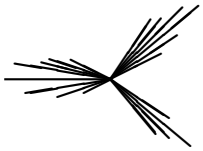

Instituto de Física Teórica
Universidade Estadual Paulista

DISSERTAÇÃO DE MESTRADO

IFT-D.003/18

Enhancement in the double Higgs boson production by e^+e^- annihilation and physics Beyond the Standard Model.

Presented by: Andrés Felipe Vásquez Tocora

Advisor: Rogerio Rosenfeld

Co-Advisor: Alberto Tonero

October 3, 2018

Vásquez Tocora, Andrés Felipe
V335e Enhancement in the double Higgs boson production by e^+e^- annihilation and physics beyond the standard model/ Andrés Felipe Vásquez Tocora. – São Paulo, 2018
120 f. : il.

Dissertação (mestrado) - Universidade Estadual Paulista (Unesp), Instituto de Física Teórica (IFT), São Paulo
Orientador: Rogerio Rosenfeld
Coorientador: Alberto Tonero

1. Modelo padrão (Física nuclear). 2. Higgs, Bosons de. 3. Teoria de campos (Física) I. Título.

Sistema de geração automática de fichas catalográficas da Unesp. Biblioteca do Instituto de Física Teórica (IFT), São Paulo. Dados fornecidos pelo autor(a).

Abstract

The main goal of this dissertation is to show the enhancement of the cross-section for the double Higgs production through pair annihilation by including effective interactions and through the non-perturbative Sommerfeld effect. Bounds to some Wilson coefficients were obtained from such enhancement, this in the scenarios of the future e^+e^--colliders (FCC-ee, ILC, CLIC). In order to achieve this, some computational tools were implemented: FeynRules, FeynArts, FormCalc, and LoopTools. It is also shown the enhancement of the double Higgs production in 2HDM and MSSM, discussing the general framework of these two models. In addition, it is studied the threshold behavior of the cross-section for the double Higgs production when a hidden sector couples to the Higgs boson, yielding resonances below the threshold energy due to non-perturbative effects.

We study the Sommerfeld effect in the double Higgs production in the scenario of e^+e^--colliders. The enhancement is discussed as generated from a hidden sector coupled to the Higgs boson. Below and above threshold enhancements are presented. Such analysis is of importance in the ILC project, which will operate up to the threshold energy $\sqrt{s} = 250\,\text{GeV}$. The results has been achieved by the use of computational tools like FeynArts, FormCalc, and LoopTools.

Keywords— Beyond the Standard Model, Effective Field Theory, Higgs boson production, Sommerfeld effect.

Resumo

O objetivo principal dessa dissertação é, mostrar o aprimoramento da seção de choque para a produção em dobro dos bósons de Higgs, por meio de aniquilação de pares, incluindo interações efetivas e através do efeito não perturbativo de Sommerfeld. De tais aprimoramentos, os limites para alguns coeficientes de Wilson foram obtidos, isso nos cenários de futuros aceleradores de e^+e^- (FCC-ee, ILC, CLIC). Para atingir estes resultados, algumas ferramentas computacionais foram implementadas: FeynRules, FeynArts, FormCalc e LoopTools. Também, é mostrado o aprimoramento da produção em dobro de bósons de Higgs no 2HDM e MSSM, discutindo o marco geral desses dois modelos. Além disso, foi estudado o comportamento, perto do limite de produção, da seção de choque da produção em dobro dos bósons de Higgs, quando um setor escondido é acoplado ao Higgs, produzindo ressonâncias abaixo da energia limite de produção, devido à efeitos não perturbativos.

To Luz Stella and Gabrielly.

Contents

Abstract **ii**

Introduction . . . 1

I The Standard Model of particle physics **1**

I.1 Strong Sector . . . 3

I.2 Higgs sector . . . 4

I.3 Electroweak Bosonic Sector . . . 5

I.4 Ghosts and gauge fixing . . . 8

I.5 Electroweak Fermion sector . . . 9

I.6 Yukawa Interactions . . . 11

I.7 Entire Standard Model Lagrangian . . . 12

II New physics **15**

II.1 Why physics beyond the Standard Model? . . . 15

II.1.1 Gravity . . . 15

II.1.2 Cosmological Constant Problem and Dark Matter . . . 16

II.1.3 Neutrino Masses . . . 17

II.1.4 Additional open problems . . . 18

II.2 Physics BSM in an effective approach . . . 18

II.3 Naturalness and Hierarchy problem . . . 24

III Two-Higgs-Doublet Model (2HDM) 30

III.1 Construction of the Model . . . 31

III.2 Types of 2HDM . . . 36

III.3 The Alignment Limit . . . 39

III.4 Constraints to the Parameters of the 2HDM . . . 40

IV Minimal Supersymmetric Standard Model 42

IV.1 Basics of Supersymmetry . . . 43

IV.2 Construction of the MSSM . . . 48

IV.3 Spontaneous Symmetry Breaking in the MSSM . . . 51

IV.4 Supersymmetry Breaking . . . 56

IV.4.1 Soft Supersymmetry Breaking terms and full MSSM Lagrangian . . . 56

IV.4.2 Spontaneous Supersymmetry Breaking . . . 57

IV.5 Mass spectrum of the MSSM . . . 64

IV.6 Phenomenological constraints on the MSSM . . . 68

V Higgs physics 70

V.1 Channels of production . . . 71

V.2 Software implementation . . . 73

V.2.1 $e^+e^- \to \mu^+\mu^-$ . . . 73

V.3 $h \to \gamma\gamma$ . . . 74

V.4 $h \to gg$ . . . 81

V.5 Branching ratios and decay widths of the Higgs boson . . . 82

VI Double Higgs production via electron-positron annihilation 89

VI.1 Double Higgs production in the SM ($e^+e^- \to hh$) . . . 91

VI.2 Enhancement of $e^+e^- \to hh$ via Effective operators . . . 93

VI.3 $e^+e^- \to h^0A^0$ (2HDM) . . . 102

VI.4 $e^+e^- \to \{h^0A^0,\ H^0A^0\}$ (MSSM) . . . 103

VI.5 Sommerfeld enhancement 104

VI.5.1 Remarks on Sommerfeld effect 104

VI.5.2 Sommerfeld effect from ladder approximation applied to the $e^+e^- \to hh$ process 107

VI.5.3 Solution to the Schrödinger equation 111

VI.5.4 Sommerfeld enhancement of $e^+e^- \to hh$ 112

VII Conclusion **115**

Bibliography **115**

List of Tables

I.1 Quark properties.[15] 1

I.2 Lepton properties.[15] 2

I.3 Properties of bosons. [15] 2

I.4 Quantum numbers Q, τ^3 and Y for the fermion and higgs fields. 5

II.1 Dimension-6 independent effective operators. The top table shows 34 operators that take into account interactions involving bosons, while in the bottom table there are 29 operators describing four-fermion interactions. Without the 4 B-violating operators, remain 59 independent operators described in Ref. [62] 21

III.1 Higgs doublets that couples to an up-, down- and charged-lepton-like fermions in different Two-Higgs Doublet Models. 37

III.2 Higgs doublets that couples to an up-, down- and charged-lepton-like fermions in different Two-Higgs Doublet Models. 38

IV.1 Conventions of the R-charge belonging to an $U(1)_R$ symmetry for some objects. 48

IV.2 Particle spectrum of the MSSM that are arranged in chiral superfields, together with their representations under the gauge symmetry of the SM. The index i stands for the generation. 49

IV.3 Particle spectrum of the MSSM that are arranged in vector superfields, together with their representations under the gauge symmetry of the SM. The indices run as $A = 1, \cdots, 8$ and $I = 1, 2, 3$ 49

V.1 The Branching Ratios for a Higgs boson with $m_h = 125\,\text{GeV}$.[15] 88

VI.1 Benchmark luminosities and energies for different future experiments.[65] 101

List of Figures

I.1 Triple and Quartic Higgs interactions. 4

I.2 Triple interactions between weak massive bosons and the Higgs 6

I.3 Quartic interactions between weak massive bosons and the Higgs 7

I.4 Yukawa interaction between Higgs boson and fermions. 12

I.5 Electroweak interactions for fermions. 13

IV.1 Corrections to the Higgs mass from scalars and fermions. 51

V.1 Main production processes for the Higgs boson in hadronic collisions. 71

V.2 Main production processes for the Higgs boson in e^+e^- colliders. 72

V.3 Cross-section for the process $e^+e^- \to \mu^+\mu^-$ (Compare to Fig. 5.1 in [54]) a) in QED, b) in the Glashow-Weinberg-Salam model with the full Z-boson propagar (Compare to Fig. 1 in [66]). . . . 75

V.4 Feynman diagrams in the unitary gauge for the Higgs decay into two photons, with $\epsilon_2^\mu = \epsilon^\mu(p_2)$ and $\epsilon_3^\nu = \epsilon^\nu(p_3)$, and where the crossed diagrams have been omitted. 75

V.5 Width for the decay $H \to \gamma\gamma$ computed theoretically (Black) and by FormCalc implementation (Magenta). 76

V.6 Feynman diagrams for the Higgs decay into two gluons. 81

V.7 Width for the decay $H \to gg$ given by FormCalc (Black) and theoretical computations from [15] (Magenta). 82

V.8 Branching ratios and their uncertainties of the Higgs boson as a function of its mass.[67] 86

VI.1 Feynman diagrams at tree-level for $e^+e^- \to hh$. 90

VI.2 (a) Triangle and (b) Box topologies at 1-loop for $e^+e^- \to hh$. 90

VI.3 Bubble topologies at 1-loop for $e^+e^- \to hh$. 90

VI.4 Total cross-section and box contribution for the process $e^+e^- \to hh$ in the SM, where it is shown that only the box topologies do contribute substantially. Here $\sigma^{(0+1)}$ stands for the total cross-section at NLO and $\sigma^{(Box)}$ for the cross-section coming just from the Box diagrams. 91

VI.5 Dependence on the trilinear Higgs coupling of the cross-section for $e^+e^- \to hh$ just for the 1-loop contribution (Left), and of the total cross section at NLO (Right). 92

VI.6 Example of the helicity structure for diagrams involving the trilinear Higgs interaction. 92

VI.7 Vanishing amplitude for the process $e^+e^- \to hh$ near threshold, where it has been fixed randomly two collision angles in order to present that the suppression is not due to such fixing. 93

VI.8 Feynman Diagram of an effective contribution that reproduces a Fermi-like interaction. 94

VI.9 Sensitivity (Left) and enhancement (Right) of the cross-section $\sigma\left(e^+e^- \to hh\right)$ due to variations of the Wilson coefficient C_1 that appears in Eq. [VI.1]. 95

VI.10 Sensitivity (Left) and enhancement (Right) of the cross-section $\sigma\left(e^+e^- \to hh\right)$ due to variations of the Wilson coefficient C_{et} introduced in the Lagrangian of Eq. [VI.15]. 97

VI.11 Chosen Feynman diagrams that introduces the effective interactions effects from Eq. [VI.15] into the cross-section $\sigma\left(e^+e^- \to hh\right)$. 98

VI.12 χ^2-distribution for the Wilson coefficients C_{eH} (left) and C_{et} (right) from the cross-section of the double Higgs production via electron-positron annihilation. Here the horizontal lines stand for the limit of 95% of confidence level from a χ^2 distribution with 1 degree of freedom. The bounds a)-b) are expected for $\mathcal{L} = 2.6\,\mathrm{ab}^{-1}$ at 350 GeV, benchmark values of the FCC-ee Project. The bounds c)-d) are expected for $\mathcal{L} = 4\,\mathrm{ab}^{-1}$ at 500 GeV, benchmark values of the ILC Project. The bounds e)-f) are expected for $\mathcal{L} = 1.5\,\mathrm{ab}^{-1}$ at 1.5 TeV, benchmark values of the CLIC Project. . 100

VI.13 χ^2-distribution for the Wilson coefficients C_{eH} and C_{et} from the cross-section of the double Higgs production via electron-positron annihilation. It is presented, from inner to outer, the 68.5%, 95% and 99% confidence regions for 1 degree of freedom for the mentioned Wilson coefficients. These bounds are expected for (a) $\mathcal{L} = 500\,\mathrm{fb}^{-1}$ at 380 GeV, (b) $\mathcal{L} = 1.5\,\mathrm{ab}^{-1}$ at 1.5 TeV, (c) $\mathcal{L} = 3\,\mathrm{ab}^{-1}$ at 3 TeV, benchmark values of the CLIC project; and (d) $\mathcal{L} = 4\,\mathrm{ab}^{-1}$ at 500 GeV, benchmark values of the ILC projects (arXiv: 1704.02333v2). 101

VI.14 Total cross-section of the process $e^+e^- \to A^0h^0$ in the 2HDM for $\tan\beta = 1$ and $\sin\alpha = 1$, at tree level and at 1-loop with different values for λ_5. 102

VI.15 Some examples of the Feynman diagrams that enter in the the process $e^+e^- \to A^0h^0$ in the 2HDM and in the MSSM. 103

VI.16Cross-sections at tree-level for the Higgs boson production $e^+e^- \to H^0A^0$ in the MSSM a) as a function of the energy ($m_{A^0} = 200\,\text{GeV}$), and b) as a function of the mass of the CP-even neutral Higgs boson H_0 ($\sqrt{s} = 3\,\text{TeV}$). Compare the above results with [70]. 104

VI.17Sommerfeld Factor (S) as a function of ϵ_ϕ with the fixed value $\epsilon_v = 10^{-3}$. Here the black solid curve represent the numerical solution of the Schrödinger equation while the red dashed curve stands for analytical solution with the approximation taking the Hulthen potential. 106

VI.18Relation that defines the amplitude of the process $e^+e^- \to e^+e^-$ mediated by Higgs bosons in terms of $\Gamma(q,p)$. 108

VI.19Relation that must be satisfied by Γ in the ladder approximation. 109

VI.20Behavior around threshold of the cross-sections for the double Higgs production when the Sommerfeld effects of a hidden scalars ϕ with $m_\phi = 10\,\text{GeV}$ are taken into account. The left plot corresponds to the Higgs boson with a width of $\Gamma_h = 0.005\,\text{GeV}$ as in the SM, while the left plot corresponds to $\Gamma_h = 0.01\,\text{GeV}$. The black solid curve represents the SM cross-section σ_0. The vertical lines in magenta represent the energies $\sqrt{s} = 227.65\,\text{GeV}$ and $\sqrt{s} = 240.35\,\text{GeV}$ of the $\ell = 0$ bound-state from the formulas [VI.78]. 113

Introduction

Huge advances have been achieved in the understanding of the basic components of matter and its dynamics. From the Fermi theory of the β-decay, many attempts were made in order to unveil the fundamental nature of the weak interactions. Thus it was introduced the Glashow-Winberg-Salam theory (GWS) of electroweak interactions, that explains the dynamics of electroweak interactions up to smaller distances than those that Fermi theory could. The GWS theory, together with Quantum Chromodynamics (QCD), compose the Standard Model (SM) of particles, a theory that has shown incredible predictive power. This theory was completely confirmed July 4 of 2012, when the resonance at 125 GeV was identified as the Higgs boson.

Despite all the success that the Standard Model represents by itself, from its creation it is known that it cannot be the full story. An ever deeper theory is needed in order to explain the known physical phenomena. The simple fact that gravity cannot be explained in the SM framework is a strong hint to say that it is required a theory that explains the physics at enough short distances, where gravity becomes comparable in strength to the other interactions, i.e. at the Planck scale. Like this, there are many other hints in the way to find theories beyond the SM: massive neutrinos, dark matter, dark energy, cosmological problem, CP violation and matter-antimatter asymmetry are some observational clues.

Theoretical arguments also can guide us in the way of looking for UV - completions of the SM. How is it possible that between the electroweak and the Planck scales there is not new physics? This is like 16 orders of magnitude in which basically nothing interesting happens. Thus the hierarchy problem guide us to seek the right underlying theory beyond the SM. This motivates the study of supersymmetric theories, compositeness models, extra-dimensions, among others.

The list of extensions of the SM model is huge, for this reason a method that can describe beyond SM effects in a model-independent way is very useful. Following the Fermi theory, an effective extension of the SM that let us parametrize the unknown physics was built. Precisely, through this effective extension, in this dissertation, the Higgs sector is studied. It is very important the full characterization of the Higgs sector. So far, we know the predictions for the parameters in the scalar potential of the SM, but the trilinear and quartic self-interactions

of the Higgs boson has not been directly measured. Thus, some deviations are expected from the predictions, in such a way that this sheds light on physics beyond the SM.

It could also happen that there exist some scalars that, from the particle spectrum of the SM, only couple to the Higgs boson. In this case, it could happen that such interactions bind Higgs bosons in order to compose a bound-state. This situation is studied in a non-relativistic way, through the Sommerfeld effect, where the effects of the hidden scalars could be relevant.

In this dissertation, the Standard Model of particle physics is discussed in chapter [I] and the motivations for going beyond the Standard Model in chapter [II]. In the same chapter, the EFT approach for physics beyond the Standard Model is presented. Chapters [III] and [IV] give the general aspects of the Two Higgs Doublet Model and the Minimal Supersymmetric Standard Model, respectively. Then, in the chapter [V], some general aspects of the Higgs boson physics are shown . Finally, in the chapter [VI], the cross-sections for the Double Higgs production by e^+e^- annihilation in the SM, 2HDM, and MSSM, are studied, including the way that some effective operators can enhance this process, then imposing bounds to their respective Wilson coefficients. Moreover, the non-perturbative effects in the double Higgs boson production due to a hidden sector are presented in the same chapter.

Chapter I

The Standard Model of particle physics

This chapter is dedicated to one of the most successful theories conceived so far: the so-called Standard Model of particles (SM). The unprecedented accuracy between the predictions yielded by the SM and the experiments have located it as the current paradigm for high energy processes.

The SM takes some of the outstanding results in particle physics of the 60's and 70's. The SM is composed by the Electroweak theory of Glashow[1], Weinberg[2] and Salam[3] (GWS theory), and by the Quantum Chromodynamics (QCD). The former gives a consistent unification of the weak and electromagnetic interactions between quark and leptons, making use of the Goldstone's theorem through the Higgs mechanism[4]-[6]. The latter describes the strong interaction between gluons and quarks, and got its theoretical structure from the works of Gell-Mann, Fritzsch, and Leutwyler in ref. [8], and Gross, Wilczek and Politzer in ref. [10][11]. The renormalizability of the theory was proven in 1972 by 't Hooft and Veltman[9].

All these ingredients have received great experimental confirmations, from the prediction of neutral currents and the baryon and meson spectra, up to the last discovery in 2012 at the LHC: the Higgs boson[13][12]. This theory, that has been tested up to 13 TeV, is the best description for the physics in particle accelerators, where the gravitational interactions are negligible.

	Flavor	Mass (GeV)	Charge (e *units*)
Up quark Sector	u	$(2.2)^{+0.6}_{-0.4} \times 10^{-3}$	$\frac{2}{3}$
	c	1.27 ± 0.03	
	t	173.21 ± 0.51	
Down quark Sector	d	$4.7^{+0.5}_{-0.4} \times 10^{-3}$	$-\frac{1}{3}$
	s	$96^{+8}_{-4} \times 10^{-3}$	
	b	$(4.18)^{+0.04}_{-0.03}$	

Table I.1: Quark properties.[15]

Flavor	Mass (GeV)	Charge (e *units*)
e^-	$(0.5109989461 \pm 0.000000031) \times 10^{-3}$	-1
μ^-	$(105.6583745 \pm 0.0000024) \times 10^{-3}$	
τ^-	1.77686 ± 0.00012	
ν_e, ν_μ, ν_τ	$< 2\,\text{eV}$ (Tritium decay)	0

Table I.2: Lepton properties.[15]

Particle	Mass (GeV)	Charge (e *units*)
γ	$< 1 \times 10^{-21}$	$< 10^{-35}$
g	0 (Theoretical)	0
$W^\pm$	80.385 ± 0.015	± 1
Z	91.1876 ± 0.0021	0
h	125.09 ± 0.24	0

Table I.3: Properties of bosons. [15]

The SM, as a quantum field theory, is determined by its degrees of freedom, that is, the particle content, and the symmetries, both global and gauge symmetries. The particle content of the theory is given by, first, six quark types and six type of leptons, with masses and charges as shown in tables [I.1] and [I.2]. Second, spin-1 fields, where it is noted that photons (long-range Coulomb interaction) and gluons (confined due to strong interaction and so a short-range interaction) are massless, and that the weak bosons are so heavy that leads to a short-range weak interaction. At last but not least, we have the Higgs boson, a spin-0 field.

It is observed that the quark masses span a range of $(10^{-3} - 10^2)\,\text{GeV}$. As it is well known, the measure of such quark masses is tricky, since the confinement phenomenon. Thus, bound states of quarks are measured, such as pions, instead of free quarks. These bound states are set by the QCD scale at $\Lambda_{QCD} \sim 200\,\text{MeV}$. Furthermore, in the fermionic sector, we have the hierarchical span of the charged leptons masses and the particular values for the neutrinos. The latter species is very special, since the unknown absolute scale for these masses, i.e. we only can measure differences between masses. In addition, there exists the possibility that just two of the three neutrinos are massive.

On the other hand, the gauge symmetry that the Lagrangian of the theory manifests is $SU(3)_C \times SU(2)_L \times U(1)_Y$, thus, in general, the covariant derivative is

$$D_\mu \quad = \partial_\mu + ig_s G_\mu^a T^a + igW_\mu^a \tau^a + ig' B_\mu \tfrac{Y}{2}, \tag{I.1}$$

where the G_μ^a correspond to the eight gauge fields of the $SU(3)_C$, i.e. the eight gluons, the W_μ^a are the three gauge fields of the $SU(2)_L$ and B_μ is the gauge field of the $U(1)_Y$. Then, we see that the interaction particles are known once the gauge group is set. Now, to endow with mass some particles of the SM it is implemented the Higgs Mechanism, thus the spontaneous symmetry breaking (SSB) of the theory must be specified. Such SSB is realized just in the electroweak sector (EW-SSB), in a way that strong interaction remains untouched.

Specifically,

$$SU(2)_L \times U(1)_Y \xrightarrow{SSB} U(1)_{em}\,, \tag{I.2}$$

i.e., three of the four generators of $SU(2)_L \times U(1)_Y$ are broken, then the Higgs field should have at least three real scalars to play the role of the Nambu-Goldstone bosons (NGB), which are "swallowed" by the three gauge fields, becoming the longitudinal degree of freedom of the new massive bosons. The complex field H, that is in the smallest representation of the gauge group and satisfies the previous requirements, is made up of four real scalars and is a singlet of the color group, a doublet of $SU(2)_L$ with $Y = +1$. Hence, an unbroken generator and a real scalar field remain, which are the photon and the Higgs, respectively.

I.1 Strong Sector

Let us set

$$G^a_{\mu\nu} = \partial_\mu G^a_\nu - \partial_\nu G^a_\mu + g_s f^{abc} G^b_\mu G^c_\nu, \tag{I.3}$$

with $a = 1, ..., 8$, g_s the gauge coupling for the QCD and f^{abc} the group structure constant, which are related to the generators T^a of the group through $[T^a, T^b] = if^{abc}T^c$. In QCD, the quarks are in the fundamental representation, and the generators can be chosen to be $T^a = \lambda^a/2$, with λ^a the Gell-Mann matrices, thus in this sector we have

$$D_\mu Q = (\partial_\mu - ig_s G_\mu)\, Q. \tag{I.4}$$

The gauge transformations are given by operators of the form $U = e^{-iT^a\alpha^a}$, so that the SM Lagrangian remains invariant under the field transformations

$$Q \;\rightarrow\; e^{-iT^a\alpha^a}Q, \qquad \delta Q = -iT^a\alpha^a Q, \tag{I.5}$$

$$G_\mu \;\rightarrow\; UG_\mu U^{-1} - \frac{i}{g_s}(\partial_\mu U)\,U^{-1}, \qquad \delta G^a_\mu = -\frac{1}{g_s}\partial_\mu\alpha^a + f^{abc}\alpha^b G^c_\mu. \tag{I.6}$$

The gauge field Lagrangian for the gluons is written as

$$\mathcal{L}^{YM}_{QCD} \;=\; -\frac{1}{4}G^a_{\mu\nu}G^{a\mu\nu}. \tag{I.7}$$

The Lagrangian including the matter fields will be introduced in a few sections.

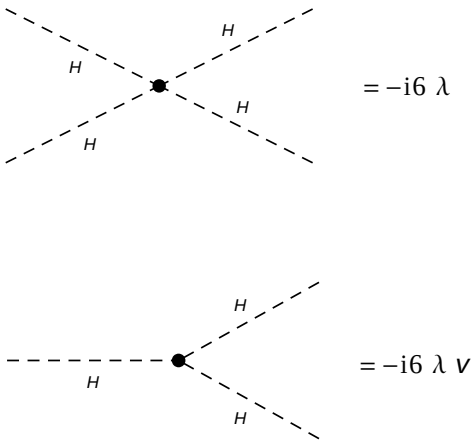

Figure I.1: Triple and Quartic Higgs interactions.

I.2 Higgs sector

The Higgs doublet used to get the EW-SSB is

$$H = \begin{pmatrix} H^+ \\ H^0 \end{pmatrix} = \frac{1}{\sqrt{2}} \begin{pmatrix} \phi_1 + i\phi_2 \\ \phi_3 + i\phi_4 \end{pmatrix}. \tag{I.8}$$

As it was already said, H transforms as a singlet of $SU(3)_C$, a doublet of $SU(2)_L$ and with an hypercharge of $+1/2$ under $U(1)_Y$ (which is noted as $H \sim (1, 2, +1/2)$). Hence, we have the covariant derivative over the Higgs field

$$D_\mu H = \partial_\mu H + igW_\mu H + ig' \frac{Y_H}{2} B_\mu H, \tag{I.9}$$

where g and g' are the gauge couplings for $SU(2)_L$ and $U(1)_Y$, respectively, and $W_\mu = W_\mu^a \tau^a$, with $\tau^a = \frac{\sigma^a}{2}$. The Lagrangian for this sector is

$$\mathcal{L}_{Higgs} = (D_\mu H)^\dagger (D^\mu H) - V(H), \tag{I.10}$$

with the potential

$$V(H) = \lambda \left(H^\dagger H - \frac{1}{2} v^2 \right)^2, \tag{I.11}$$

where the mass dimensions of the parameters in the potential are $[\lambda] = 0$ and $[v] = 1$, with $v > 0$. Now, let

Field	ℓ_L	ℓ_R	ν_L	u_L	d_L	u_R	d_R	H^+	H^0
T^3	$-\frac{1}{2}$	0	$\frac{1}{2}$	$\frac{1}{2}$	$-\frac{1}{2}$	0	0	$\frac{1}{2}$	$-\frac{1}{2}$
Y	-1	-2	-1	$\frac{1}{3}$	$\frac{1}{3}$	$\frac{4}{3}$	$-\frac{2}{3}$	1	1
Q	-1	-1	0	$\frac{2}{3}$	$-\frac{1}{3}$	$\frac{2}{3}$	$-\frac{1}{3}$	1	0

Table I.4: Quantum numbers Q, τ^3 and Y for the fermion and higgs fields.

us focus on the vacuum expectation value (VEV) of the Higgs field. In general, it must be $\langle H\rangle = \begin{pmatrix} a \\ b \end{pmatrix}$, but without loss of generality, it can be set to

$$\langle H\rangle \quad = \quad \begin{pmatrix} 0 \\ \frac{v}{\sqrt{2}} \end{pmatrix}, \tag{I.12}$$

this by using transformations of the type $\phi \to \exp(-2i\theta_{2,3}\tau_{2,3})\phi$. From the Goldstone theorem, it is known that, to get an unbroken generator, this must annihilate the vacuum. With the generators in the form presented so far, naively, we can say that all the four generators are broken, but with the linear combinations $Q = \tau^3 + \frac{1}{2}\mathbf{1}_{2\times 2}$ we find an unbroken generator. Here Q is identified as the electric charge.

We want to identify the would-be NGB's, then the exponential parametrization is the more suitable realization. In general:

$$H \quad = \quad \frac{1}{\sqrt{2}}\,(h+v)\,e^{-i\chi^a\tau^a}\begin{pmatrix} 0 \\ 1 \end{pmatrix}, \tag{I.13}$$

where the χ^a are the NGB's ($a = 1, 2, 3$) and the radial mode h is the Higgs boson. After spontaneous symmetry breaking, we have that the potential of the scalar sector is

$$V(H) \quad = \quad \lambda\left(H^\dagger H - \frac{1}{2}v\right)^2 = \frac{\lambda}{4}\left(2vh + h^2\right)^2 \tag{I.14}$$

$$\quad = \quad \frac{1}{2}m_h h^2 + \lambda v h^3 + \frac{\lambda}{4}h^4, \tag{I.15}$$

where the Higgs mass comes to be $m_h^2 = 2\lambda v^2$. From this, the Feynman rules of the figure [I.1] are derived.

I.3 Electroweak Bosonic Sector

The Yang-Mills Lagrangian for this sector is

$$\mathcal{L}_{EW} \quad = \quad -\frac{1}{4}W^a_{\mu\nu}W^{a\mu\nu} - \frac{1}{4}B_{\mu\nu}B^{\mu\nu} + |D_\mu H|^2. \tag{I.16}$$

For the electroweak bosons, it would be useful to see the interactions with the Higgs boson. For this sake, we

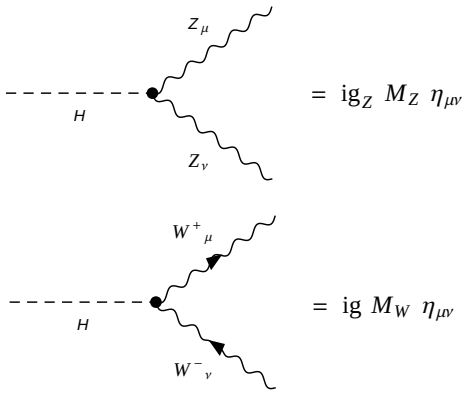

Figure I.2: Triple interactions between weak massive bosons and the Higgs

take into account the covariant derivative of the latter in the following analysis. So far, we know that the SSB is in the form of Eq. [I.2], thus, in the end, we must be able to recover the electromagnetic field. With this in mind, we change the gauge field basis. With $\tau^\pm = \tau^1 \pm i\tau^2$, the following commutation relations are obtained

$$\left[Q, \tau^\pm\right] \quad = \quad \left[\tau^3, \tau^\pm\right] = \pm\tau^\pm, \tag{I.17}$$

which suggests that the gauge bosons corresponding to τ^+ and τ are electrically positive and negative charged, respectively. We can define $W_\mu^\pm = \frac{1}{\sqrt{2}}\left(W_\mu^1 \mp iW_\mu^2\right)$, so that

$$g\left(W_\mu^1\tau^1 + W_\nu^2\tau^2\right) \quad = \quad \frac{g}{\sqrt{2}}\left(W_\mu^+\tau^+ + W_\mu^-\tau^-\right). \tag{I.18}$$

In the same way, we rotate the other gauge fields by doing

$$Z_\mu = c_W W_\mu^3 - s_W B_\mu, \qquad\qquad A_\mu = s_W W_\mu^3 + c_W B_\mu, \tag{I.19}$$

where $c_W \equiv \cos\theta_W = \frac{g}{\sqrt{g^2+g'^2}}$, $s_W \equiv \sin\theta_W = \frac{g'}{\sqrt{g^2+g'^2}}$, so that $\tan\theta_W = \frac{g'}{g}$. In the canonical normalization of the kinetic terms, we have the equivalence

$$-\frac{1}{4}\sum_{a=1,2}\left(\partial_\mu W_\nu^a - \partial_\nu W_\mu^a\right)\left(\partial^\mu W^{\nu a} - \partial^\nu W^{\mu a}\right) = -\frac{1}{2}\left(\partial_\mu W_\nu^+ - \partial_\nu W_\mu^+\right)\left(\partial^\mu W^{\nu-} - \partial^\nu W^{\mu-}\right). \tag{I.20}$$

We can also check that

$$gW_\mu^2\tau^3 + \frac{Y}{2}g'B_\mu = g\left(c_W Z_\mu + s_W A_\mu\right)\tau^3 + g'\left(c_W A_\mu - s_W Z_\mu\right)\frac{Y}{2} \quad \text{(I.21)}$$

$$= gs_W A_\mu\left(\tau^3 + \frac{Y}{2}\right) + \frac{g}{c_W}Z_\mu\left(c_w^2\tau^3 - s_W^2\frac{Y}{2}\right). \quad \text{(I.22)}$$

There are two remarks from the last equation:

- A_μ is coupled to $Q = \tau^3 + \frac{Y}{2}$ (This relation can be tested with the values of the table [I.2]).
- It can be identified the electromagnetic constant by doing $e = g\,s_W = g'c_W$.

With this rotation on the fields, we can see the way the Higgs mechanism endows with mass the weak bosons:

$$|D_\mu H|^2 = \left|\frac{1}{\sqrt{2}}\begin{pmatrix}0\\ \partial_\mu h\end{pmatrix} + \frac{i}{2\sqrt{2}}(v+h)\begin{pmatrix}\sqrt{2}gW_\mu^+\\ -g_Z Z_\mu\end{pmatrix}\right|^2 \quad \text{(I.23)}$$

$$= \frac{1}{2}\partial_\mu h\partial^\mu h + M_W^2 W_\mu^+ W^{-\mu} + \frac{1}{2}M_Z^2 Z_\mu Z^\mu + \frac{1}{8}\left(2vh + h^2\right)\left(2g^2 W_\mu^+ W^{-\mu} + g_Z^2 Z_\mu Z^\mu\right), \quad \text{(I.24)}$$

where it has been identified

$$M_Z = \frac{1}{2}\sqrt{g^2 + g'^2}v, \qquad M_W = \frac{1}{2}gv, \quad \text{(I.25)}$$

which allows us to define $\rho \equiv \frac{M_W}{M_Z c_W}$, in such a way that at tree-level $\rho = 1$. After the SSB, which led us to Eq. [I.24], we see that the photon remains massless. The last term in Eq. [I.24] yields the interactions shown in the Figures [I.2] and [I.3].

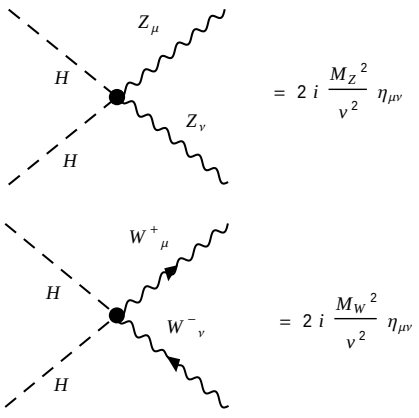

Figure I.3: Quartic interactions between weak massive bosons and the Higgs

I.4 Ghosts and gauge fixing

In the previous section we saw that just the physical Higgs field h appeared. In general, it is known that all the four fields introduced in the Higgs doublet are able to be in our Lagrangian. So far, we have worked in the unitary gauge. Now, we discuss a generalization of the class of Lorenz gauges: the R_χ-gauge. We can use the following parametrization for the Higgs field:

$$H = \begin{pmatrix} \varphi^+ \\ \frac{1}{\sqrt{2}}(v+h+i\varphi_Z) \end{pmatrix}, \qquad \tilde{H} = i\sigma_2 H^* = \begin{pmatrix} \frac{1}{\sqrt{2}}(v+h-i\varphi_Z) \\ -\varphi^- \end{pmatrix}, \tag{I.26}$$

where $\varphi^\pm = \chi^1 \pm \chi^2$ and $\varphi_Z = \chi^3$. The Lagrangian in this gauge is written as

$$\mathcal{L}_{R_\xi} = -\frac{1}{2\xi}F_G^2 - \frac{1}{2\xi}F_A^2 - \frac{1}{2\xi}F_Z^2 - \frac{1}{\xi}F_-F_+, \tag{I.27}$$

with

$$F_G^a = \partial^\mu G_\mu^a, \qquad F_A = \partial^\mu A_\mu, \qquad F_Z = \partial^\mu Z_\mu - \xi M_Z \varphi_Z, \tag{I.28}$$

$$F_+ = \partial^\mu W_\mu^+ - i\xi M_W \varphi^+, \tag{I.29}$$

$$F_- = \partial^\mu W_\mu^- + i\xi M_W \varphi^-. \tag{I.30}$$

Then we must specify the Lagrangian for the ghosts. With the Faddeev-Popov technique, we have

$$\begin{aligned} \mathcal{L}_{Ghost} = & \sum_{i=1}^{4}\left[\bar{c}_+\frac{\partial(\delta F_+)}{\partial\alpha^i} + \bar{c}_-\frac{\partial(\delta F_+)}{\partial\alpha^i} + \bar{c}_Z\frac{\partial(\delta F_Z)}{\partial\alpha^i} + \bar{c}_A\frac{\partial(\delta F_A)}{\partial\alpha^i}\right]c_i \\ & + \sum_{a,b=1}^{8}\bar{\omega}^a\frac{\partial(\delta F_G^a)}{\partial\beta^b}\omega^b, \end{aligned} \tag{I.31}$$

where the ghosts related to the QCD sector are denoted with ω^a, transforming as $U = e^{-iT^a\beta^a}$ $(a = 1, ..., 8)$, and the ghosts associated with the electroweak sector are denoted with $c_\pm$, c_A, c_Z, transforming as $U = e^{-iT^a\alpha^a}$ $(a = 1, 2, 3)$ and $U = e^{iY\alpha^4}$. To be more explicit, we redefine the parameters of the electroweak sector as

$$\alpha^\pm = \frac{\alpha^1 \mp \alpha^2}{\sqrt{2}}, \alpha_Z = \alpha^3\cos\theta_W + \alpha^4\sin\theta_W, \alpha_A = -\alpha^3\sin\theta_W + \alpha^4\cos\theta_W. \tag{I.32}$$

Then, we have the set of transformations

$$\delta F_G^a = -\partial_\mu\beta^a + g_s f^{abc}\beta^b G_\mu^c, \tag{I.33}$$

$$\delta F_A = -\partial_\mu\alpha_A, \tag{I.34}$$

$$\delta F_Z = \partial_\mu (\delta Z^\mu) - M_Z \delta\varphi_Z, \tag{I.35}$$

$$\delta F_+ = \partial_\mu \left(\delta W_\mu^+\right) - iM_W \delta\varphi^+, \tag{I.36}$$

$$\delta F_- = \partial_\mu \left(\delta W_\mu^-\right) - iM_W \delta\varphi^-. \tag{I.37}$$

where, for the electroweak bosons,

$$\delta Z_\mu = -\partial_\mu \alpha_Z + igc_W \left(W_\mu^+ \alpha^- - W_\mu^- \alpha^+\right), \tag{I.38}$$

$$\delta W_\mu^\pm = -\partial_\mu \alpha^\pm \pm ig \left[\alpha^\pm \left(Z_\mu c_W - A_\mu s_W\right) - \left(\alpha_Z c_W - \alpha_A s_W\right) W_\mu^\pm\right], \tag{I.39}$$

while, for the unphysical scalars,

$$\delta\varphi_Z = -\frac{1}{2} g \left(\alpha^- \varphi^+ + \alpha^+ \varphi^-\right) + \frac{g}{2c_W} \alpha_Z (v + h), \tag{I.40}$$

$$\delta\varphi^\pm = \mp i \frac{g}{2} \left(v + h \pm i\varphi_Z\right) \alpha^\pm \mp i \frac{g c_{2W}}{2c_W} \varphi^\pm \alpha_Z \pm ie\varphi^+ \alpha_A. \tag{I.41}$$

I.5 Electroweak Fermion sector

Now, we focus on the fermions and the $SU(2)_L \times U(1)_Y$ part of the Standard Model. The GWS theory is known to be a chiral gauge theory, i.e. left- and right-handed components of the fermions can have different quantum numbers under the gauge group. Specifically, just the left-handed components of the fermions are sensitive to the weak interaction, while the right-handed do not. Hence, the sensitive components to $SU(2)_L$ transform in the fundamental representation, thus we define the quark and lepton doublets

$$Q_1 = \begin{pmatrix} u_L \\ d_L \end{pmatrix}, \quad Q_2 = \begin{pmatrix} c_L \\ s_L \end{pmatrix}, \quad Q_3 = \begin{pmatrix} t_L \\ b_L \end{pmatrix}, \tag{I.42}$$

$$L_1 = \begin{pmatrix} \nu_{e_L} \\ e_L \end{pmatrix}, \quad L_2 = \begin{pmatrix} \nu_{\mu_L} \\ \mu_L \end{pmatrix}, \quad L_3 = \begin{pmatrix} \nu_{\tau_L} \\ \tau_L \end{pmatrix}. \tag{I.43}$$

The right-handed components are then $SU(2)_L$-singlets: $U_1 = u_R$, $U_2 = c_R$, $U_3 = t_R$, $D_1 = d_R$, $D_2 = s_R$, $D_3 = b_R$, $E_1 = e_R$, $E_2 = \mu_R$, $E_3 = \tau_R$. With these definitions, we can specify the couplings of fermions to the gauge bosons of the electroweak sector. We can use now the hypercharges that we have already set on the table [I.2]. The covariant derivatives explicitly are

$$D_\mu Q_i = \left(\partial_\mu + igW_\mu^a \tau^a + ig' B_\mu \frac{Y_Q}{2}\right) Q_i, \tag{I.44}$$

$$D_\mu L_i = \left(\partial_\mu + igW_\mu^a \tau^a + ig' B_\mu \frac{Y_L}{2}\right) L_i, \tag{I.45}$$

$$D_\mu U_i = \left(\partial_\mu + ig' B_\mu \frac{Y_U}{2}\right) U_i, \tag{I.46}$$

$$D_\mu D_i = \left(\partial_\mu + ig' B_\mu \frac{Y_D}{2}\right) D_i, \tag{I.47}$$

$$D_\mu E_i = \left(\partial_\mu + ig' B_\mu \frac{Y_E}{2}\right) E_i. \tag{I.48}$$

With these relations, the Lagrangian for the kinetic terms in the electroweak sector of the fermions is written as

$$\mathcal{L}^{kin}_{Fermion} = i\bar{Q}_i \not{D} Q_i + i\bar{U}_i \not{D} U_i + i\bar{D}_i \not{D} D_i + i\bar{L}_i \not{D} L_i + i\bar{E}_i \not{D} E_i, \tag{I.49}$$

where a sum over the generation index i is implicit. Here, we must note that the hypercharges of the two components of any doublet are the same, because of the commutation between $SU(2)_L$ and $U(1)_Y$. A fundamental difference can be noticed between leptons and quarks: the former are singlets of the $SU(3)_C$ while the latter are in the fundamental representation. Thus, the covariant derivatives used for the quarks in this section must include the term with the gluon fields that appears in Eq. [I.4]. Now, we can write the Lagrangian in Eq. [I.49] explicitly as

$$\begin{aligned}\mathcal{L}^{kin}_{Fermion} =& i\bar{Q}_i \not{\partial} Q_i + i\bar{U}_i \not{\partial} U_i + i\bar{D}_i \not{\partial} D_i + i\bar{L}_i \not{\partial} L_i + i\bar{E}_i \not{\partial} E_i \\ &- \frac{g}{\sqrt{2}} W^+_\mu J^{\mu+} - \frac{g}{\sqrt{2}} W^-_\mu J^{\mu-} - eA_\mu J^\mu_Q - \frac{e}{s_W c_W} Z_\mu J^\mu_Z,\end{aligned} \tag{I.50}$$

with the Noether currents given by

$$J^{\mu+} = \bar{\Psi}\tau^+\gamma^\mu\Psi = \sum_i \left(\bar{U}_{iL}\gamma^\mu D_{iL} + \bar{N}_{iL}\gamma^\mu E_{iL}\right), \tag{I.51}$$

$$J^{\mu-} = \bar{\Psi}\tau^-\gamma^\mu\Psi = \sum_i \left(\bar{D}_{iL}\gamma^\mu U_{iL} + \bar{E}_{iL}\gamma^\mu N_{iL}\right), \tag{I.52}$$

$$J^\mu_Q = \bar{\Psi} Q \gamma^\mu \Psi = \sum_i \left(\frac{2}{3}\bar{U}_i\gamma^\mu U_i - \frac{1}{3}\bar{D}_i\gamma^\mu D_i - \bar{E}_i\gamma^\mu E_i\right), \tag{I.53}$$

$$\begin{aligned}J^\mu_Z =& \bar{\Psi}\left(\tau^3 - s^2_W Q\right)\gamma^\mu\Psi \\ =& \sum_i \left[\bar{U}_{iL}\left(\frac{1}{2} - \frac{2}{3}s^2_W\right)\gamma^\mu U_{iL} + \bar{D}_{iL}\left(-\frac{1}{2} + \frac{1}{3}s^2_W\right)\gamma^\mu D_{iL}\right. \\ &+ \bar{U}_{iR}\left(-\frac{2}{3}s^2_W\right)\gamma^\mu U_{iR} + \bar{D}_{iR}\left(\frac{1}{3}s^2_W\right)\gamma^\mu D_{iR} + \bar{E}_{iL}\left(-\frac{1}{2} + s^2_W\right)\gamma^\mu E_{iL} \\ &\left. + \bar{E}_{iR}\left(s^2_W\right)\gamma^\mu E_{iR} + + \bar{N}_{iL}\left(\frac{1}{2}\right)\gamma^\mu N_{iL}\right],\end{aligned} \tag{I.54}$$

where N_{iL} stands for the neutrinos of the SM, i.e. left-handed neutrinos. Thus, the interactions of the figure [I.5] are generated. The interactions between the fermions and Z-boson can be written in a suitable way. For

this, we take into account that the left- and right-handed terms can be combined by making

$$\begin{aligned}\left(\tau^3 - s_W^2 Q\right) P_L - s_W^2 Q P_R &= \tau^3 P_L - s_W^2 Q \\ &= \frac{1}{2}\left[\left(\tau^3 - 2s_W^2 Q\right) - \tau^3\gamma_5\right] \\ &= \frac{1}{2}\left(g_V^i - g_A^i\right), \end{aligned} \tag{I.55}$$

with $g_V^i = \tau_i^3 - 2s_W^2 Q_i$ and $g_A^i = \tau_i^3\gamma_5$. It is observed that there are two kinds of interactions involving fermions in the weak sector: the flavor-changing charged currents, generated by the $W^\pm$ bosons, and the flavor-preserving neutral currents, mediated by the Z and the A bosons.

I.6 Yukawa Interactions

The usual mass terms $m\bar{\psi}\psi$ spoil the $SU(2)_L \times U(1)_Y$ symmetry. In the SM, the fermions get their masses through EW-SSB. We are able to write

$$\mathcal{L}_{Yuk} = -\lambda_{ij}^u \bar{Q}_i \tilde{H} U_j - \lambda_{ij}^d \bar{Q}_i H D_j - \lambda_{ij}^e \bar{L}_i H E_j + \text{h.c.} \tag{I.56}$$

Now, for simplicity let us work in the unitary gauge, thus after SSB

$$\mathcal{L}_{Yuk} = -\frac{1}{\sqrt{2}}(v+h)\left[\lambda_{ij}^u \bar{U}_{iL} U_{jR} + \lambda_{ij}^d \bar{D}_{iL} D_{jR} + \lambda_{ij}^e \bar{E}_{iL} E_{jR} + \text{h.c.}\right]. \tag{I.57}$$

Then, there appear the fermion-mass matrices $M^u = \frac{v}{\sqrt{2}}\lambda^u$, $M^d = \frac{v}{\sqrt{2}}\lambda^d$ and $M^e = \frac{v}{\sqrt{2}}\lambda^e$. We can rotate the fermionic field basis such that these matrices are diagonalized, with the eigenvalues being the real and positive masses m_f. Therefore:

$$\begin{aligned}\mathcal{L}_{Yuk} = \left(1 + \frac{h}{v}\right)\big[&m_u \bar{u}u + m_c \bar{c}c + m_t \bar{t}t + m_d \bar{d}d + m_u \bar{s}s + m_b \bar{b}b \\ &m_e \bar{e}e + m_\mu \bar{\mu}\mu + m_\tau \bar{\tau}\tau\big]. \end{aligned} \tag{I.58}$$

With this, it is readily visible the Yukawa interactions between the Higgs and different fermions, being the coupling proportional to the mass of the given fermion, as is shown in the figure [I.4]. There is another important remark: the flavor-changing interaction terms, appearing in the Lagrangian of Eq. [I.50], are manifestly modified by the field-basis change used to diagonalize the mass matrices. To see this, we take the change of the field basis to be $U_L' = L^u U_L$ and $D_L' = L^d D_L$, then $\bar{U}_L \gamma^\mu D_L = \bar{U}_L' L^u \gamma^\mu L^{d\dagger} D_L' = \bar{U}_L' \gamma^\mu V_{CKM} D_L'$, where $V_{CKM} \equiv L^u L^{d\dagger}$

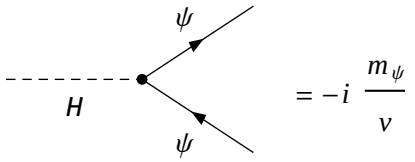

Figure I.4: Yukawa interaction between Higgs boson and fermions.

is the Cabibbo-Kobayashi-Maskawa (CKM) mixing matrix. Hence,

$$\mathcal{L}^{kin}_{Fermion} \subset -\frac{g}{\sqrt{2}} W^+_\mu \left(\begin{array}{ccc} \bar{u}', & \bar{c}', & \bar{t}' \end{array} \right)_L \left(\begin{array}{ccc} V_{ud} & V_{us} & V_{ub} \\ V_{cd} & V_{cs} & V_{cb} \\ V_{td} & V_{ts} & V_{tb} \end{array} \right) \gamma^\mu \left(\begin{array}{c} d' \\ s' \\ b' \end{array} \right)_L + \text{h.c.} \tag{I.59}$$

The CKM matrix can be parametrized through three angles and one complex phase that takes into account CP violation.

I.7 Entire Standard Model Lagrangian

The full Lagrangian of the SM is then given by adding up the different Lagrangians listed in the previous sections:

$$\mathcal{L}_{SM} \quad = \quad \mathcal{L}^{YM}_{QCD} + \mathcal{L}_{Higgs} + \mathcal{L}_{EW} + \mathcal{L}_{R_\xi} + \mathcal{L}_{Ghost} + \mathcal{L}^{kin}_{Fermion} + \mathcal{L}_{Yuk}. \tag{I.60}$$

The fermionic fields contained in this Lagrangian transform under $SU(3)_C \times SU(2)_L \times U(1)_Y$ as

$$Q_i \sim \left(3, 2, \frac{1}{3}\right), \quad U_i \sim \left(3, 1, \tfrac{4}{3}\right), \quad D_i \sim \left(3, 1, -\frac{2}{3}\right), \tag{I.61}$$

$$L_i \sim (1, 2, -1), \quad E_i \sim (1, 1, -2), \quad H \sim (1, 2, 1). \tag{I.62}$$

The Standard Model is determined by a total of 18 parameters: there are 3 gauge couplings, 2 constants from the Higgs potential, 3 lepton masses, 6 quark masses and 4 CKM parameters. Thus, we must choose the best 18 measured quantities that allow us to determine the full set of parameters. So far, in the context of the SM, all the fermion masses are known, as well as the CKM parameters, obtained from flavor physics experiments. The parameters of the Higgs sector have been measured through the Higgs mass and the VEV, the latter known through EW relations.

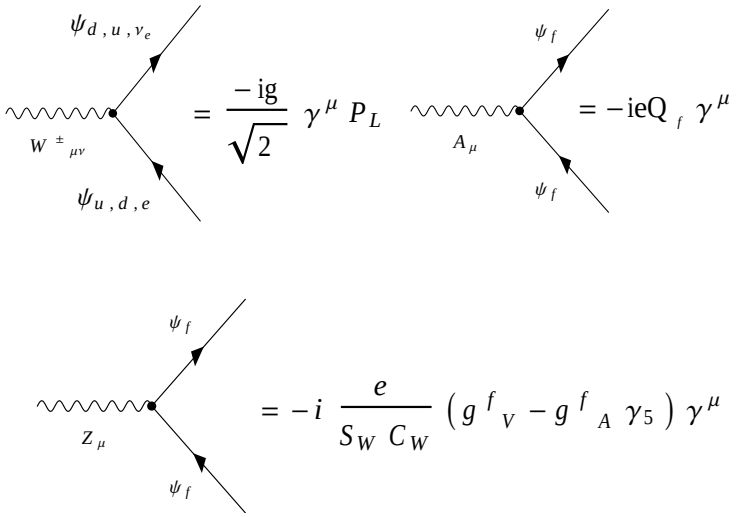

Figure I.5: Electroweak interactions for fermions.

The best-measured quantities in the SM are

$$\begin{aligned}
\text{Electron magnetic moment :} \quad & \tfrac{g_e-2}{2} &&= (1159.65218091 \pm 0.00000026) \times 10^{-6}, \\
\text{Muon lifetime :} \quad & \tau_\mu^{-1} &&= 2.99588(1) \times 10^{-19}\ \text{GeV}, \\
\text{Z pole mass :} \quad & m_Z &&= 91.1876 \pm 0.0021\ \text{GeV},
\end{aligned}$$

where the first two are measured at rest. The Z pole mass is measured at the electroweak scale, $\sqrt{s} = m_Z$. We also have

$$\begin{aligned}
\text{Z decay width :} \quad & \Gamma_Z &&= 2.4952 \pm 0.0023\ \text{GeV}, \\
\text{Z asymmetry :} \quad & A_e &&= \frac{\sigma\left(e_L^+ e_L^- \to Z\right) - \sigma\left(e_R^+ e_R^- \to Z\right)}{\sigma\left(e_L^+ e_L^- \to Z\right) + \sigma\left(e_R^+ e_R^- \to Z\right)} = 0.1515 \pm 0.0019, \\
\text{W pole mass :} \quad & m_W &&= 80.385 \pm 0.015\ \text{GeV},
\end{aligned}$$

which are measured at the electroweak scale. The electric magnetic moment gives the fine-structure constant through the 1-loop relation $g_e - 2 = \frac{\alpha(0)}{\pi}$, so that $\alpha^{-1}(0) = 137.035999139(31)$. The muon lifetime enables the determination of the Fermi constant (G_F) by using the formula $\Gamma_\mu = \frac{G_F^2 m_\mu^5}{192\pi^3}$, yielding $1.1663787(6) \times 10^{-5}\ \text{GeV}^{-2}$. The last result unveils the value of the VEV since $\frac{G_F}{\sqrt{2}} = \frac{g^2}{8m_W^2} = \frac{1}{2v^2}$, hence $v = 246\,\text{GeV}$. The weak mixing angle is measured through asymmetries in some processes, for example $e^+e^- \to \mu^+\mu^-$ forward-backward asymmetry and neutrino-electron processes, so that $s_W^2 = 0.23129(5)$ at $\sqrt{s} = m_Z$. Once some SM parameters are known, we can make some predictions about other parameters. For instance, we can predict through the formula

$m_W = \frac{ev}{2s_W}$ that at tree-level $m_W = 79.794\,\text{GeV}$, and similarly, at tree-level $A_e = 0.1252$. These predictions are close to the measured values, but can be improved by including radiative corrections. This motivates the important high precision program of electroweak observables[18][19].

Chapter II

New physics

In this chapter, it is briefly discussed why the Standard Model (SM), presented in the Chapter [I], is incomplete, and why it is needed a new underlying theory. Also, a discussion of effective extensions of the SM is made.

II.1 Why physics beyond the Standard Model?

Despite the fact that the SM of particles has been broadly tested, showing an unprecedented accuracy on its predictions, there are several experimental facts that escape to its scope, which have led us to the conclusion that this theory should be extended in order to take account for those experimental results. In the following a brief discussion of some of such phenomena is done.

II.1.1 Gravity

So far, it is well known that in our universe there are four fundamental interactions that dictate its dynamics. Three of them are described within the frame of the SM, they being the electromagnetic, the strong and the weak interactions. The remaining interaction, gravity, is not contained in the description given by the SM. For the predictions made in the SM, it is not so relevant the inclusion of gravity due to its weakness at the scales where experiments are made in particle colliders, which explains the fact that excellent predictions can be done without taking into account gravity.

Our knowledge of gravitational interactions comes from the theory of general relativity, which is not a quantum theory. With this in mind, it is expected that new physics should appear at scales where a quantum description

of gravity should be needed, and at scales where the strength of this interaction can have effects on our measurements, i.e. at the Planck scale $M_P = \sqrt{\frac{\hbar c}{G_N}} = 1.22093(7) \times 10^{19}\text{GeV}/c^2$.

Below the Planck scale, the effects of gravity are completely negligible. This fact has been shown through an effective quantum version of gravity, which is valid up to the Planck scale. In such description, the leading corrections to general relativity come from very weak couplings with a typical strength of $\sim 10^{-40}$, at a distance of one fermi[20].

II.1.2 Cosmological Constant Problem and Dark Matter

Through the different collaborations in cosmological observations, it has been observed that the SM gives a description of roughly 5% of the energy present in our universe. Actually, it is well known that, the present-day density parameter of the vacuum is $\Omega_v = 0.68 \pm 0.02$, and the present-day density parameter of the pressureless matter is $\Omega_m = 0.32 \pm 0.01$, for a universe spatially flat[15] (The updated measurements for the cosmological parameters given by the Planck collaboration can be found in [21]). The energy stored in the vacuum has been called as dark energy, and as is shown by Ω_v. Our present-day universe is dominated by such vacuum energy. This constituent of our universe represents one of the current greatest puzzles in physics, since the measurements of the cosmological constant conclude that it is many orders of magnitude smaller than the expected value from the SM[22].

In addition to this, about of 26% of the composition of the universe corresponds the so-called dark matter, i.e. non-luminous and non-absorbing matter, which is also not described by the SM. The existence of dark matter is well established from the measurement of galactic rotation curves, gravitational lensing and anisotropy of the cosmic microwave background (CMB)[23]. On the other hand, the actual nature of the dark matter remains to be unveiled, even though, we already have much information about its features. For instance, from analysis of structure formation in the universe, it is known that the most of the dark matter should be cold, i.e. should be non-relativistic.

In order to characterize the nature of the dark matter, it should be taken into account that the candidates to compose non-baryonic dark matter must be stable on cosmological time scales, as well as very weakly interacting with electromagnetic radiation, and must reproduce the known relic density. Among the candidates we can find sterile neutrinos (massive neutrinos that are also $SU(2)_L \times U(1)_Y$ singlets), gravitinos, axions, weakly interacting massive particles (so-called WIMPs) and primordial black holes.

II.1.3 Neutrino Masses

The observation of neutrino oscillations is understood as the mixing phenomenon between flavor eigenstates (N_e, N_μ, N_τ) due to the fact that it can be chosen other basis $N_\alpha = \sum_i U_{\alpha i} N_i$, that describes the mass states for the neutrinos, with α running in the flavors and $i = 1, 2, 3$ the mass eigenstates. Thus, in the simplest case of two flavors, the probabilities for a flavor change in a neutrino's journey through a distance x is

$$P_{change}(x) \quad = \quad \sin^2 2\theta \sin^2\left(\frac{|\Delta m^2|}{4E} x\right), \tag{II.1}$$

with $|\Delta m^2| = |m_1^2 - m_2^2|$, and where θ parametrizes the change of the basis. From this, it is remarkable that we can only measure the difference between masses, not absolute values. This last feature yields different possible hierarchies for the neutrino masses. Usually, we refer as normal and inverted hierarchies when $\Delta m^2 > 0$ and $\Delta m^2 < 0$, respectively.

In analogy to the CKM matrix in the quark sector, the PMNS (Pontecorvo-Maki-Nakagawa-Sakata) matrix is defined by the elements $U_{\alpha i}$, which arise in the unitary transformation for the change of basis of the neutrinos. Following this, the neutrinos coupled to charged leptons of a given flavor through the W bosons are not mass eigenstates, but a coherent superposition of mass eigenstates[25]

$$\mathcal{L}_{CC} \quad = \quad \frac{g}{\sqrt{2}} W_\mu^- \bar{L}_\alpha \gamma^\mu N_\alpha + \text{h.c.} = \frac{g}{\sqrt{2}} W_\mu^- \bar{L}_\alpha \gamma^\mu U_{\alpha i} N_i + \text{h.c.}, \tag{II.2}$$

where sum in the indices α and i is understood.

So far, there are three experimental sectors to measure the important parameters in neutrino oscillations:

1. Solar neutrinos and the reactor experiment KamLAND, sensitive mainly to Δm^2_{21} and θ_{12}. (Solar sector)
2. Atmospheric neutrino studies, K2K and MINOS accelerator experiments are sensitive to Δm^2_{23} and θ_{23}. (Atmospheric sector)
3. The CHOOZ experiment yields bounds to θ_{13} as a function of Δm^2_{31}

From such experiments it is known that the measured values for the parameters in neutrino oscillations are (Normal hierarchy)[15]

$$\Delta m^2_{21} \equiv \Delta m^2_\odot = 7.54^{+0.26}_{-0.22} \times 10^{-5}\ \text{eV}^2, \qquad \sin^2\theta_{13} = 0.0234^{+0.0020}_{-0.0019} \tag{II.3}$$

$$\Delta m^2_{32} \equiv \Delta m^2_A = (2.51 \pm 0.10) \times 10^{-3}\text{eV}^2, \qquad \sin^2\theta_{23} = 0.437^{+0.033}_{-0.023} \tag{II.4}$$

$$\delta/\pi = 1.39^{+0.38}_{-0.27}, \qquad \sin^2\theta_{12} = 0.308 \pm 0.017 \tag{II.5}$$

These results have established the necessity of an extension for the SM where it could be possible to describe massive neutrinos. In order to have massive neutrinos, it is needed the inclusion of right-handed neutrinos. In this way, it is where seesaw models arise[24][26][27]. The seesaw models are minimal extensions of the SM that add one heavy right-handed neutrino per family so that N_L and N_R can form a mass term that is similar to those for charged leptons and quarks. Since the right-handed neutrinos are colorless and singlets under $SU(2)_L$ with hypercharge zero, their kinetic terms are of the form $\bar{N}_R \partial\!\!\!/ N_R$. Therefore, the mass terms of the neutrinos (with one flavor) can be obtained after spontaneous symmetry breaking from

$$\mathcal{L}_{seesaw} = Y_D \bar{L}_e \tilde{H} N_R + \frac{M_R}{2} N_R^T C N_R + \text{h.c.}, \tag{II.6}$$

without a spoiling of the gauge symmetries of the usual SM. From this Lagrangian, it is not difficult to see that the smaller the mass of the light neutrino is, the bigger the mass of the heavy neutrino becomes. The latter feature gives the name for this mechanism.

The main goals in neutrino physics are

1. To determine the individual values of the neutrino masses.
2. To determine whether they are Majorana-like.
3. To discover Leptonic CP-violation.

II.1.4 Additional open problems

In addition to the above mentioned open problems, currently, there are other issues of big interest in particle physics. The strong CP poblem and the matter-antimatter asymmetry are of remarkable importance.

II.2 Physics BSM in an effective approach

In order to discover physics beyond the Standard Model, one could go in two ways: first, seek new matter particles, or second, looking for unknown interactions between the already known particles. The Standard Model extended through effective interactions lies in the latter situation, and can be seen as a way to parametrize the unknown physics, through the known matter fields.

Following the discussion in the previous sections, we know that there should be some new physics at energies above the scale of the electroweak spontaneous symmetry breaking. Whichever be the theory that successes in solving the current problems in high energy physics, we can consider that it is possible to integrate out the

unknown degrees of freedom, so that the respective effective field theory (EFT) is left only with the Standard Model particle content. The quantum field theory obtained through this procedure stands up to a scale (Λ), at which we are able to see the new particles.

In this construction, it is important the fact that the $SU(2)_L \times U(1)_Y$ symmetry is spontaneously broken for energies below the Higgs mass, while holds for energies above such mass. Thus, the interactions in the effective field theory must respect the full gauge symmetry of the SM.

As well, another condition that can be taken into account is the fact that if we remove the cutoff by doing $\Lambda \to \infty$, the remaining theory should be the Standard Model. The SM does only contain renormalizable operators. In the scheme of an EFT, the absence of non-renormalizable operators in the SM is understood from the fact that the new interactions are proportional to factors of $\frac{1}{\Lambda}$, being suppressed as the scale for new physics is sufficiently above.

The dominant effective interactions are expected to be of order $\mathcal{O}(\frac{1}{\Lambda})$. For one generation of fermions, there is only one operator, which leads to mass terms for the neutrinos, and corresponds to an effective term coming from underlying theories. All the operators of dimension five violate lepton and(or) baryon number, and actually, any odd-dimensional operator does not respect the conservation of lepton and baryon number[28].

When we go on, the dimension-six operators follow, which are $\mathcal{O}(\frac{1}{\Lambda^2})$. At this level, there are 5 different operators for one generation that violate lepton and baryon number, while there are 59 independent interactions that preserve them. The interactions that involve L and(or) B violation are highly constrained for light fermions, mainly from proton decay experiments. The interactions that do preserve such numbers are less restricted. At this point, it is clear the simplicity of the SM, which just has 14 operators for one generation.

A classic example for an EFT is the V-A model postulated by Fermi, which remains as a valid QFT up to energies close to the W boson mass. In this model, weak interactions were postulated as touch interactions between two currents, where the corresponding term in the action is of order six and the coupling constant is given by $\frac{G_F}{\sqrt{2}} = \frac{g^2}{8m_W^2}$. Here, it is remarkable that, in this model, the action describes the effective interactions, but the Fermi constant does not give information about the new energy scale, just the ratio between the strength of the underlying interaction (g) and the new energy scale (m_W), which individuals values just can be known through the underlying theory.

The above facts for the Fermi model are general facts and serve as a guide to build an effective extension of the SM. Thus, we start by expanding the possible new interactions in terms of SM degrees of freedom, as

$$\mathcal{L}_{SM}^{eff} = \mathcal{L}_{SM} + \sum_i \frac{c_i}{\Lambda}\mathcal{O}_i^{(5)} + \sum_i \frac{c_i}{\Lambda^2}\mathcal{O}_i^{(6)} + \dots \tag{II.7}$$

In the above equation we can have effective operators of dimension 5, 6,... and so on, multiplied by adimensional coefficients, named Wilson coefficients, and divided by powers of the cutoff energy in a consistent way, so that the mass dimension of the Lagrangian remains to be 4. In this fashion, the ratio between Wilson coefficients and the new scale energy is restricted by experimental values, as in the case of the Fermi constant. When we are interested in an analysis preserving lepton and baryon number, some Wilson coefficients are set to zero. For instance, the only dimension-five operator that is allowed by the SM symmetry is the operator

$$Q_{\nu\nu} = (\widetilde{H}^\dagger L_p)^T C(\widetilde{H}^\dagger L_r), \tag{II.8}$$

known as the Weinberg operator, but by imposing lepton number conservation its contribution vanishes. Above, r and p stand for generation indices. It also can be observed that by integrating out the right-handed degrees of freedom in $\mathcal{L}_{seesaw}$ in Eq. [II.6], the effective operator $Q_{\nu\nu}$ is yielded.

Now, let us think about the possibility of having a fundamental interaction between fermions of the Standard Model mediated by some new vectorial boson X. We are not able to see this boson at energies below its mass, but we can see some of its effects indirectly as 4-fermion interactions. Thus, in the effective Lagrangian, such effects of the X boson, will appear through dimension-6 operators with four fermionic fields. We can also see that this dimension-6 operator comes from a process between four fermions mediated by the X boson, then from its propagator arises a factor $\frac{1}{m_X^2}$ at energies much below the boson mass. Hence, it is identified the factor $\frac{1}{m_X^2} \sim \frac{1}{\Lambda^2}$.

The main advantage of this approach is the model-independence of the procedure. The new physics implies new interactions between the already known particles. With this, we are able to study these effects without a full fundamental description in this EFT approach. Currently, there is no evidence for the existence of a dimension-6 operator for the Standard Model. Instead, some bounds for combinations of the coefficients in Eq. [II.7] are known.

With the fields of the Standard Model is possible to construct a total of 80 dimension-6 operators, as was shown by Buchmüller and Wyler in 1986[29]. After that, some works presented equivalences between some operators[30], i.e. not all of the 80 operators are linearly independent. In the end, taking away all the redundancies, stands a set of 59 independent operators, mentioned before. Another possible dimension-6 operator can be obtained by means of the equations of motion, integration by parts, Fierz identities or by a suitable redefinition of the fields. The first work presenting the full reduced list of operators was Ref. [62], where Grzadkowski et al published an updated list of the effective operators.

There are different ways of choosing a given basis that allows the parametrization of new physics. Currently, there is no convention for a preferred basis, so that we can find different options, such that, according to

X^3		φ^6 and $\varphi^4 D^2$		$\psi^2\varphi^3$	
Q_G	$f^{ABC}G_\mu^{A\nu}G_\nu^{B\rho}G_\rho^{C\mu}$	Q_φ	$\left(H^\dagger H\right)^3$	$Q_{e\varphi}$	$\left(H^\dagger H\right)\left(\bar{L}_p E_r H\right)$
$Q_{\widetilde{G}}$	$f^{ABC}\widetilde{G}_\mu^{A\nu}G_\nu^{B\rho}G_\rho^{C\mu}$	$Q_{\varphi\Box}$	$\left(H^\dagger H\right)\Box\left(H^\dagger H\right)$	$Q_{u\varphi}$	$\left(H^\dagger H\right)\left(\bar{Q}_p U_r \widetilde{H}\right)$
Q_W	$\varepsilon^{IJK}W_\mu^{I\nu}W_\nu^{J\rho}W_\rho^{K\mu}$	$Q_{\varphi D}$	$\left(H^\dagger D^\mu H\right)^*\left(H^\dagger D_\mu H\right)$	$Q_{d\varphi}$	$\left(H^\dagger H\right)\left(\bar{Q}_p D_r H\right)$
$Q_{\widetilde{W}}$	$\varepsilon^{IJK}\widetilde{W}_\mu^{I\nu}W_\nu^{J\rho}W_\rho^{K\mu}$				

$X^2\varphi^2$		$\psi^2 X\varphi$		$\psi^2\varphi^2 D$	
$Q_{\varphi G}$	$H^\dagger H G_{\mu\nu}^A G^{A\mu\nu}$	Q_{eW}	$\left(\bar{L}_p\sigma^{\mu\nu}E_r\right)\tau^I H W_{\mu\nu}^I$	$Q_{\varphi l}^{(1)}$	$\left(H^\dagger i\overleftrightarrow{D}_\mu H\right)\left(\bar{L}_p\gamma^\mu L_r\right)$
$Q_{\varphi\widetilde{G}}$	$H^\dagger H\widetilde{G}_{\mu\nu}^A G^{A\mu\nu}$	Q_{eB}	$\left(\bar{L}_p\sigma^{\mu\nu}E_r\right)H B_{\mu\nu}$	$Q_{\varphi l}^{(3)}$	$\left(H^\dagger i\overleftrightarrow{D}_\mu^I H\right)\left(\bar{L}_p\tau^I\gamma^\mu L_r\right)$
$Q_{\varphi W}$	$H^\dagger H W_{\mu\nu}^I W^{I\mu\nu}$	Q_{uG}	$\left(\bar{Q}_p\sigma^{\mu\nu}T^A U_r\right)\widetilde{H}G_{\mu\nu}^A$	$Q_{\varphi e}$	$\left(H^\dagger i\overleftrightarrow{D}_\mu H\right)\left(\bar{E}_p\gamma^\mu E_r\right)$
$Q_{\varphi\widetilde{W}}$	$H^\dagger H\widetilde{W}_{\mu\nu}^I W^{I\mu\nu}$	Q_{uW}	$\left(\bar{Q}_p\sigma^{\mu\nu}U_r\right)\tau^I\widetilde{H}W_{\mu\nu}^I$	$Q_{\varphi q}^{(1)}$	$\left(H^\dagger i\overleftrightarrow{D}_\mu H\right)\left(\bar{Q}_p\gamma^\mu Q_r\right)$
$Q_{\varphi B}$	$H^\dagger H B_{\mu\nu}B^{\mu\nu}$	Q_{uB}	$\left(\bar{Q}_p\sigma^{\mu\nu}U_r\right)\widetilde{H}B_{\mu\nu}$	$Q_{\varphi q}^{(3)}$	$\left(H^\dagger i\overleftrightarrow{D}_\mu^I H\right)\left(\bar{Q}_p\tau^I\gamma^\mu Q_r\right)$
$Q_{\varphi\widetilde{B}}$	$H^\dagger H\widetilde{B}_{\mu\nu}B^{\mu\nu}$	Q_{dG}	$\left(\bar{Q}_p\sigma^{\mu\nu}T^A D_r\right)H G_{\mu\nu}^A$	$Q_{\varphi u}$	$\left(H^\dagger i\overleftrightarrow{D}_\mu H\right)\left(\bar{U}_p\gamma^\mu U_r\right)$
$Q_{\varphi WB}$	$H^\dagger\tau^I H W_{\mu\nu}^I B^{\mu\nu}$	Q_{dW}	$\left(\bar{Q}_p\sigma^{\mu\nu}D_r\right)\tau^I H W_{\mu\nu}^I$	$Q_{\varphi d}$	$\left(H^\dagger i\overleftrightarrow{D}_\mu H\right)\left(\bar{D}_p\gamma^\mu D_r\right)$
$Q_{\varphi\widetilde{W}B}$	$H^\dagger\tau^I H\widetilde{W}_{\mu\nu}^I B^{\mu\nu}$	Q_{dB}	$\left(\bar{Q}_p\sigma^{\mu\nu}D_r\right)H B_{\mu\nu}$	$Q_{\varphi ud}$	$\left(\widetilde{H}^\dagger D_\mu H\right)\left(\bar{U}_p\gamma^\mu D_r\right)$

$(\bar{L}L)\,(\bar{L}L)$		$(\bar{R}R)\,(\bar{R}R)$		$(\bar{L}L)\,(\bar{R}R)$	
Q_{ll}	$\left(\bar{L}_p\gamma_\mu L_r\right)\left(\bar{L}_s\gamma^\mu L_t\right)$	Q_{ee}	$\left(\bar{E}_p\gamma_\mu E_r\right)\left(\bar{E}_s\gamma^\mu E_t\right)$	Q_{le}	$\left(\bar{L}_p\gamma_\mu L_r\right)\left(\bar{E}_s\gamma^\mu E_t\right)$
$Q_{qq}^{(1)}$	$\left(\bar{Q}_p\gamma_\mu Q_r\right)\left(\bar{Q}_s\gamma^\mu Q_t\right)$	Q_{uu}	$\left(\bar{U}_p\gamma_\mu U_r\right)\left(\bar{U}_s\gamma^\mu U_t\right)$	Q_{lu}	$\left(\bar{L}_p\gamma_\mu L_r\right)\left(\bar{U}_s\gamma^\mu U_t\right)$
$Q_{qq}^{(3)}$	$\left(\bar{Q}_p\gamma_\mu\tau^I Q_r\right)\left(\bar{Q}_s\gamma^\mu\tau^I Q_t\right)$	Q_{dd}	$\left(\bar{D}_p\gamma_\mu D_r\right)\left(\bar{D}_s\gamma^\mu D_t\right)$	Q_{ld}	$\left(\bar{L}_p\gamma_\mu L_r\right)\left(\bar{D}_s\gamma^\mu D_t\right)$
$Q_{lq}^{(1)}$	$\left(\bar{L}_p\gamma_\mu L_r\right)\left(\bar{Q}_s\gamma^\mu Q_t\right)$	Q_{eu}	$\left(\bar{E}_p\gamma_\mu E_r\right)\left(\bar{U}_s\gamma^\mu U_t\right)$	Q_{qe}	$\left(\bar{Q}_p\gamma_\mu Q_r\right)\left(\bar{E}_s\gamma^\mu E_t\right)$
$Q_{lq}^{(3)}$	$\left(\bar{L}_p\gamma_\mu\tau^I l_r\right)\left(\bar{Q}_s\gamma^\mu\tau^I Q_t\right)$	Q_{ed}	$\left(\bar{E}_p\gamma_\mu E_r\right)\left(\bar{D}_s\gamma^\mu D_t\right)$	$Q_{qu}^{(1)}$	$\left(\bar{Q}_p\gamma_\mu Q_r\right)\left(\bar{U}_s\gamma^\mu U_t\right)$
		$Q_{ud}^{(1)}$	$\left(\bar{U}_p\gamma_\mu U_r\right)\left(\bar{D}_s\gamma^\mu D_t\right)$	$Q_{qu}^{(8)}$	$\left(\bar{Q}_p\gamma_\mu T^A Q_r\right)\left(\bar{U}_s\gamma^\mu T^A U_t\right)$
		$Q_{ud}^{(8)}$	$\left(\bar{U}_p\gamma_\mu T^A U_r\right)\left(\bar{D}_s\gamma^\mu T^A D_t\right)$	$Q_{qd}^{(1)}$	$\left(\bar{Q}_p\gamma_\mu Q_r\right)\left(\bar{D}_s\gamma^\mu D_t\right)$
				$Q_{qd}^{(8)}$	$\left(\bar{Q}_p\gamma_\mu T^A Q_r\right)\left(\bar{D}_s\gamma^\mu T^A D_t\right)$

$(\bar{L}R)\,(\bar{R}L)$ and $(\bar{L}R)\,(\bar{L}R)$		B-violating	
Q_{ledq}	$\left(\bar{L}_p^j E_r\right)\left(\bar{D}_s Q_t^j\right)$	Q_{duq}	$\varepsilon^{\alpha\beta\gamma}\varepsilon_{jk}\left[\left(D_p^\alpha\right)^T C U_r^\beta\right]\left[\left(Q_s^{\gamma j}\right)^T C L_t^k\right]$
$Q_{quqd}^{(1)}$	$\left(\bar{Q}_p^j U_r\right)\varepsilon_{jk}\left(\bar{Q}_s^k D_t\right)$	Q_{qqu}	$\varepsilon^{\alpha\beta\gamma}\varepsilon_{jk}\left[\left(Q_p^{\alpha j}\right)^T C Q_r^{\beta k}\right]\left[\left(U_s^\gamma\right)^T C E_t\right]$
$Q_{quqd}^{(8)}$	$\left(\bar{Q}_p^j T^A U_r\right)\varepsilon_{jk}\left(\bar{Q}_s^k T^A D_t\right)$	Q_{qqq}	$\varepsilon^{\alpha\beta\gamma}\varepsilon_{jn}\varepsilon_{km}\left[\left(Q_p^{\alpha j}\right)^T C Q_r^{\beta k}\right]\left[\left(Q_s^{\gamma m}\right)^T C L_t^n\right]$
$Q_{lequ}^{(1)}$	$\left(\bar{L}_p^j E_r\right)\varepsilon_{jk}\left(\bar{Q}_s^k U_t\right)$	Q_{duu}	$\varepsilon^{\alpha\beta\gamma}\left[\left(D_p^\alpha\right)^T C U_r^\beta\right]\left[\left(U_s^\gamma\right)^T C E_t\right]$
$Q_{lequ}^{(3)}$	$\left(\bar{L}_p^j\sigma_{\mu\nu}E_r\right)\varepsilon_{jk}\left(\bar{Q}_s^k\sigma^{\mu\nu}U_t\right)$		

Table II.1: Dimension-6 independent effective operators. The top table shows 34 operators that take into account interactions involving bosons, while in the bottom table there are 29 operators describing four-fermion interactions. Without the 4 B-violating operators, remain 59 independent operators described in Ref. [62]

our necessities, we can choose one of those. The reduced list mentioned above is usually referred as Warsaw basis[62]. The full set of operators in the Warsaw basis is listed in table [II.2]. There, the generation and color indices are denoted by $p = 1, 2, 3$ and $\alpha = 1, 2, 3$, respectively, while the $SU(2)_L$ index appears as $j = 1, 2$. The generators of the $SU(3)_c$ and $SU(2)_L$ groups are $T^A = \frac{1}{2}\lambda^A$ and $S^I = \frac{1}{2}\tau^I$, respectively, with λ^A the Gell-Mann matrices and τ^I the Pauli matrices. Also, in this part, the convention is such that Q_r (r being the generation index) stands for the isospin doublets, which are made up of left-handed quarks, and L_r the isospin doublets of left-handed leptons; the U_r, D_r and E_r correspond to right-handed components. The duals of the strength field tensors are defined as $\widetilde{X}_{\mu\nu} = \frac{1}{2}\varepsilon_{\mu\nu\rho\sigma}X^{\rho\sigma}$. The hermitian derivatives are defined as:

$$H^\dagger i\overset{\leftrightarrow}{D}_\mu H \equiv H^\dagger i\left(D_\mu - \overset{\leftarrow}{D}_\mu\right)H, \qquad H^\dagger i\overset{\leftrightarrow}{D}{}^I_\mu H \equiv H^\dagger i\left(\tau^I D_\mu - \overset{\leftarrow}{D}_\mu\tau^I\right)H. \tag{II.9}$$

In the table [II.1], the purely bosonic operators are all hermitian. In the same table, the operators containing $\widetilde{X}_{\mu\nu}$, with X being the dual to a strength field tensor, are the only CP-odd operators involving bosons. For the operators involving currents of fermions (which are written in brackets), with fields of the same chirality, the hermitian conjugate corresponds to exchanging the generation indices. For the other operators the hermitian conjugates were not written.

Among the other possible bases, we find a basis that maximizes the number of operators describing interactions between electroweak bosons and the Higgs field, then, in this way, the works in Ref. [31] are useful. After the discovery of the Higgs boson, some modified bases were published, giving an updated lists, as for instance Ref. [32]. The latter basis presents an interesting feature: it is possible to identify if the new physics is of strong character or not.

In the following section, we will see the hierarchy paradox in particle physics, but now we anticipate that supersymmetric theories and compositeness are among the possible scenarios that would provide a solution. The advantage of the approach presented in Ref. [32] is that, it is possible to identify if the new physics correspond to a compositeness model (where the Higgs boson turns out to be a composite state in the fundamental theory) or not.

In the development of the basis in Ref. [32], it was very important the work done in Ref. [33]. In the latter, it is studied the situation in which the Higgs field arises as a pseudo-Goldstone boson from a strongly-interacting sector. Also, it was shown an effective approach for the scenario of a light composite Higgs in analogy to the Chiral effective theory. Through such analysis, the SILH (Strongly-Interacting Light Higgs) Lagrangian can be

reached, which looks like

$$\begin{aligned}\Delta\mathcal{L}_{SILH} &= \frac{\bar{c}_H}{2v^2}\partial^\mu\left(H^\dagger H\right)\partial_\mu\left(H^\dagger H\right)+\frac{\bar{c}_T}{2v^2}\left(H^\dagger\overleftrightarrow{D^\mu}H\right)\left(H^\dagger\overleftrightarrow{D}_\mu H\right)-\frac{\bar{c}_6\lambda}{v^2}\left(H^\dagger H\right)^3\\ &+\left(\left(\frac{\bar{c}_u}{v^2}y_u H^\dagger H\bar{Q}H^c U+\frac{\bar{c}_d}{v^2}y_d H^\dagger H\bar{Q}HD+\frac{\bar{c}_l}{v^2}y_l H^\dagger H\bar{L}HE\right)+h.c.\right)\\ &+\frac{i\bar{c}_W g}{2m_W^2}\left(H^\dagger\sigma^i\overleftrightarrow{D^\mu}H\right)\left(D^\nu W_{\mu\nu}\right)^i+\frac{i\bar{c}_B g'}{2m_W^2}\left(H^\dagger\overleftrightarrow{D^\mu}H\right)\left(\partial^\nu B_{\mu\nu}\right)\\ &+\frac{i\bar{c}_{HW}g}{m_W^2}\left(D^\mu H\right)^\dagger\sigma^i\left(D^\nu H\right)W^i_{\mu\nu}+\frac{i\bar{c}_{HB}g'}{m_W^2}\left(D^\mu H\right)^\dagger\left(D^\nu H\right)B_{\mu\nu}\\ &+\frac{\bar{c}_\gamma g'^2}{m_W^2}H^\dagger H B_{\mu\nu}B^{\mu\nu}+\frac{\bar{c}_g g_S^2}{m_W^2}H^\dagger H G^a_{\mu\nu}G^{a\mu\nu}.\end{aligned}\tag{II.10}$$

Here, some operators readily equivalent to those shown in the top of the table [II.2] can be seen. Precisely are these operators that enter in the basis defined in Ref. [32]. This last basis is suitable for Higgs physics. In such basis, the effective Lagrangian reads,

$$\mathcal{L} = \mathcal{L}_{SM}+\sum_i \bar{c}_i\mathcal{O}_i \equiv \mathcal{L}_{SM}+\Delta\mathcal{L}_{SILH}+\Delta\mathcal{L}_{F_1}+\Delta\mathcal{L}_{F_2},\tag{II.11}$$

where $\Delta\mathcal{L}_{SILH}$ was already defined, and with

$$\begin{aligned}\Delta\mathcal{L}_{F_1} &= \frac{i\bar{c}_{Hq}}{v^2}\left(\bar{Q}\gamma^\mu Q\right)\left(H^\dagger\overleftrightarrow{D}_\mu H\right)+\frac{i\bar{c}'_{Hq}}{v^2}\left(\bar{Q}\gamma^\mu\sigma^i Q\right)\left(H^\dagger\sigma^i\overleftrightarrow{D}_\mu H\right)\\ &+\frac{i\bar{c}_{Hu}}{v^2}\left(\bar{U}\gamma^\mu U\right)\left(H^\dagger\overleftrightarrow{D}_\mu H\right)+\frac{i\bar{c}_{Hd}}{v^2}\left(\bar{D}\gamma^\mu D\right)\left(H^\dagger\overleftrightarrow{D}_\mu H\right)\\ &+\left(\frac{i\bar{c}_{Hud}}{v^2}\left(\bar{U}\gamma^\mu D\right)\left(H^{c\dagger}\overleftrightarrow{D}_\mu H\right)+h.c\right)\\ &+\frac{i\bar{c}_{HL}}{v^2}\left(\bar{L}\gamma^\mu L\right)\left(H^\dagger\overleftrightarrow{D}_\mu H\right)+\frac{i\bar{c}'_{HL}}{v^2}\left(\bar{L}\gamma^\mu\sigma^i L\right)\left(H^\dagger\sigma^i\overleftrightarrow{D}_\mu H\right)\\ &+\frac{i\bar{c}_{Hl}}{v^2}\left(\bar{E}\gamma^\mu E\right)\left(H^\dagger\overleftrightarrow{D}_\mu H\right),\end{aligned}\tag{II.12}$$

$$\begin{aligned}\Delta\mathcal{L}_{F_2} =& \frac{\bar{c}_{uB}g'}{m_W^2}y_u\bar{Q}H^c\sigma^{\mu\nu}UB_{\mu\nu}+\frac{\bar{c}_{uW}g}{m_W^2}y_u\bar{Q}\sigma^i H^c\sigma^{\mu\nu}UW^i_{\mu\nu}+\frac{\bar{c}_{uG}g_S}{m_W^2}y_u\bar{Q}H^c\sigma^{\mu\nu}\lambda^a UG^a_{\mu\nu}\\ &+\frac{\bar{c}_{dB}g'}{m_W^2}y_d\bar{Q}H\sigma^{\mu\nu}DB_{\mu\nu}+\frac{\bar{c}_{dW}g}{m_W^2}y_d\bar{Q}\sigma^i H\sigma^{\mu\nu}DW^i_{\mu\nu}+\frac{\bar{c}_{dG}g_S}{m_W^2}y_d\bar{Q}H\sigma^{\mu\nu}\lambda^a DG^a_{\mu\nu}\\ &+\frac{\bar{c}_{lB}g'}{m_W^2}y_l\bar{L}H\sigma^{\mu\nu}EB_{\mu\nu}+\frac{\bar{c}_{lW}g}{m_W^2}y_l\bar{L}\sigma^i H\sigma^{\mu\nu}LW^i_{\mu\nu}+h.c.\end{aligned}\tag{II.13}$$

By counting, we note that the leading operators in Higgs physics are given by a set of $12+8+8=28$ operators. When this basis is compared to the Warsaw one, it is noted that in order to have a complete set of operators, there must be added the 25 four-fermion operators, and 2 X^3-like operators for the strength tensors of the $SU(3)_c$ and $SU(2)_L$ groups. It must be noted that, in the SILH basis, a CP-even Higgs is assumed, so that CP-odd terms do not appear here, thus, by relaxing the CP-condition, 6 operators can be added: $Q_{\widetilde{G}}$, $Q_{\widetilde{W}}$,

$Q_{\varphi\widetilde{W}}B$ and $Q_{\varphi\tilde{X}}$, with $X = G, W, B$. Hence, we would have a set of 61 operators, but actually, there are two redundant operators in the $\Delta\mathcal{L}_{F_1}$ Lagrangian, so that the minimal set of 59 independent operators appears.

To conclude this section, we have seen the usefulness of this EFT approach in order to get hints of new physics. It is interesting the fact that a non-renormalizable theory can be so helpful. The important issue is that we are conscious that this is a theory valid at low energies, so that the contributions of the effective operators are suppressed by positive powers of the ratio between the energy and the scale Λ (This can be seen by simple dimensional analysis), then at sufficiently low energies we do not have to worry about the full expansion in the Lagrangian, and thus the epistemological problem of dealing with a non-renormalizable theory is of no matter.

II.3 Naturalness and Hierarchy problem

Now, we have seen that the SM must be extended, and we have a model-independent approach for studying new physics. Then, we focus now on the search for the appropriate underlying and fundamental description of nature that extends the SM. In this section, a guidance in such search is discussed: the naturalness principle.

Let us first recall the main classes of symmetries relevant in quantum field theory:

- Gauge symmetries: in this class we found local symmetries, which relate different non-observable properties of the fields. This symmetries tells us that there are non-physical degrees of freedom in our descriptions.
- Global symmetries: This class of symmetries encloses accidental symmetries or accidental approximate symmetries. An example of accidental symmetries is Parity in QED, since actually Parity is violated in the electroweak model. Even though, global symmetries are normally broken they take an important role in order to understand the dynamics of the system.

We can analyze the situation where a physical system presents an underlying global symmetry, which is broken by a small interaction controlled by a given parameter. Such controlled breaking of symmetries can be reflected in the observables, modifying them. Then, these modifications are completely understood in terms of symmetries. Now, an unnatural situation happens when the experiments go in contradiction to our understanding in terms of symmetries. What could we expect in an unnatural situation? the answer is that there should be additional symmetries that were out of the starting analysis.

We can move on to unnatural situations in QFT, where it can be seen natural and unnatural mass hierarchies from the point of view of RG-flow. It can be thought that, we have an infrared physical description at some scale Λ_{IR}, and that there is new physics above some ultraviolet scale Λ_{UV}. With this, by definition, we are saying that there is a separation of scales and that nothing interesting is happening in between, i.e. there is not

any dramatical change in the dynamics. Thus, we are able to state that, in a situation where a separation of scale has been stated, the theory is almost scale-invariant. Now, we can ask, under which conditions is such a separation of scales natural?

To see this, first, let us recall the meaning of the β-function of a given coupling. It can be defined

$$t \equiv \log \frac{\Lambda_{UV}}{\mu}, \qquad \frac{d}{dt}\lambda \equiv \mu \frac{d}{d\mu}\lambda = \beta(\lambda),$$

thus, it is understood t as an RG-time, and the β-function of the coupling λ turns out to be a kind of velocity. Then, we can see that the β-function gives information of how fast some scale is reached along the RG evolution. In this sense, the naturalness of the hierarchy is just the question of the slowness of the motion in the parameter space as we move along the RG evolution. In the limit of $\beta \to 0$, the couplings do not change, or equivalently, the theory does not "move", what corresponds to a scale-invariant theory (SFT), this happens in the so-called fixed points. The smallness of the β-function in an RG-flow sense means the stability of the fixed point.

Hence, the notion of naturalness is related to the features of the β-function around a fixed point, or equivalently with the deformations of the fixed point. In this way, an unnatural case arises when the fixed point admits relevant deformations, coming from relevant operators ($d < 4$), such as a scalar mass term. In the latter case, simple dimensional analysis tells us that the corrections for the mass should be proportional to some energy scale, $m^2 \sim c\Lambda^2$, and the coefficient c should be understood in terms of symmetries. In the situation where the difference between the two scales is huge, the coefficient must be extremely small, here the problem arises when there is no explanation in terms of symmetries about such smallness.

The standard definition for the principle of naturalness, broadly used in particle physics, was given by Gerardus 't Hooft as

" *any energy scale μ, a physical parameter or a set of physical parameters $\alpha_i(\mu)$ is allowed to be very small only if the replacement $\alpha_i(\mu) = 0$ would increase the symmetry of the system*".[14]

There are some well-known situations, where the truthfulness of this principle can be seen. In QED, for instance, an enhancement in the symmetries of the theory arises when the electron is taken to be massless. The chiral symmetry $\psi \to e^{i\omega\gamma_5}\psi$, in QED, is broken just by the mass term of the electron. Hence, following the 't Hooft naturalness principle, we have that the electron mass is allowed to be small. Moreover, any quantum correction to the electron mass must respect the chiral symmetry, then, it is expected that these quantum corrections vanish in the limit $m_e \to 0$. Precisely, this is what we get by doing the complete computation:

$$m_e = m_e^{(0)} \left(1 - \frac{6\alpha}{4\pi} \log\left(\frac{m_e}{\mu}\right)\right). \tag{II.14}$$

Another interesting situation happens in QCD. We can think about the contributions to the proton mass, $m_p = 0.9382$ GeV, coming from the Planck scale, so that $m_p^2 \sim \epsilon M_P^2$. Then, it is addressed the question of the smallness of the parameter ϵ because of the huge difference between the scales. In this situation, we recall that, the masses of the quarks from which the proton is made up are very small compared to m_p, so that the mass terms of the QCD Lagrangian are negligible. Is in this situation where we have classically conformal symmetry. This symmetry is broken by quantum effects, and, is in this way, that the proton acquires the most of its mass. Therefore, the smallness of ϵ is understood in terms of the quantum breaking of the conformal symmetry. Actually, from the renormalization group of QCD, we can write for the strong coupling, α_s,

$$\frac{d\alpha_s}{dt} = -2b_0\alpha_s^2, \tag{II.15}$$

with $t = \log(M_P/\mu)$, where b_0 is a constant that could depend on the number of colors, among other factors, particularly $b_0 = 7$ in QCD. Therefore, by solving this equation, and at the scale $\mu = m_p$

$$m_p = e^{-\frac{2\pi}{b_0\alpha_s(M_P)}} M_P, \tag{II.16}$$

then, with $g_s(M_p) = 0.5$, the exponential factor is extremely small. Particularly, it is from the renormalization group analysis that the conformal symmetry is broken.

Now, we want to see the hierarchy problems in the SM. For this, we start by analyzing at which scale new physics should come.

It was defined, at the end of Section 1.3, the quantity ρ, which gives information of the similarity between the masses of the electroweak bosons. We can rewrite at tree-level the relation between these masses as $M_W^2 = (1 - s_W^2)M_Z^2$, thus we see that the difference between them is related to s_W, or equivalently to g', so that for $s_W = 0$ then $g' = 0$. This situation correspond to that when we are not taking into account the $U(1)_Y$ interaction, hence all of the three W bosons are equivalent and the term $W_\mu^a W^{a\mu}$ is $SO(3)$ invariant. We can go even deeper, to note that the four degrees of freedom of the scalar Higgs sector can be rearranged as

$$H = \begin{pmatrix} H^+ \\ H^0 \end{pmatrix} = \frac{1}{\sqrt{2}} \begin{pmatrix} \phi_1 + i\phi_2 \\ \phi_3 + i\phi_4 \end{pmatrix} \Rightarrow \Phi = \frac{1}{\sqrt{2}} \begin{pmatrix} \phi_3 - i\phi_4 & \phi_1 + i\phi_2 \\ -\phi_1 + i\phi_2 & \phi_3 + i\phi_4 \end{pmatrix}, \tag{II.17}$$

where there is an underlying invariant $\phi_1^2 + \phi_2^2 + \phi_3^2 + \phi_4^2$, which leads to a $SO(4) \simeq SU(2)_L^{Gauge} \times SU(2)_R^{Global}$ symmetry. The bi-doublet can be taken to transform as $\Phi(x) \to U_L(x)\Phi U_R^\dagger$. After symmetry breaking, it is seen $SU(2)_L \times SU(2)_R \to SU(2)_{diag}$. This remnant symmetry is the so-called custodial symmetry, that is equivalent to the $SO(3)$ symmetry mentioned before. When we do $g' \neq 0$, the global $SU(2)_R$ symmetry is broken, remaining $U(1)_Y$. Therefore, the custodial symmetry protects the relation $\rho \sim 1$. A more detailed

analysis can be found in Ref. [34].

Such protection in the ρ parameter puts strong bounds on new physics. This symmetry can be broken by the irrelevant term

$$\frac{1}{\Lambda^2}\left(H^\dagger D_\mu H\right)\left(H^\dagger D_\mu H\right), \tag{II.18}$$

from which $\delta\rho = \frac{m_W^2}{\Lambda^2}$. In order to control such violations in the custodial symmetry, we must set a sufficient big scale Λ.

On the other hand, as was discussed before, the term that leads to neutrino masses, by using the degrees of freedom of the Standard Model, is the dimension-5 Weinberg operator. Hence, the separation of scales generically implies that the charged leptons (with mass terms coming from marginal terms) are much heavier than the neutrinos. It also occurs that the accidental lepton number global symmetry could be violated. Such new term can be written as

$$\frac{Y_\nu}{\Lambda}(L^T i\sigma_2 H)C(H^T i\sigma_2 L), \tag{II.19}$$

which after electroweak symmetry breaking generates the mass-terms for the neutrinos.

Now, from the bounds set by the measurements of ρ and neutrino masses, it is concluded from our breaking of the approximate symmetries that, at least, $\Lambda_{UV} \gg$ TeV. Actually, there are more bounds measured, from the $K - \bar{K}$ mixing and the proton decay, that constraint other irrelevant operators, such as the four fermions contact interactions.

There exist a marginal operator that is not already contained in the Standard Model Lagrangian:

$$\theta\tilde{G}_{\mu\nu}G^{\mu\nu}, \tag{II.20}$$

where $G_{\mu\nu}$ is the QCD strength tensor and, as usual, $G_{\mu\nu} = \frac{1}{2}\epsilon_{\mu\nu\alpha\beta}G^{\alpha\beta}$ is its dual. This term is known to be a total derivative, thus it does not appear in the equations of motion. Despite this fact, it induces an electric dipole moment (d_n) in the neutron, a quantity that has been searched in the experiments. Current measurements yield the maximal value $d_n < 3 \times 10^{-26} e \cdot$ cm, but by using current algebra we can find the dependence

$$d_n \;=\; 5.2 \times 10^{-16} \cdot \theta \text{ cm}, \tag{II.21}$$

thus, it turns out that $\theta < 10^{-10}$. The term in Eq. [II.20] also violates CP, although, other sources of CP violations are known even in the Standard Model, coming from the Yukawa sector.

So far, in our analysis, unnaturalness has not come. The paradoxical situations arise when we start to analyze

the relevant operators. We consider the Higgs mass, written as

$$c\Lambda_{UV}^2 H^\dagger H, \tag{II.22}$$

which is a dimension 2 operator. Here, through selection rules, we can set the coefficient of the Higgs mass from dilatations (the selection rule dictated by dimensional analysis), so that a given fundamental scale Λ_{UV}^2 should appear multiplied by some coefficient constrained by symmetries. In this sense, there is a shift symmetry of the Higgs Goldstone boson that is broken by the Yukawa interaction. Then, the coefficient should be controlled by the same parameter that breaks the shift symmetry. Thus $c \sim \frac{\lambda_t^2}{16\pi^2}$, since the biggest Yukawa coupling is that corresponding to the heaviest fermion, i.e. the top quark. Actually, the corrections to the Higgs mass are given by

$$\delta m_h^2 = \frac{3\lambda_t^2}{4\pi^2}\Lambda_t^2 - \frac{9g^2}{32\pi^2}\Lambda_g^2 - \frac{3g'^2}{32\pi^2}\Lambda_{g'}^2 - \frac{3\lambda}{8\pi^2}\Lambda_h^2 + \dots. \tag{II.23}$$

It is already known that the Higgs mass is of order $\sim 10^2$GeV, and from the irrelevant operators, we have seen that $\Lambda_{UV} \sim 10^{15}$GeV, so c is suppressed by more than 20 orders of magnitude. At this stage, we start to see a huge difference between selection rules and the results of the experiments. This is the naturalness problem and the hierarchy paradox in the Standard Model: we do not have a whole understanding of the parameter structure in terms of symmetries. The situation could be even worst: there could be a relevant term of null dimension:

$$\Lambda_{UV}^4\sqrt{g}, \tag{II.24}$$

which is related to the Cosmological constant term. Here the problem could exist even if Λ_{UV} were the electron mass.

Under this light, the θ parameter in Eq. [II.20] can be seen as an unnatural quantity, since its smallness cannot be explained in terms of some symmetry. It could be argued that the CP violation could lead to such smallness, but we know that CP is already violated in other sectors.

With all this, we see that some paradoxical situations happen in the Standard Model, and, if we want to solve them, we have to propose new models that give explanations for the smallness of some parameters in terms of new symmetries. Is in this fashion that it is preferred the kind of models that solve the Hierarchy problem. There are several models that do not have this SM problem, among those the supersymmetric and compositeness scenarios are found.

For the supersymmetric scenario, a new fundamental symmetry is introduced: the physics at fundamental scales is invariant under the exchange between fermion and bosons. Under supersymmetry (SUSY), the Higgs mass

parameters acquire a new symmetry, so that their smallness can be understood in terms of SUSY, thus the Higgs mass is protected. Hence, it is said that, such smallness is explained by the fact that SUSY is broken by small effects that can be even non-perturbative. With this the t' Hooft criterion is satisfied.

On the other scenario, in compositeness, the Higgs is viewed as a composite field in the fundamental theory. The basic idea in this approach is that, above the weak scale, the Higgs field does not have dimension 1 anymore, instead, such dimension is bigger than 1, in such a way that the mass operator of the Higgs has dimension bigger than 2. This diminishes its relevance, then the RG-evolution of the parameters is slower, explaining the separation between scales.

Another option to solve the Hierarchy problem is the introduction of large extra-dimensions, which solve the problem by changing the fundamental scale, bringing it closer to the weak scale.

Chapter III

Two-Higgs-Doublet Model (2HDM)

In the chapter [II], it was shown why there should be physics beyond the Standard Model. Also, it was presented a model-independent approach to study the effects of such new physics. Now, in this chapter, we want to see a simple extension of the SM, where an additional copy of the $SU(2)_L$ Higgs doublet is introduced. This is the two Higgs doublet model (2HDM), where the Higgs boson discovered in 2012 is assumed to be one of the physical fields contained in the two scalar $SU(2)$ doublets, which appear in the scalar potential of this new model.

When it is intended to extend the SM, an important parameter that allows measuring the phenomenological validity of such extensions is the ρ parameter discussed in the previous chapter. The new models cannot spoil the custodial symmetry. This imposes that, the deviations ($\Delta\rho$) from the tree-level value of ρ in the SM must be $|\Delta\rho| \lesssim 10^{-3}$. It can be shown that for $SU(2)$ singlets ($T = 0$) and doublets ($T = 1/2$), with hypercharges $Y = 0$ and $Y = \pm 1$, respectively, it must be satisfied $\rho = 1$ at tree level. The simplest extension of the SM that fits in the latter option is the 2HDM.

This chapter is dedicated to the review of the basic features of this SM extension. There is a vast literature concerning the theory and phenomenology of the 2HDM, thus, here, we are focused on the construction of the model, with the current constraints on the parameter space after the detection of the Higgs boson, which usually come from unitarity and stability of the potential.

III.1 Construction of the Model

The model starts by introducing a new $SU(2)_L$ doublet of scalars. In this fashion, our new scalar sector will be made up of the two doublets

$$\Phi_1 = \begin{pmatrix} \Phi_1^+ \\ \Phi_1^0 \end{pmatrix} \ (Y=+1)\,, \qquad \Phi_2 = \begin{pmatrix} \Phi_2^+ \\ \Phi_2^0 \end{pmatrix} \ (Y=+1)\,. \tag{III.1}$$

With this, the kinetic terms of the scalars, the Yukawa, and the potential terms are modified. We can write

$$\mathcal{L}^{scalar} = \mathcal{L}^{Kin} + \mathcal{L}^{Yuk} - V\left(\Phi_1, \Phi_2\right), \tag{III.2}$$

where, naturally,

$$\mathcal{L}^{Kin} = \left(D_\mu \Phi_i\right)^\dagger \left(D^\mu \Phi_i\right), \quad (i=1,2) \text{ and with } \quad D_\mu = \partial_\mu + igW_\mu^a \tau^a + ig'\frac{Y}{2}B_\mu. \tag{III.3}$$

The Yukawa interactions in $\mathcal{L}$ can be chosen in different ways that will be studied in the next section. Now, we can write the most general Higgs potential so that the conditions of CP-conservation, gauge invariance and renormalizability are satisfied, and even more, we can ask for a discrete Z_2 symmetry to be present in a way that the potential is symmetric under transformations

$$\Phi_i \to (-1)^i \Phi_i, \ \ i=1,2. \tag{III.4}$$

This Z_2 symmetry forbids the appearance of big contributions to Flavor-Changing-Neutral-Current (FCNC) effects

$$\begin{aligned} V(\Phi_1,\Phi_2) = {} & \lambda_1\left(\Phi_1^\dagger\Phi_1 - \frac{v_1^2}{2}\right)^2 + \lambda_2\left(\Phi_2^\dagger\Phi_2 - \frac{v_2^2}{2}\right)^2 + \lambda_3\left[\left(\Phi_1^\dagger\Phi_1 - \frac{v_1^2}{2}\right) + \left(\Phi_2^\dagger\Phi_2 - \frac{v_2^2}{2}\right)\right]^2 \\ & + \lambda_4\left[\left(\Phi_1^\dagger\Phi_1\right)\left(\Phi_2^\dagger\Phi_2\right) - \left(\Phi_1^\dagger\Phi_2\right)\left(\Phi_2^\dagger\Phi_1\right)\right] + \lambda_5\left[\mathrm{Re}\left(\Phi_1^\dagger\Phi_2\right) - \frac{v_1 v_2}{2}\right]^2 + \lambda_6\left[\mathrm{Im}\left(\Phi_1^\dagger\Phi_2\right)\right]^2, \end{aligned} \tag{III.5}$$

with the λ_i being dimensionless parameters and where the vacuum expectation values of the neutral part of the scalar fields correspond to $\langle\Phi_i^0\rangle = v_i/\sqrt{2}$. In addition, in order to get the usual electroweak symmetry breaking

$SU(2)_L \times U(1)_Y \to U(1)_{em}$ we choose the minimum of the potential to be[1]

$$\langle \Phi_1 \rangle = \frac{1}{\sqrt{2}} \begin{pmatrix} 0 \\ v_1 \end{pmatrix}, \qquad \langle \Phi_2 \rangle = \frac{1}{\sqrt{2}} \begin{pmatrix} 0 \\ v_2 \end{pmatrix}. \tag{III.6}$$

In general, the physical scalars may be a linear combination of the different degrees of freedom contained among the complex components of the Φ_i's. By writing

$$\Phi_1 = \begin{pmatrix} \phi_1^+ \\ \frac{v_1+\eta_1+i\chi_1}{\sqrt{2}} \end{pmatrix}, \qquad \Phi_2 = \begin{pmatrix} \phi_2^+ \\ \frac{v_2+\eta_2+i\chi_2}{\sqrt{2}} \end{pmatrix}, \tag{III.7}$$

we can extract the mass terms from the potential in terms of the field components. We start by recognizing

$$\begin{aligned} \Phi_i^\dagger \Phi_i &= \phi_i^- \phi_i^+ + \frac{1}{2}\left(v_i + \eta_i - i\chi_i\right)\left(v_i + \eta_i + i\chi_i\right) \\ &= \phi_i^- \phi_i^+ + \frac{1}{2}\left(v_i + \eta_i\right)^2 + \frac{1}{2}\chi_i^2, \end{aligned} \tag{III.8}$$

so that it is readily visible that

$$\begin{aligned} \left(\Phi_i^\dagger \Phi_i - \frac{v_i^2}{2}\right)^2 = v_i^2\eta_i^2 + \left(\phi_i^-\phi_i^+\right)^2 + \frac{1}{4}\eta_i^4 - \frac{1}{4}\chi_i^4 + \phi_i^-\phi_i^+\eta_i^2 + 2v_i\phi_i^-\phi_i^+\eta_i \\ - \phi_i^-\phi_i^+\chi_i^2 + v_i\eta_i^3 - v_i\eta_i\chi_i^2 - \frac{1}{2}\chi_i^2\eta_i^2, \end{aligned} \tag{III.9}$$

where just the first term will contribute to the mass expressions for each $i = 1, 2$. By taking advantage of the relation above, we also can extract mass terms from the expression

$$\left(\Phi_1^\dagger\Phi_1 + \Phi_2^\dagger\Phi_2 - \frac{v_1^2+v_2^2}{2}\right)^2 \supset v_1^2\eta_1^2 + v_2^2\eta_2^2 + 2v_1v_2\eta_1\eta_2. \tag{III.10}$$

In the potential of the 2HDM appears the expression $\Phi_1^\dagger\Phi_2$, as well as its conjugate, and its real and imaginary part, thus, it is useful to fully expand it:

$$\begin{aligned} \Phi_1^\dagger\Phi_2 &= \phi_1^-\phi_2^+ + \frac{1}{2}\eta_1\eta_2 + \frac{1}{2}v_2\eta_1 + \frac{1}{2}v_1\eta_2 + \frac{v_1v_2}{2} + \frac{1}{2}\chi_1\chi_2 \\ &\quad + \frac{i}{2}\left(\eta_1\chi_2 + v_1\chi_2 - \chi_1\eta_2 - v_2\chi_1\right). \end{aligned} \tag{III.11}$$

[1] Here, we are using a specific parametrization of the scalar potential. In [39] it is discussed vacuum stability in 2HDMs with a different parametrization. It is possible to obtain the potential in eq. [III.5] from that in [39], but not vice-versa. In addition, there can be seen that the minimization of the scalar potential could lead to different local minima, and that the form of the vev's in eq. [III.6] is subtle. In some cases, there could be a non-zero upper component in the vev's, which corresponds to the so-called charged vacuum, leading to a $U(1)_{em}$ symmetry spontaneously broken. In this work, we decide to take the most common vev's in 2HDMs.

Hence, we extract the mass terms,

$$\begin{aligned}\left(\Phi_2^\dagger\Phi_1\right)\left(\Phi_1^\dagger\Phi_2\right) \supset & \frac{1}{2}v_1v_2\phi_1^-\phi_2^+ + \frac{1}{2}v_1v_2\phi_1^+\phi_2^- + \frac{1}{4}v_1^2\chi_2^2 + \frac{1}{4}v_2^2\chi_1^2 \\ & + \frac{1}{4}v_2^2\eta_1^2 + \frac{1}{4}v_1^2\eta_2^2 + v_1v_2\eta_1\eta_2, \end{aligned} \tag{III.12}$$

but this contribution is subtracted from the expression

$$\begin{aligned}\left(\Phi_1^\dagger\Phi_1\right)\left(\Phi_2^\dagger\Phi_2\right) \supset & \frac{1}{2}v_2^2\phi_1^-\phi_1^+ + \frac{1}{2}v_1^2\phi_2^-\phi_2^+ + \frac{1}{4}v_1^2\chi_2^2 + \frac{1}{4}v_2^2\chi_1^2 \\ & + \frac{1}{4}v_2^2\eta_1^2 + v_1v_2\eta_1\eta_2 + \frac{1}{4}v_1^2\eta_2^2, \end{aligned} \tag{III.13}$$

where from Eq.[III.12-III.13] we can see that almost all the mass terms cancel out, except those related to the charged scalars. The mass terms coming from the real and imaginary part of $\Phi_1^\dagger\Phi_2$ are easy to get from Eq. [III.11]. Thus, for the neutral scalars:

$$\begin{aligned}\mathcal{L}_{neutral}^{mass} &= \lambda_1v_1^2\eta_1^2 + \lambda_2v_2^2\eta_2^2 + \lambda_3\left(v_1^2\eta_1^2 + v_2^2\eta_2^2 + 2v_1v_2\eta_1\eta_2\right) \\ &\quad + \lambda_5\left(\frac{1}{4}v_2^2\eta_1^2 + \frac{1}{4}v_1^2\eta_2^2 + \frac{1}{2}v_1v_2\eta_1\eta_2\right) \\ &= \frac{1}{2}\left(\eta_1,\eta_2\right)M_{neutral}^2\begin{pmatrix}\eta_1\\ \eta_2\end{pmatrix}, \end{aligned} \tag{III.14}$$

where the mass matrix is given by

$$M_{neutral}^2 = \begin{pmatrix} m_{11} & m_{12} \\ m_{12} & m_{22}\end{pmatrix}, \tag{III.15}$$

with

$$m_{11} = 2\left(\lambda_1+\lambda_3\right)v_1^2 + \frac{1}{2}\lambda_5v_2^2, \quad m_{12} = \left(2\lambda_3 + \frac{1}{2}\lambda_5\right)v_1v_2, \quad m_{22} = 2\left(\lambda_2+\lambda_3\right)v_2^2 + \frac{1}{2}\lambda_5v_1^2. \tag{III.16}$$

Analogously, we have for the pseudo-scalars

$$\begin{aligned}\mathcal{L}_{p-s}^{mass} &= \frac{1}{4}\lambda_6\left(v_1^2\chi_2^2 + v_2^2\chi_1^2 - 2v_1v_2\chi_1\chi_2\right) \\ &= \frac{1}{2}\left(\chi_1,\chi_2\right)M_{p-s}^2\begin{pmatrix}\chi_1\\ \chi_2\end{pmatrix}, \end{aligned} \tag{III.17}$$

with the mass matrix in this case given by

$$M^2_{p-s} = \frac{\lambda_6}{2}\begin{pmatrix} v_2^2 & -v_1v_2 \\ -v_1v_2 & v_1^2 \end{pmatrix}. \tag{III.18}$$

Finally, for the charged scalars it is yielded

$$\begin{aligned} \mathcal{L}^{mass}_{charged} &= \lambda_4\left(\frac{1}{2}v_2^2\phi_1^-\phi_1^+ + \frac{1}{2}v_1^2\phi_2^-\phi_2^+ - \frac{1}{2}v_1v_2\phi_1^-\phi_2^+ - \frac{1}{2}v_1v_2\phi_1^+\phi_2^-\right) \\ &= \left(\phi_1^+, \phi_2^+\right) M^2_{charged}\begin{pmatrix} \phi_1^- \\ \phi_2^- \end{pmatrix}, \end{aligned} \tag{III.19}$$

where

$$M^2_{charged} = \frac{\lambda_4}{2}\begin{pmatrix} v_2^2 & -v_1v_2 \\ -v_1v_2 & v_1^2 \end{pmatrix}. \tag{III.20}$$

With these mass expressions, we are able to write the physical scalars states by diagonalizing the mass matrices. For this task, we note the similitude between $M^2_{charged}$ and M^2_{p-s}, then both of these matrices will be diagonalized by the same rotation in the field basis. Then, we change our field basis by applying the rotations,

$$\begin{pmatrix} H^0 \\ h^0 \end{pmatrix} = R_1\begin{pmatrix} \eta_1 \\ \eta_2 \end{pmatrix}, \qquad \begin{pmatrix} G^0 \\ A^0 \end{pmatrix} = R_2\begin{pmatrix} \chi_1 \\ \chi_2 \end{pmatrix}, \qquad \begin{pmatrix} G^\pm \\ H^\pm \end{pmatrix} = R_2\begin{pmatrix} \phi_1^\pm \\ \phi_2^\pm \end{pmatrix}, \tag{III.21}$$

with

$$R_1 = \begin{pmatrix} \cos\alpha & \sin\alpha \\ -\sin\alpha & \cos\alpha \end{pmatrix}, \qquad R_2 = \begin{pmatrix} \cos\beta & \sin\beta \\ -\sin\beta & \cos\beta \end{pmatrix}. \tag{III.22}$$

Then, the diagonalization of the mass matrix in Eq. [III.15] for the scalar bosons is

$$\begin{aligned} R_1\left(M^2_{neutral}\right)R_1^T &= \begin{pmatrix} m_{11}\cos^2\alpha + m_{12}\sin 2\alpha + m_{22}\sin^2\alpha & m_{12}\cos 2\alpha + \frac{1}{2}\left(-m_{11}+m_{22}\right)\sin 2\alpha \\ m_{12}\cos 2\alpha + \frac{1}{2}\left(-m_{11}+m_{22}\right)\sin 2\alpha & m_{11}\sin^2\alpha - m_{12}\sin 2\alpha + m_{22}\cos^2\alpha \end{pmatrix} \\ &= \begin{pmatrix} m_h^2 & 0 \\ 0 & m_H^2 \end{pmatrix}, \end{aligned} \tag{III.23}$$

where in order to get a diagonal matrix we do:

$$m_{12}\cos 2\alpha + \frac{1}{2}\left(-m_{11}+m_{12}\right)\sin 2\alpha = 0 \quad \Rightarrow \quad \tan 2\alpha = \frac{2m_{12}}{m_{11}-m_{22}}, \tag{III.24}$$

but, by recalling that the components m_{ij} are given in the relations [III.16], it turns out that the rotation angle α is given by

$$\tan 2\alpha \;=\; \frac{2\left(\lambda_3+\frac{1}{4}\lambda_5\right)v_1v_2}{\lambda_1v_1^2-\lambda_2v_2^2+\left(\lambda_3+\frac{1}{4}\lambda_5\right)\left(v_1^2-v_2^2\right)}. \tag{III.25}$$

The masses of the CP-even scalars can be obtained by solving the characteristic equation of the matrix, so that

$$\begin{aligned} m_h^2 &= \frac{1}{2}\left[(m_{11}+m_{22})-\sqrt{(m_{11}-m_{22})^2+m_{12}^2}\right], \\ m_H^2 &= \frac{1}{2}\left[(m_{11}+m_{22})+\sqrt{(m_{11}-m_{22})^2+m_{12}^2}\right]. \end{aligned} \tag{III.26}$$

Similarly, it can be done for the other mass matrices. The matrix where the mass of the pseudo-scalar is contained (Eq. [III.18]) can be diagonalized by:

$$R_2\left(M_{p-s}^2\right)R_2^T=\frac{\lambda_6}{2}\begin{pmatrix} (v_2\cos\beta-v_1\sin\beta)^2 & v_1v_2\left(\sin^2\beta-\cos^2\beta\right)-\left(-v_1^2+v_2^2\right)\sin\beta\cos\beta \\ v_1v_2\left(\sin^2\beta-\cos^2\beta\right)-\left(-v_1^2+v_2^2\right)\sin\beta\cos\beta & (v_2\cos\beta+v_1\sin\beta)^2 \end{pmatrix}, \tag{III.27}$$

so that in order to get a diagonal matrix, the β-angle must be

$$v_1v_2\left(\sin^2\beta-\cos^2\beta\right)-\left(-v_1^2+v_2^2\right)\sin\beta\cos\beta=0 \;\;\Rightarrow\;\; \tan\beta=\frac{v_2}{v_1}. \tag{III.28}$$

This is equivalent to $v_2\cos\beta=v_1\sin\beta$, then, the diagonal entries are

$$(v_2\cos\beta-v_1\sin\beta)^2=0, \qquad \text{and} \qquad (v_2\cos\beta+v_1\sin\beta)^2=v_1^2+v_2^2\equiv v^2, \tag{III.29}$$

where it was made the identification $v=\sqrt{v_1^2+v_2^2}=246\,\text{GeV}$. We note that the fact of having a diagonal zero value in the matrix corresponds to a Goldstone boson, G^0, while the mass of the pseudo-scalar is given by

$$m_A^2 \;=\; \frac{1}{2}\lambda_6v^2. \tag{III.30}$$

The same analysis stands for the matrix of the charged bosons, as was mentioned before. Then, we also have a couple of charged Goldstone bosons $G^\pm$, while the physical charged Higgses have mass

$$m_{H^+}^2=\frac{1}{2}\lambda_4v^2. \tag{III.31}$$

Let us summarize. Through diagonalization it was yielded the scalar spectrum made up of eight real fields h^0,

H^0, $H^\pm$, A^0, G^0 and $G^\pm$, from which three of them, the massless one, would be eaten by the electroweak vector fields in order to get their longitudinal degrees of freedom, so that in the end just the first five scalars compose the physical particle spectrum from the scalar sector.

By looking at the potential in Eq. [III.5], we note that there are eight parameters in it, where six of them are couplings and two are the vev's. The vev's are related through their relation to the vev in the SM, thus we are introducing seven new parameters in the 2HDM. Usually, those seven parameters are chosen to be the four masses of the physical scalars, the parameter $\tan\beta$, the mixing angle α and the coupling λ_5:

$$(m_h, m_H, m_A, m_{H^+}, \tan\beta, \alpha, \lambda_5)\,. \tag{III.32}$$

Then, the couplings must be given in terms of the input parameters. This is not a difficult task. By inverting the relations [III.26], [III.30, [III.31] and with the definitions of the mixing angles, we obtain:

$$\begin{aligned}
\lambda_1 &= \frac{1}{2v^2\cos^2\beta}\left[m_H^2\cos^2\alpha + m_h^2\sin^2\alpha - \frac{\sin\alpha\cos\alpha}{\tan\beta}\left(m_H^2 - m_h^2\right)\right] - \frac{\lambda_5}{4}\left(\tan^2\beta - 1\right),\\
\lambda_2 &= \frac{1}{2v^2\sin^2\beta}\left[m_h^2\cos^2\alpha + m_H^2\sin^2\alpha - \sin\alpha\cos\alpha\tan\beta\left(m_H^2 - m_h^2\right)\right] - \frac{\lambda_5}{4}\left(\cot^2\beta - 1\right),\\
\lambda_3 &= \frac{1}{2v^2}\frac{\sin\alpha\cos\alpha}{\sin\beta\cos\beta}\left(m_H^2 - m_h^2\right) - \frac{\lambda_5}{4},\\
\lambda_4 &= \frac{2}{v^2}m_{H^+}^2,\\
\lambda_5 &= \frac{2}{v^2}m_A^2.
\end{aligned} \tag{III.33}$$

We note that from the eight parameters introduced in the potential of the 2HDM, two of them are already known. One is given by the vev already known in the SM, $v = 246\,\text{GeV}$, and the other is given by $m_h = 125\,\text{GeV}$. This assuming that the detected scalar in the LHC is the lightest CP-even scalar of the 2HDM. The other parameters must be bounded by theoretical and experimental constraints.

III.2 Types of 2HDM

So far, we have established the physical spectrum of the 2HDM. In this section, we want to see the way the new physical states interact with the SM particles. This issue is basically what defines the different possible types of 2HDM. Then, we discuss here the possible forms of $\mathcal{L}^{Yuk}$ in Eq. [III.2]. In general, we can have couplings of the form

$$-y_{ij}^a\bar{\Psi}_L^i\Phi_a\Psi_R^j + h.c. \tag{III.34}$$

Model	Type I	Type II	Lepton-specific	Flipped
U	Φ_2	Φ_2	Φ_2	Φ_2
D	Φ_2	Φ_1	Φ_2	Φ_1
E	Φ_2	Φ_1	Φ_1	Φ_2

Table III.1: Higgs doublets that couples to an up-, down- and charged-lepton-like fermions in different Two-Higgs Doublet Models.

Here, we can have two different Yukawa couplings for each fermionic field. This does not allow in the 2HDM to ensure that the mass matrices can be diagonalized together with the Yukawa coupling matrices, as in the SM. This leads to a Higgs neutral boson to mediate flavor-changing interactions among fermion mass eigenstates. Such situation is very constrained from the Kaon, D and B meson phenomenology. To avoid this situation it is taken into account the Glashow-Weinberg criterion[2], which states the necessary conditions to have flavor conservation in the neutral current interactions[35][36]. By following this criterion it is enough that each charged fermionic field couples to just one of the Higgs doublet.

The Yukawa interactions in different Two-Higgs Doublet models that satisfy the Glashow-Weinberg criterion are shown in the table [III.1]. In type-I models just one Higgs doublet couples to the up, down and charged-lepton fermions, while the other does not couple to any of them. Thus, the Yukawa Lagrangian of type-I 2HDM is

$$\mathcal{L}^{Yuk}_{Type-I} = -y^d_{ij}\bar{Q}_i\Phi_2 D_j - y^u_{ij}\bar{Q}_i\widetilde{\Phi}_2 U_j - y^e_{ij}\bar{L}_i\Phi_2 E_j + h.c. \tag{III.35}$$

The type-II 2HDM Yukawa interactions are chosen such that one of the Higgs doublets couples to the down-like fermions and to the charged-leptons, while the other doublet couples to the up-like fermions. To get vanishing the dangerous FCNC, the right-handed components should transform under the discrete symmetry as $D_i \to -D_i$ and $U_i \to U_i$. The Lagrangian for this type of models is

$$\mathcal{L}^{Yuk}_{Type-II} = -y^d_{ij}\bar{Q}_i\Phi_1 D_j - y^u_{ij}\bar{Q}_i\widetilde{\Phi}_2 U_j - y^e_{ij}\bar{L}_i\Phi_1 D_j + h.c. \tag{III.36}$$

In the next chapter, we shall see that the Higgs sector of the MSSM corresponds to a type-II 2HDM.

The Yukawa interactions can be written explicitly in terms of the mass eigenstates. Let us see the way this happens for the type-I 2HDM. In this model, all the mass matrices are defined as $m_{ij} = \frac{v_2}{\sqrt{2}}y_{ij}$, so that they can be diagonalized by rotations in the fermionic basis, as it was done for the SM (see Section [I.6]). The relations

[2]In order to avoid FCNC at tree-level it is necessary and sufficient that all fermions of the same charge and helicity transform under the same irreducible representation of SU(2), have the same T_3 eigenvalue and that a basis exists in which they receive their contributions in the mass matrix from a single source[37].

Model	Type I	Type II	Lepton-specific	Flipped
ξ_h^u	$\cos\alpha/\sin\beta$	$\cos\alpha/\sin\beta$	$\cos\alpha/\sin\beta$	$\cos\alpha/\sin\beta$
ξ_h^d	$\cos\alpha/\sin\beta$	$-\sin\alpha/\cos\beta$	$\cos\alpha/\sin\beta$	$-\sin\alpha/\cos\beta$
ξ_h^ℓ	$\cos\alpha/\sin\beta$	$-\sin\alpha/\cos\beta$	$-\sin\alpha/\cos\beta$	$\cos\alpha/\sin\beta$
ξ_H^u	$\sin\alpha/\sin\beta$	$\sin\alpha/\sin\beta$	$\sin\alpha/\sin\beta$	$\sin\alpha/\sin\beta$
ξ_H^d	$\sin\alpha/\sin\beta$	$\cos\alpha/\cos\beta$	$\sin\alpha/\sin\beta$	$\cos\alpha/\cos\beta$
ξ_H^ℓ	$\sin\alpha/\sin\beta$	$\cos\alpha/\cos\beta$	$\cos\alpha/\cos\beta$	$\sin\alpha/\sin\beta$
ξ_A^u	$\cot\beta$	$\cot\beta$	$\cot\beta$	$\cot\beta$
ξ_A^d	$-\cot\beta$	$\tan\beta$	$-\cot\beta$	$\tan\beta$
ξ_A^ℓ	$-\cot\beta$	$\tan\beta$	$\tan\beta$	$-\cot\beta$

Table III.2: Higgs doublets that couples to an up-, down- and charged-lepton-like fermions in different Two-Higgs Doublet Models.

$v_2 = v\sin\beta$ and $ev = 2M_W\sin\theta_W$ allow us to write

$$\begin{aligned}
\mathcal{L}^{Yuk}_{Type-I} &= -\frac{1}{\sqrt{2}}y^d_{ij}\left(v_2+\eta_2+i\chi_2\right)\bar{d}_{Li}d_{Rj} - y^d_{ij}\phi_2^+\bar{u}_{Li}d_{Rj} - \frac{1}{\sqrt{2}}y^u_{ij}\left(v_2+\eta_2+i\chi_2\right)\bar{u}_{Li}u_{Rj} + y^u_{ij}\phi_2^-\bar{d}_{Li}u_{Rj} \\
&\quad -\frac{1}{\sqrt{2}}y^e_{ij}\left(v_2+\eta_2+i\chi_2\right)\bar{e}_{Li}e_{Rj} - y^e_{ij}\phi_2^+\bar{\nu}_{Li}e_{Rj} + h.c. \\
&\supset -m_d^{(i)}\bar{d}_i d_i - \frac{e}{2M_W\sin\theta_W\sin\beta}m_d^{(i)}\eta_2\bar{d}_i d_i - \frac{ie}{2M_W\sin\theta_W\sin\beta}m_d^{(i)}\chi_2\left(\bar{d}_i\gamma_5 d_i\right) \\
&\quad -\left\{\frac{e}{\sqrt{2}M_W\sin\theta_W\sin\beta}\phi_2^+V^{ij}_{CKM}\bar{u}_i\left(m_d^{(j)}P_R - m_u^{(i)}P_L\right)d_j + h.c.\right\} \\
&= -m_d^{(i)}\bar{d}_i d_i - \frac{e}{2M_W\sin\theta_W\sin\beta}m_d^{(i)}\bar{d}_i d_i\left[H^0\sin\alpha + h^0\cos\alpha\right] - \frac{ie\cot\beta}{2M_W\sin\theta_W}m_d^{(i)}\bar{d}_i\gamma_5 d_i A_0 \\
&\quad -\left\{\frac{e\cot\beta}{\sqrt{2}M_W\sin\theta_W}V^{ij}_{CKM}\bar{u}_i\left(m_d^{(j)}P_R - m_u^{(i)}P_L\right)d_j H^+ + h.c.\right\},
\end{aligned} \tag{III.37}$$

where the Cabibbo-Kobayashi-Maskawa matrix arises after diagonalization of the mass matrices, and where the expressions for the up-like quarks and leptons are very similar. It is also understood that the computations are made in the unitary gauge, where the ghosts and the would-be Nambu-Goldstone bosons do not appear. In fact, the Yukawa interactions can be written in a very general way, following the notation in [43]

$$\begin{aligned}
\mathcal{L}^{Yuk} = &-\sum_{f=u,d,\ell}\frac{e}{2M_W\sin\theta_W}m_f\left(\xi_h^f\bar{f}fh^0 + \xi_H^f\bar{f}fH^0 - i\xi_A^f\bar{f}\gamma_5 fA^0\right) \\
&+\left\{\frac{e}{\sqrt{2}M_W\sin\theta_W}V_{CKM}\bar{u}\left(m_u\xi_A^u P_L + m_d\xi_A^d P_R\right)d\,H^+ + \frac{e}{\sqrt{2}M_W\sin\theta_W}m_\ell\xi_A^\ell\bar{\nu}_L\ell_R H^+ + h.c.\right\},
\end{aligned} \tag{III.38}$$

with the generation indices omitted. The parameters ξ_h^f, ξ_H^f and ξ_A^f are enlisted for various 2HDM in the table [III.2]. The way to reach such couplings is the same as the shown above. The difference in the couplings come from the vev that defines the masses of the fermions and the rotation between the scalar bases. For instance, in type-II 2HDM the masses are defined as $m_{u\,ij} = \frac{v_2}{\sqrt{2}}y^u_{ij}$, $m_{d\,ij} = \frac{v_1}{\sqrt{2}}y^d_{ij}$ and $m_{e\,ij} = \frac{v_1}{\sqrt{2}}y^e_{ij}$, so that for down-like quarks and leptons instead of $v_2 = v\sin\beta$, it enters $v_1 = v\cos\beta$. In a phenomenological sense, it is worth mentioning that the Yukawa couplings can be enhanced or suppressed depending on the type of 2HDM.

For instance, in the type I the couplings of the pseudoscalar and the charged Higgs bosons get suppressed for $\tan\beta > 1$.

III.3 The Alignment Limit

In the 2HDM it is possible to recover a physical CP-even scalar with the same gauge, Yukawa and self-coupling interactions at tree level as those in the SM for the Higgs boson. This situation in the 2HDM is known as the alignment limit. To see this limit we start by noting that the trilinear coupling of the W-bosons with the Higgs is of the form

$$\begin{aligned}\mathcal{L}^{Kin} &\supset \frac{1}{8}g^2\left(W_\mu^1+iW_\mu^2\right)\left(W_\mu^1-iW_\mu^2\right)(v_1+\eta_1)^2+\frac{1}{8}g^2\left(W_\mu^1+iW_\mu^2\right)\left(W_\mu^1-iW_\mu^2\right)(v_2+\eta_2)^2 \\ &\supset \frac{1}{2}g^2W_\mu^-W_\mu^+\left(v_1\eta_1+v_2\eta_2\right). \end{aligned} \tag{III.39}$$

Now, by comparing with the SM model situation (see Eq. [I.24]), the identification

$$H_1' = \frac{1}{v}\left(v_1h_1+v_2h_2\right), \tag{III.40}$$

leads to an interaction between a scalar and the charged weak bosons like that in the SM. The orthogonal combination (H_2') of h_1 and h_2 does not present a trilinear coupling with the weak bosons. Then, let us write

$$\begin{pmatrix} H_1' \\ H_2' \end{pmatrix} = \begin{pmatrix} \cos\beta & \sin\beta \\ -\sin\beta & \cos\beta \end{pmatrix}\begin{pmatrix} h_1 \\ h_2 \end{pmatrix}. \tag{III.41}$$

In general, the fields H_i' not need to be physical. The alignment limit states the situation under which H_1' is a CP-even physical scalar, but these physical states are given by the transformation

$$h^0 = \sin(\beta-\alpha)\,H_1' + \cos(\beta-\alpha)\,H_2', \tag{III.42}$$

$$H^0 = \cos(\beta-\alpha)\,H_1' - \sin(\beta-\alpha)\,H_2'. \tag{III.43}$$

Then, the alignment limit is at $\sin(\beta-\alpha)=1$. The measurements at the LHC regarding the Higgs boson decays are in a good agreement with the SM, thus, it is expected the parameters to be near the alignment limit. Let us also note that the alignment condition fixes one parameter. It is also remarkable that in the alignment limit the trilinear Higgs coupling takes the same form as in the SM.

III.4 Constraints to the Parameters of the 2HDM

After the measurement of the resonance identified with the Higgs boson, the parameters of the 2HDMs got stronger constraints. Bounds to these parameters come from experiments and from theoretical arguments. In the former, we can find direct bounds to the masses of the non-standard scalars and measurements on FCNC; in the latter enter unitary and stability constraints, as well as small deviations from $\rho = 1$.

Measurements in the LHC set that at 95% of C.L. the masses of the non-standard Higgs bosons should be[15]

$$m_{H^\pm} > 80 \text{ GeV}, \qquad \text{and} \quad m_{A^0} > 93.4 \text{ GeV} \quad \text{for } \tan\beta > 0.4. \tag{III.44}$$

Other constraints on the mass of the charged Higgs bosons can be found from quantum corrections to the FCNC through the charged-current interactions. Measurements on the B-meson decays [38] claim that $m_{H^\pm} > 295\,\text{GeV}$ for $\tan\beta > 1$.

Constraints on $\tan\beta$ can also be established from measurements of $Z^0 \to \bar{b}b$ and $B - \bar{B}$ mixing processes. This parameter can take values from a wide range of values. The mentioned experiments pointed out that situations in which $\tan\beta \ll 1$ are disfavoured[40].

In the Standard Model, it is straightforward the identification of the conditions that the parameters on the potential should satisfy in order to have it bounded from below at tree-level. The quartic coupling (λ) should be positive. Actually, a deeper analysis including quantum corrections through the effective potential shows that at Planck energies the SM presents instabilities. An instructive review on this topic is presented in [41]. Such analysis in the 2HDM is more complicated, but it is known that this extension of the SM does not solve the stability problem of the effective potential without the soft-breaking term. Even more, when including the soft breaking term, a bound of $\tan\beta \gtrsim 3$ is obtained near the alignment limit. A recent summary at tree-level is found in [42]. By imposing that at large values in the field directions the potential cannot be infinitely negative the following constraints are found

$$\begin{aligned} &\lambda_1 + \lambda_3 > 0, \qquad (2\lambda_3 + \lambda_4) + 2\sqrt{(\lambda_1 + \lambda_3)(\lambda_2 + \lambda_3)} > 0, \\ &\lambda_2 + \lambda_3 > 0, \qquad 2\lambda_3 + \frac{\lambda_5 + \lambda_6}{2} - \frac{|\lambda_5 - \lambda_6|}{2} + 2\sqrt{(\lambda_1 + \lambda_3)(\lambda_2 + \lambda_3)} > 0, \end{aligned} \tag{III.45}$$

Unitarity conditions are obtained through the study in partial-waves of amplitudes involving four scalars. By joining stability and unitarity conditions strong implications on the non-standard Higgs masses and $\tan\beta$ are obtained. In particular, for $\lambda_5 = 0$:

$$\frac{1}{8} < \tan\beta < 8, \qquad m_{H^0},\, m_{A^0},\, m_{H^+} < 1\,\text{TeV}, \tag{III.46}$$

where it is also taken into account that the 2HDM must be near the alignment limit. From the unitarity constraints, it is found that the difference between m_{A^0} and m_{H^+} is always restricted independent on the values of the other parameters. The constraint that gives evidence of this fact is

$$|m_A^2 - m_{H^+}^2| \quad < \quad \frac{16\pi}{3}v^2. \tag{III.47}$$

An interesting upshot is also obtained through

$$0 < \quad \left(m_{H^0}^2 - \tfrac{1}{2}\lambda_5 v^2\right)\left(\tan^2\beta + \cot^2\beta\right) + 2m_{h^0}^2 \quad < \frac{32\pi}{3}v^2, \tag{III.48}$$

which is obtained by an interplay between unitarity and stability conditions. For $\lambda_5 < 0$ the allowed values for $\tan\beta$ must be very close to 1, while for λ_5 positive $\tan\beta$ can be in a wide range of values. For situations where $\tan\beta$ gets away from 1 it is expected $m_{H^0}^2$ close to $\lambda_5 v^2/2$.

If instead of a Z_2 symmetry it is imposed a softly broken $U(1)$ global symmetry so that $\Phi_1 \to \Phi_1$ and $\Phi_2 \to e^{i\alpha}\Phi_2$, an interesting relation among the masses m_{A^0} and m_{H^0} emerges, [42]:

$$0 \leq \quad \left(m_{H^0}^2 - m_{A^0}^2\right)\left(\tan^2\beta + \cot^2\beta\right) + 2m_{h^0}^2 \quad \leq \frac{32\pi}{3}v^2, \tag{III.49}$$

where it is manifested that the masses of the pseudoscalar A^0 and the CP-even scalar H are degenerate for big values of $\tan\beta$. This comes from the fact that when the $U(1)$ symmetry is exact $\lambda_5 = \lambda_6$. An analogous situation happens between the m_{H^0} and m_{H^+}. For this global symmetry, the masses can grow arbitrarily, the bounds are on the differences of the non-standard masses, not on their absolute values.

It is important to clarify that the above degeneracies depend on the $U(1)$ symmetry. On the other hand, for the Z_2 symmetry the bounds are on the absolute values of the masses and restrict them. This is due to the fact that for the Z_2 symmetry to be exact λ_5 must vanish, which can be seen from the unitarity bounds

$$|m_{A^0}^2 - \frac{1}{2}\lambda_5 v^2| < \frac{16\pi}{3}v^2, \qquad\qquad |m_{H^+}^2 - \frac{1}{2}\lambda_5 v^2| < \frac{16\pi}{3}v^2. \tag{III.50}$$

Finally, we mention that when the constraints on the ρ-parameter are combined with the previous theoretical bounds, the splitting between m_H and m_{H^+} is $\sim 50\,\text{GeV}$ for $\tan\beta$ greater than 1. In this case, the constraints from the ρ-parameter are stronger than those coming from unitarity and stability. For $\tan\beta = 1$ the ρ-parameter cannot give conclusive bounds on the non-standard masses space.

Chapter IV

Minimal Supersymmetric Standard Model

In the chapter [II], we discussed the Hierarchy paradox in the SM framework and, at the end, it was very briefly discussed that supersymmetry (SUSY) is capable to give a dynamical explanation for the smallness of the parameters that enter in the corrections of the Higgs boson mass. Now, in this chapter, it is intended to study SUSY in a general approach, the way supersymmetric theories can be built and, in particular, present the Minimal Supersymmetric Standard Model (MSSM) that is broadly studied in particle physics. Also, it is pretended to see the mechanism that SUSY introduces to protect the Higgs mass.

The basic idea behind SUSY is that the observables can remain unchanged under the exchange between bosons and fermions. To achieve such symmetry, a given particle must exhibit the same physical properties as its partner of opposite statistics (Known as superpartner). Here supersymmetric transformations are extensions of the Poincarè transformations, then new generators Q_α and $\bar{Q}_{\dot{\alpha}}$ are defined and the algebra must be extended. Thus, the transformations can be performed in the new directions defined by the supersymmetric generators.

In general, SUSY sets the framework for unification at the Planck scale, and is of fundamental importance in different theories, as is the case of String theory. But at scales where the current experiments run it is noted that SUSY was not directly confirmed. If SUSY exists the SM particles should have some superpartners that so far were not detected (There are not known fundamental particles with the same physical features and with opposite statistic), then in the case that SUSY was confirmed, it should be broken at electroweak scale. This raises the question of which is the mechanism of supersymmetry breaking. There are many options, among which we can find that non-perturbative effects are interesting sources of SUSY breaking. Such options will be also discussed.

Appart from the unexpected and nice extension that represents SUSY, there are many phenomenological motivations to study this theory. One of them was already mentioned: the hierarchy paradox. Among such motivations we also find the fact that in the set of new superpartners there could be some candidates to be WIMP, giving hints about the nature of dark matter. Also, the MSSM provides a good example of gauge coupling unification. In addition, some new CP-violation sources can be introduced, guiding us to a solution to the matter-antimatter asymmetry problem.

This chapter is based on the reviews [44][45][46][47] and the books [48][68].

IV.1 Basics of Supersymmetry

In this section, we want to review enough concepts of superfields and superspace formalism in order to construct globally supersymmetric Lagrangians. Let us start by writing the supersymmetric algebra:

$$\left\{Q_\alpha, \bar{Q}_{\dot{\beta}}\right\} = 2\sigma^\mu_{\alpha\dot{\beta}} P_\mu. \tag{IV.1}$$

Here we must specify that the number of copies of this algebra (N) that we will take into account is $N = 1$, this because in phenomenology we are usually interested in chiral theories, while theories with $N > 1$ are non-chiral. In addition to this, we will also be interested in supersymmetry breaking, so that for $N > 1$ there are two options, either we find a way to partially break the full supersymmetry to $N = 1$, or a potential that allows for the complete breaking of the symmetry must be included, but with global supersymmetry none of these two ways can be reached.

The more natural environment to study supersymmetric theories is in the superspace, which is an extension of the space-time, where four additional anti-commuting coordinates are introduced, θ_α and $\dot{\theta}_{\dot{\alpha}}$, with α, $\dot{\theta} = 1, 2$. In such space, the supersymmetric operators take the differential form:

$$Q_\alpha = \frac{\partial}{\partial\theta_\alpha} - i\sigma^\mu_{\alpha\dot{\alpha}}\bar{\theta}^{\dot{\alpha}}\partial_\mu, \qquad \bar{Q}^{\dot{\alpha}} = \frac{\partial}{\partial\bar{\theta}_{\dot{\alpha}}} - i\bar{\sigma}^{\mu\dot{\alpha}\alpha}\theta_\alpha\partial_\mu. \tag{IV.2}$$

It is also useful to introduce the couple of operators:

$$D_\alpha = \frac{\partial}{\partial\theta_\alpha} + i\sigma^\mu_{\alpha\dot{\alpha}}\bar{\theta}^{\dot{\alpha}}\partial_\mu, \qquad \bar{D}^{\dot{\alpha}} = \frac{\partial}{\partial\bar{\theta}_{\dot{\alpha}}} + i\bar{\sigma}^{\mu\dot{\alpha}\alpha}\theta_\alpha\partial_\mu. \tag{IV.3}$$

The supersymmetric algebra possesses two irreducible representations, which are manifested as chiral and vector fields, the former identified by $\bar{D}_{\dot{\alpha}}\Phi = 0$ while the latter corresponds to the real condition $V = V^\dagger$. These fields,

in general, are functions of the coordinates $\{\theta,\,\bar{\theta},\,x^{\mu}\}$. Thus, by expanding the chiral fields we have:

$$\Phi\left(y^{\mu},\theta^{\alpha}\right) = \varphi\left(y\right)+\sqrt{2}\theta^{\alpha}\psi_{\alpha}(y)+\theta^{\alpha}\theta_{\alpha}F(y), \tag{IV.4}$$

$$\bar{\Phi}\left(\bar{y}^{\mu},\bar{\theta}^{\dot{\alpha}}\right) = \bar{\varphi}\left(\bar{y}\right)+\sqrt{2}\bar{\theta}_{\dot{\alpha}}\bar{\psi}^{\dot{\alpha}}\left(\bar{y}\right)+\bar{\theta}_{\dot{\alpha}}\bar{\theta}^{\dot{\alpha}}\bar{F}\left(\bar{y}\right), \tag{IV.5}$$

where $y^{\mu}=x^{\mu}+i\theta\sigma^{\mu}\bar{\theta}$ and $\bar{y}^{\mu}=x^{\mu}-i\theta\sigma^{\mu}\bar{\theta}$. It is noted that the superfield is composed in its components of a complex scalar (φ), a Weyl fermion (ψ) and an auxiliary field (F) usually introduced to close off-shell the supersymmetric algebra. Under supersymmetric transformations, the relation $\delta_{Q}\Phi(y,\theta)=(\xi Q+\bar{\xi}\bar{Q})\Phi(y,\theta)$ in components yields

$$\delta_{Q}\varphi=\sqrt{2}\xi\psi,\quad \delta_{Q}\psi_{\alpha}=i\sqrt{2}(\sigma^{\mu}\bar{\xi})_{\alpha}\partial_{\mu}\varphi+\sqrt{2}\xi_{\alpha}F,\quad \delta_{Q}F=i\sqrt{2}\bar{\xi}\bar{\sigma}^{\mu}\partial_{\mu}\psi. \tag{IV.6}$$

On the other hand, vector superfields have a different expansion in components, which in a full form is

$$\begin{aligned}V\left(x,\theta,\bar{\theta}\right) = {} & C\left(x\right)+i\theta x\left(x\right)-i\bar{\theta}\bar{\chi}\left(x\right)+\frac{i}{2}\theta\theta\left(M\left(x\right)+iN\left(x\right)\right)-\frac{i}{2}\bar{\theta}\bar{\theta}\left(M\left(x\right)-iN\left(x\right)\right)-\left(\theta\sigma^{\mu}\bar{\theta}\right)A_{\mu}\left(x\right)\\ & +i\theta\theta\bar{\theta}\left(\bar{\lambda}\left(x\right)+\frac{i}{2}\bar{\sigma}^{\mu}\partial_{\mu}\chi\left(x\right)\right)-i\bar{\theta}\bar{\theta}\theta\left(\lambda\left(x\right)+\frac{i}{2}\sigma^{\mu}\partial_{\mu}\bar{\chi}\left(x\right)\right)+\frac{1}{2}\theta\theta\bar{\theta}\bar{\theta}\left(d\left(x\right)+\frac{1}{2}\Box C\left(x\right)\right).\end{aligned} \tag{IV.7}$$

The usual gauge transformations of vector fields, $\delta_{gauge}A_{\mu}=\partial_{\mu}\Lambda$ can be written in superspace formalism as

$$\delta_{gauge}V\left(x,\theta,\bar{\theta}\right) = \Lambda\left(y,\theta\right)+\bar{\Lambda}\left(\bar{y},\bar{\theta}\right), \tag{IV.8}$$

where it must be satisfied $\bar{D}_{\dot{\alpha}}\Lambda=0=D_{\alpha}\bar{\Lambda}$. By expanding in components:

$$\Lambda\left(y,\theta\right)=a\left(y\right)+\sqrt{2}\theta b\left(y\right)+\theta\theta f\left(y\right), \tag{IV.9}$$

it is not difficult to see that

$$\begin{aligned}&\delta C=a+a^{*}, && \delta\chi=-i\sqrt{2}b, && \delta\left(M+iN\right)=-2if,\\ &\delta A_{\mu}=-i\partial_{\mu}\left(a-a^{*}\right), && \delta\lambda=0, && \delta d=0,\end{aligned}$$

so that the vector field transforms as usual, and even more, some components of $\Lambda\left(y,\theta\right)$ can be taken in such a way that we can eliminate certain components of the vector superfield. We will work in the Wess-Zumino gauge, in which we can write

$$V\left(x,\theta,\bar{\theta}\right) = -\theta\sigma^{\mu}\bar{\theta}A_{\mu}+i\theta\theta\bar{\theta}\bar{\lambda}-i\bar{\theta}\bar{\theta}\theta\lambda+\frac{1}{2}\theta\theta\bar{\theta}\bar{\theta}d. \tag{IV.10}$$

The gauge transformations on chiral superfields can be read as

$$\Phi \quad \rightarrow \quad e^{\Lambda}\Phi, \tag{IV.11}$$

so that the element $\Phi^{\dagger}e^{gV}\Phi$ remains invariant under gauge transformations. Here we can see that:

$$\begin{aligned} e^{gV} &= 1 + gV + g^2V^2 + \dots \\ &= 1 - g\theta\sigma^{\mu}\bar{\theta}A_{\mu} + ig\theta\theta\bar{\theta}\bar{\lambda} - ig\bar{\theta}\bar{\theta}\theta\lambda + \frac{1}{2}g\theta\theta\bar{\theta}\bar{\theta}\left(d - gA_{\mu}A^{\mu}\right). \end{aligned} \tag{IV.12}$$

We note that the in form as we have written our equations, the gauge symmetry corresponds to $U(1)$, but this analysis stands for the non-abelian case, where Λ is a matrix. The strength field tensor also has an analogous in the superspace formalism. For the abelian situation:

$$\mathcal{W}_{\alpha} \quad = \quad -\frac{1}{4}\bar{D}\bar{D}D_{\alpha}V, \tag{IV.13}$$

and in components

$$\mathcal{W}_{\alpha} \quad = \quad -i\lambda_{\alpha} + \theta_{\alpha}d - \frac{i}{2}\left(\sigma^{\mu}\bar{\sigma}^{\nu}\theta\right)_{\alpha}F_{\mu\nu} + \theta\theta\left(\sigma^{\mu}\partial_{\mu}\bar{\lambda}\right)_{\alpha}. \tag{IV.14}$$

The generalization of the strength superfield to the non-abelian case is read as

$$\left(\mathcal{W}_{\alpha}\right)_{A}^{B} \quad = \quad -\frac{1}{4}\bar{D}\bar{D}\left(e^{-gV}D_{\alpha}e^{gV}\right)_{A}^{B}, \tag{IV.15}$$

which transforms as $\mathcal{W}_{\alpha} \rightarrow e^{-\Lambda}\mathcal{W}_{\alpha}e^{\Lambda}$. Now, we want to be able to write the action in the superspace formalism, where some features of the supersymmetric theory are readily visible. In order to achieve this, we start by reviewing in Grassmann variables the integral rules

$$\int d^2\theta\ \theta\theta = \int d^2\bar{\theta}\ \bar{\theta}\bar{\theta} = 1, \qquad\qquad \int d^4\theta\ \theta\theta\bar{\theta}\bar{\theta} = 1, \tag{IV.16}$$

thus, in general, for an arbitrary function f, it is defined

$$\int d^4\theta\, f\left(x,\theta,\bar{\theta}\right) \quad = \quad \int d^4\theta\left(A\left(x\right) + \theta B\left(x\right) + \dots + \theta\theta\bar{\theta}\bar{\theta}D\left(x\right)\right) \equiv D\left(x\right), \tag{IV.17}$$

or equivalently,

$$\int d^4\theta\, f \quad = \quad \frac{1}{16}\left(\frac{\partial}{\partial\theta_{\alpha}}\frac{\partial}{\partial\theta^{\alpha}}\frac{\partial}{\partial\bar{\theta}^{\dot{\alpha}}}\frac{\partial}{\partial\bar{\theta}_{\dot{\alpha}}}f\right)\Big|_{\theta=\bar{\theta}=0}. \tag{IV.18}$$

In a very similar way, for chiral and anti-chiral functions $f(y,\theta)$ and $\bar{f}(\bar{y},\bar{\theta})$,

$$\int d^2\theta\, f = \frac{1}{4}\left(\frac{\partial}{\partial\theta_\alpha}\frac{\partial}{\partial\theta^\alpha}f\right)\Big|_{\theta=\bar{\theta}=0}, \qquad \int d^2\bar{\theta}\,\bar{f} = \frac{1}{4}\left(\frac{\partial}{\partial\bar{\theta}^{\dot{\alpha}}}\frac{\partial}{\partial\bar{\theta}_{\dot{\alpha}}}\bar{f}\right)\Big|_{\theta=\bar{\theta}=0}. \tag{IV.19}$$

With this, integrals of the kind

$$\int d^4x \int d^4\theta f\left(x,\theta,\bar{\theta}\right) D_\alpha g\left(x,\theta,\bar{\theta}\right), \tag{IV.20}$$

will be supersymmetric, in which can be used the fact that $\{D_\alpha, Q_\beta\} = \{D_\alpha, \bar{Q}_{\dot{\beta}}\} = \{\bar{D}_{\dot{\alpha}}, Q_\beta\} = \{\bar{D}_{\dot{\alpha}}, \bar{Q}_{\dot{\beta}}\} = 0$. Let us see, the way to get the kinetic terms for a theory with one fermion and one scalar. First, it is noted that by expanding in components:

$$\Phi(y,\theta) = \varphi(x) + i\theta\sigma^\mu\bar{\theta}\partial_\mu\varphi(x) + \frac{1}{4}\theta\theta\bar{\theta}\bar{\theta}\Box\varphi(x) + \sqrt{2}\theta\psi(x) - \frac{i}{\sqrt{2}}\theta\theta\partial_\mu\psi(x)\,\sigma^\mu\bar{\theta} + \theta\theta F(x), \tag{IV.21}$$

and a similar result can be achieved for the anti-chiral superfield. Hence:

$$\begin{aligned}\int d^4\theta\Phi(y,\theta)\,\bar{\Phi}\left(\bar{y},\bar{\theta}\right) &= \frac{1}{4}\left(\varphi(x)\,\Box\bar{\varphi}(x) + \bar{\varphi}(x)\,\Box\varphi(x)\right) - \frac{1}{2}\partial_\mu\varphi(x)\,\partial^\mu\bar{\varphi}(x) \\ &\quad -\frac{i}{2}\left(\psi(x)\,\sigma^\mu\partial_\mu\bar{\psi}(x) - \partial_\mu\psi(x)\,\sigma^\mu\bar{\psi}(x)\right) + F(x)\,\bar{F}(x),\end{aligned} \tag{IV.22}$$

thus, if we use integration by parts in x-coordinates, we finally get

$$\int d^4x \int d^4\theta\Phi(y,\theta)\,\bar{\Phi}\left(\bar{y},\bar{\theta}\right) = \int d^4x\left(-\partial_\mu\varphi\partial^\mu\bar{\varphi} - i\psi\sigma^\mu\partial_\mu\bar{\psi} + F\bar{F}\right). \tag{IV.23}$$

Mass terms or Yukawa interactions can appear by chiral polynomial terms in Φ. From Eq. [IV.21] it is easy to see that

$$\begin{aligned}S &= \int d^4x\left[\int d^4\theta\Phi\bar{\Phi} + \int d^2\theta\left(\lambda\Phi + \frac{M}{2}\Phi^2 + \frac{g}{3}\Phi^3\right) + h.c.\right] \\ &= \int d^4x\left[-\left(\partial_\mu\varphi\right)^2 - i\psi\sigma^\mu\partial_\mu\bar{\psi} + F\bar{F} + \left(\lambda F + M\left(\varphi F - \frac{1}{2}\psi\psi\right) + g\left(\varphi^2 F - \psi\psi\varphi\right) + h.c.\right)\right],\end{aligned} \tag{IV.24}$$

so that the equation of motion for the auxiliary field is $\bar{F} = -\lambda - M\varphi - g\varphi^2$, and, hence, when this relation is used to eliminate the auxiliary fields we get the desired mass terms and even a quartic potential.

Similarly, we can write a supersymmetric version of the Maxwell action by means of the strength superfields. With aid of the Eq. [IV.14] it can be shown

$$\begin{aligned}S_{sMaxwell} &= \int d^4x\left(\int d^2\theta\mathcal{W}^\alpha\mathcal{W}_\alpha + \int d^2\bar{\theta}\bar{\mathcal{W}}_{\dot{\alpha}}\bar{\mathcal{W}}^{\dot{\alpha}}\right) \\ &= \int d^4x\left(-\frac{1}{4}F_{\mu\nu}F^{\mu\nu} - i\lambda\sigma^\mu\partial_\mu\bar{\lambda} + \frac{1}{2}d^2\right),\end{aligned} \tag{IV.25}$$

where a surface term has been ignored. For the sake of including matter, we can use the gauge invariant terms discussed previously. Thus, the matter action in this scheme is given by

$$S_{Matter} = \int d^4x \left(\int d^4\theta \left(\bar{\Phi} e^{2eV} \Phi + \bar{\Sigma} e^{-2eV} \Sigma \right) + M \int d^2\theta \Phi \Sigma + M \int d^2\bar{\theta} \bar{\Phi} \bar{\Sigma} \right), \tag{IV.26}$$

where it is understood $\Sigma(y,\theta) = \phi + \sqrt{2}\theta\chi(y) + \theta\theta E(y)$, so that a Dirac spinor associated to electrons and positrons (ψ_α, $\bar{\chi}^{\dot{\alpha}}$), and new particles have been included, the supersymmetric partners of the above mentioned: the selectron φ and the spositron ϕ. With this, we write

$$S^{sQED} = S_{sMaxwell} + S_{Matter}. \tag{IV.27}$$

With all these facts, it is noted that Lagrangians can be built from the general form

$$\mathcal{L} = \int d^4\theta K\left(\Phi^\dagger, e^V \Phi\right) + \left[\frac{1}{g^2} \int d^2\theta f_{\alpha\beta} \mathcal{W}^\alpha \mathcal{W}^\beta + h.c. \right] + \left[\int d^2\theta W(\Phi) + h.c. \right], \tag{IV.28}$$

where the $K\left(\Phi^\dagger, e^V\Phi\right)$ is known as Kähler potential, due to its importance in the Kähler geometry approach, and stands for the kinetic terms for matter and gauge interactions contributions to the scalar potential; the term $W(\Phi)$ is usually named as superpotential, and together with the anti-chiral part give rise to the Yukawa interactions and contribute to the scalar potential through the auxiliary fields. The peculiar function $f_{\alpha\beta}$ in the gauge kinetic term is a symmetric function in their indices and may depend analytically on chiral superfields.

To close this section, we introduce a new class of symmetries that arises in supersymmetric actions. We allowed the Grassmann variables θ and $\bar{\theta}$ to transform under such symmetries, being this the main feature of the new symmetries, since under the known symmetries the Grassmann variables remain invariant. Such class is named as R-symmetries. Being R a generator of R-transformations, the aforementioned feature can be better represented by

$$[R, Q^\alpha] = -Q^\alpha, \qquad \left[R, Q^\dagger_{\dot{\alpha}}\right] = Q^\dagger_{\dot{\alpha}}. \tag{IV.29}$$

An important fact that can be glimpsed from this, is that the R-charge can be different for the components in a supermultiplet, but a charge associated to non-R-symmetries must be the same for all the components of a given supermultiplet.

To see the way R-symmetry works, we allow $\theta \to e^{iK}\theta$ and $\bar{\theta} \to e^{-iK}\bar{\theta}$, and

$$\Phi(y,\theta) \to e^{irK} \Phi\left(y, e^{-iK}\theta\right), \qquad \bar{\Phi}\left(\bar{y},\bar{\theta}\right) \to e^{-irK} \bar{\Phi}\left(\bar{y}, e^{iK}\bar{\theta}\right). \tag{IV.30}$$

	θ_α	$d^2\theta$	Q_α	D_α	$\mathcal{W}_\alpha$	A_μ	λ_α	d
R - charge	+1	-2	-1	-1	+1	0	+1	0

Table IV.1: Conventions of the R-charge belonging to an $U(1)_R$ symmetry for some objects.

With these transformations, we see that setting $\lambda = g = 0$ in the Eq. [IV.24] the action is invariant with $r = 1$, since $d^2\theta \to e^{-2iK} d^2\theta$, while $\frac{M}{2}\Phi^2 \to \frac{M}{2} e^{2iK}\Phi^2$. In this case, it is usually said that the R-charge of the $U(1)_R$ symmetry of Φ is +1. Analogously, the R-charge of θ_α is +1. The R-charge of chiral fields depends on the explicit form of the action, while some objects have an R-charge that may depend just on conventions. In this work, the convention is as shown in table [IV.1].

IV.2 Construction of the MSSM

In order to have a supersymmetric extension of the SM we must start by doubling its particle spectrum, being the new particles the supersymmetric partners of those that we know in the SM. is in this sense that the resulting model is minimal: we are including the minimal number of particles in order to have a supersymmetric version of the SM. Then, with these new degrees of freedom we want to build a Lagrangian that, in addition to be gauge invariant, must be supersymmetric invariant.

We will arrange each SM matter field and its super-partners in a chiral superfield, while to each vector field corresponds a vector superfield, where also must be the associated super-partner of spin 1/2 (gauginos). The supermultiplets that will serve to build the supersymmetric Lagrangian are arranged in the tables [IV.2] and [IV.3]. It can be seen that the super-partners of the fermions are called with an "s" before the known name of the SM fermion. In chiral superfields we use the conjugates of the right-hand particles, where $u^c = u_R^\dagger$ and $\widetilde{u}^c = \widetilde{u}_R^*$.

The superpartners of the Higgs boson are named higgsinos, and it is remarkable that in the MSSM are used two different chiral superfields, one of them gives the masses to up-type quarks, while the other endows with mass down-type quarks. In the MSSM two different Higgs superfields are introduced in order to write a holomorphic superpotential that leads to Yukawa interactions. We also note the main feature that the Higgs superfields have opposite hypercharge, this is chosen in such a way that the MSSM is anomaly free.

Now, with the vector superfields shown in table [IV.3], we can construct the Kähler potential of the MSSM, which must involve the three vector superfields. Then

$$\mathcal{L}_{Kin} = \int d^2\theta d^2\bar{\theta} \sum_{SU(3)_c, SU(2)_L, U(1)_Y} \bar{\Phi}_\beta e^{gV} \Phi_\beta, \tag{IV.31}$$

with $\Phi_\beta = \{Q_i, U_i, D_i, L_i, E_i, H_1, H_2\}$. As it was discussed in the previous section, this part of the Lagrangian,

Fields		spin-0	spin-1/2	$SU(3)_C$, $SU(2)_L$, $U(1)_Y$
Squarks, quarks	Q	$\left(\widetilde{u}_L, \widetilde{d}_L\right)_i$	$(u_L, d_L)_i$	$\left(3,\, 2\,, \frac{1}{3}\right)$
	U_i	$\widetilde{u}_i^c$	u_i^c	$\left(\bar{3},\, 1\,, -\frac{4}{3}\right)$
	D_i	$\widetilde{d}_i^c$	d_i^c	$\left(\bar{3},\, 1\,, \frac{2}{3}\right)$
Sleptons, leptons	L_i	$(\widetilde{\nu}_L,\, \widetilde{e}_L)_i$	$(\nu_L,\, e_L)_i$	$(1,\, 2,\, -1)$
	E_i	e_i^c	$\widetilde{e}_i^c$	$(1,\, 1,\, 2)$
Higgs, higgsinos	H_1	$\left(H_1^0,\, H_1^-\right)$	$\left(\widetilde{H}_1^0,\, \widetilde{H}_1^-\right)$	$(1,\, 2,\, -1)$
	H_2	$\left(H_2^+,\, H_2^0\right)$	$\left(\widetilde{H}_2^+,\, \widetilde{H}_2^0\right)$	$(1,\, 2,\, 1)$

Table IV.2: Particle spectrum of the MSSM that are arranged in chiral superfields, together with their representations under the gauge symmetry of the SM. The index i stands for the generation.

when is expanded in components, brings us the kinetic terms of the SM fermions, sfermions, the Higgs fields and their fermionic super-partners, as well as their interactions with the gauge bosons, moreover yields Yukawa interactions of the kind fermion-sfermion-gaugino where the Yukawa coupling is the gauge one. Analogous interactions for the Higgs are obtained: Higgs-higgsino-gaugino.

Regarding the superpotential, we can have interactions that are independent of the gauge couplings. The superpotential is constructed to be renormalizable so that its mass-dimension must be equal or less than three. The most general form of a renormalizable superpotential is

$$W \;=\; W_1 + W_2, \tag{IV.32}$$

with

$$W_1 \;=\; h^u_{ij} Q_i U_j H_2 + h^d_{ij} Q_i D_j H_1 + h^e_{ij} L_i E_j H_1 + \mu H_1 H_2, \tag{IV.33}$$

$$W_2 \;=\; \epsilon_i L_i H_2 + \lambda_{ijk} L_i L_j E^c_k + \lambda'_{ijk} L_i Q_j D_k + \lambda"_{ijk} U_i D_j D_k, \tag{IV.34}$$

where, as usual, the index i runs among the generations. It is not difficult to see that the interactions yielded in W_2 violate Lepton and Baryon numbers. It is known that such interactions lead to an unstable proton through squark mediation, in opposition to the observation. Then, to avoid such situations, it is imposed a discrete type of R-symmetry: R-parity. Hence, in order to respect R-parity W_2 must vanish. Then we are left with $W = W_1$.

Fields		spin-1/2	spin-1	$SU(3)_C$, $SU(2)_L$, $U(1)_Y$
Gluino, gluon	V_s^A	$\widetilde{G}^A$	G_μ^A	$(8,\, 1\,, 0)$
Winos, W bosons	V_W^I	$\widetilde{W}^\pm,\, \widetilde{W}^0$	$W_\mu^\pm,\, W_\mu^0$	$(1,\, 3,\, 0)$
Bino, B boson	V_Y	$\widetilde{B}$	B_μ	$(1,\, 1,\, -0)$

Table IV.3: Particle spectrum of the MSSM that are arranged in vector superfields, together with their representations under the gauge symmetry of the SM. The indices run as $A = 1, \cdots, 8$ and $I = 1, 2, 3$

So that the superpotential part is given by

$$\mathcal{L}_{Yuk} = \int d^2\theta\, W(\Phi) + h.c. \tag{IV.35}$$

with W given in Eq. [IV.32] with $W_2 = 0$. R-parity (R_p) is known to act on the component fields as:

$$R_p = (-1)^{3(B-L)+2s}, \tag{IV.36}$$

being B and L the Baryon and Lepton numbers, respectively, and s stands for the spin of the particle. With this, we see that under R-parity is possible to distinguish a particle from its super-partner. Then, by looking at Eq. [IV.36] it is noted that each vertex interaction should have at least two supersymmetric partners in order to have R-parity conserved. Thus, let us think about the lightest supersymmetric particle, such particle must be stable, since by definition cannot decay into another supersymmetric particle, and also cannot decay into a pair of SM particles. This is why such light state can be a candidate to be dark matter.

As a remark, in Eq. [IV.34] the gauge indices were omitted. With $SU(2)_L$ index α, the "μ-term" is written in a gauge invariant way through the Levi-Civita symbol as $\mu\epsilon^{\alpha\beta}H_{1\beta}H_{2\alpha}$. Similarly, with a a color index, we have

$$h^u_{ij}\epsilon^{\alpha\beta}Q_{ia\alpha}U^a_j H_{2\beta}. \tag{IV.37}$$

The Lagrangian in Eq. [IV.35] leads to the usual Yukawa interactions of the fermions with the Higgs, it also yields fermion-sfermion-higgsino interactions and pure scalar interactions.

Finally, for the kinetic terms of the gauge fields, we must include the Lagrangian

$$\mathcal{L}_{Gauge} = \int d^2\theta \mathcal{W}^\alpha \mathcal{W}_\alpha + h.c. \tag{IV.38}$$

for each vector superfield in table [IV.3]. The d component of the vector superfields will lead to contributions to the scalar potential. With all this, the Lagrangian of the MSSM takes the form

$$\mathcal{L}^{(0)}_{MSSM} = \mathcal{L}_{Kin} + \mathcal{L}_{Gauge} + \mathcal{L}_{Yuk}, \tag{IV.39}$$

where these different Lagrangians are given by Eq. [IV.31], [IV.38] and [IV.35].

Now, we are able to see that the hierarchy paradox discussed in section [II.3] is solved in the MSSM. A broad discussion can be found in section 5.2 of [68]. Here we only consider the basic idea. When we consider the quantum corrections to the mass of the Higgs there can be the contributions shown in Fig. [IV.1]. As was

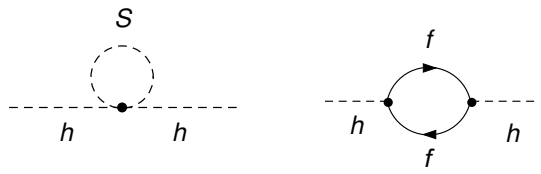

Figure IV.1: Corrections to the Higgs mass from scalars and fermions.

previously discussed, the corrections to the Higgs mass coming from four scalar interactions goes like

$$\sim \quad \lambda\Lambda^2 h^\dagger h, \tag{IV.40}$$

while the fermion part corresponds to

$$\left(-g_f^2 \int^\Lambda d^4k \,\mathrm{Tr}\left[\frac{1}{(\not{k} - m_f)^2}\right]\right) h^\dagger h \quad = \quad \left(-4g_f^2 \int^\Lambda d^4k \,\frac{k^2 + m_f^2}{\left(k^2 - m_f^2\right)^2}\right) h^\dagger h, \tag{IV.41}$$

where the minus sign comes from the fermionic character of the loop. This integral diverges quadratically, then the total correction is like

$$\left(\lambda - g_f^2\right) \Lambda^2 h^\dagger h, \tag{IV.42}$$

so that we see the possibility of eliminating the quadratically sensitivity of the Higgs mass to quantum corrections by having $\lambda = g_f^2$, what is if the coupling of the Higgs to the scalar is intimately related to the coupling of the Higgs to the fermion that runs in the loop. This can occur in a SUSY scenario and is precisely in this direction that the MSSM solves the Hierarchy paradox. In terms of the t' Hooft definition of naturalness, supersymmetry is the symmetry that protects the mass of the Higgs.

IV.3 Spontaneous Symmetry Breaking in the MSSM

We start by looking at the scalar potential contained in the MSSM that contributes to the SSB, i.e. we will not include contributions from sleptons and squarks. To get this potential let us first note that for chiral superpotentials Φ_i and Φ_j,

$$\Phi_i \Phi_j|_{\theta\theta} = -\psi_i \psi_j + F_i \phi_j + F_j \phi_i, \tag{IV.43}$$

so that, with α and β being $SU(2)_L$ indices:

$$\begin{aligned} \mu H_1 H_2 &= \mu \epsilon^{\alpha\beta} H_{2\alpha} H_{1\beta} \\ &= \mu \left(H_1^{(2)} H_2^{(1)} - H_1^{(1)} H_2^{(2)} \right), \end{aligned} \tag{IV.44}$$

which must contain the following terms involving scalar fields:

$$\mu H_1 H_2 \supset \mu \left(F_1^- H_2^+ + H_1^- F_2^+ - F_1^0 H_2^0 - H_1^0 F_2^0 \right), \tag{IV.45}$$

where we have taken $F_1 = \left(F_1^0, F_1^-\right)^T$ and $F_2 = \left(F_1^+, F_1^0\right)^T$. This part of the superpotential also has off-diagonal mass terms for the higgsinos, which we have not written. The anti-holomorphic superpotential will also contribute to the scalar potential, moreover, by recalling that from the Kähler potential there is a term like $F\bar{F}$, the equations of motion for F yield relations such as

$$\bar{F}_1^0 = -\mu H_2^0, \qquad\qquad F_1^0 = -\mu^* \bar{H}_2^0, \tag{IV.46}$$

that when are used to eliminate the auxiliary fields give the term

$$\mu^2 \left(|H_1^0|^2 + |H_2^0|^2 + |H_1^-|^2 + |H_2^+|^2 \right). \tag{IV.47}$$

On the other hand, there are "d-terms" that also contribute to the scalar potential. By expanding in components it is noted that

$$\mathcal{L}_{Kin} \supset g d^A \bar{\varphi} T^A \varphi, \qquad\qquad \mathcal{L}_{Gauge} \supset \frac{1}{2} d^A d^A \tag{IV.48}$$

where φ is the scalar component of the chiral superfields, T^A are the generators, A is an index that runs in the adjoint representation of the gauge group, and where the indices of the fundamental representation were omitted. Then, the equations of motion yield

$$d^A = g \sum_\beta \bar{\varphi}_\beta T^A \varphi^\beta. \tag{IV.49}$$

Thus, when we want to eliminate the auxiliary field it must be computed

$$\frac{1}{2} d^A d^A = \frac{g^2}{2} \left(\sum_\beta \bar{\varphi}_\beta T^A \varphi^\beta \right)^2. \tag{IV.50}$$

Then, in the MSSM must be computed for the $SU(2)_L$ generators

$$\begin{aligned}&\frac{g^2}{2}\left(\bar{H}_1\cdot\tau^A\cdot H_1+\bar{H}_2\cdot\tau^A\cdot H_2\right)\left(\bar{H}_1\cdot\tau^A\cdot H_1+\bar{H}_2\cdot\tau^A\cdot H_2\right)\\&\quad=\frac{g^2}{2}\left(\bar{H}_1\cdot\tau^A\cdot H_1\right)\left(\bar{H}_1\cdot\tau^A\cdot H_1\right)+2\left(\bar{H}_2\cdot\tau^A\cdot H_2\right)\left(\bar{H}_1\cdot\tau^A\cdot H_1\right)+\left(\bar{H}_2\cdot\tau^A\cdot H_2\right)\left(\bar{H}_2\cdot\tau^A\cdot H_2\right).\end{aligned} \tag{IV.51}$$

By expanding explicitly, it is found the contribution from the $SU(2)_L$ part:

$$\frac{g^2}{8}\left[\left(|H_1^0|^2+|H_1^-|^2-|H_2^0|^2-|H_2^-|^2\right)^2+4\left(H_2^+\bar{H}_1^0+H_2^0\bar{H}_1^-\right)\left(\bar{H}_2^+H_1^0+\bar{H}_2^0H_1^-\right)\right]. \tag{IV.52}$$

From the $U(1)_Y$ a similar computation follows, where it must be remembered the hypercharges values for the fields, and that in our normalization there is an additional $1/2$ factor in each term involving one hypercharge, then

$$\frac{1}{4}\cdot\frac{g'^2}{2}\left(\bar{H}_2H_2-\bar{H}_1H_1\right)^2 \;=\; \frac{g'^2}{8}\left(|H_1^0|^2+|H_1^-|^2-|H_2^0|^2-|H_2^-|^2\right)^2. \tag{IV.53}$$

With all these results, it is found that the scalar potential contained in Eq. [IV.39] is

$$\begin{aligned}V_{scalar}^{(0)} \;=\;& \mu^2\left(|H_1^0|^2+|H_1^-|^2\right)+\mu^2\left(|H_2^0|^2+|H_2^+|^2\right)+\frac{g^2}{2}|H_2^+\bar{H}_1^0+H_2^0\bar{H}_1^-|^2\\&+\frac{1}{8}\left(g^2+g'^2\right)\left(|H_2^0|^2-|H_1^0|^2+|H_2^+|^2-|H_1^-|^2\right)^2.\end{aligned} \tag{IV.54}$$

Here, the first two terms are precisely mass terms, similar to those obtained in the SM, with a key difference: the expression μ^2 arose from the substitution of the equations of motion, and explicitly is $\mu\cdot\mu^*$, so it only can have positive values. We recall that in order to get spontaneous symmetry breaking the mass terms in the potential should have a negative sign. The potential in Eq. [IV.54] cannot be the full potential of the MSSM. For this reason, we have to include terms that softly break SUSY. The scalar potential coming from the superpotential together with the soft-SUSY-breaking terms is read

$$\begin{aligned}V_{scalar} \;=\;& \left(m_{H_1}^2+\mu^2\right)\left(|H_1^0|^2+|H_1^-|^2\right)+\left(m_{H_2}^2+\mu^2\right)\left(|H_2^0|^2+|H_2^+|^2\right)\\&+\left(b\left(H_1^-H_2^+-H_1^0H_2^0\right)+h.c.\right)+\frac{g^2}{2}|H_2^+\bar{H}_1^0+H_2^0\bar{H}_1^-|^2\\&+\frac{1}{8}\left(g^2+g'^2\right)\left(|H_2^0|^2-|H_1^0|^2+|H_2^+|^2-|H_1^-|^2\right)^2.\end{aligned} \tag{IV.55}$$

Here we have introduced terms parametrized by $m_{H_1}^2$, $m_{H_2}^2$ and b, where the latter is taken to be positive. In addition, it has to be said that the SUSY-breaking terms were put by hand, but in the next section, we will see their possible sources. An additional feature in this potential is the quartic coupling of the neutral fields: it is

given by the couplings g and g', which is in contrast to the situation in the SM, where the λ coupling is a free parameter.

Now, we want to see under which conditions the potential V_{scalar} has a minimum and under which conditions it leads to the SSB of the SM. As is well-known in the SM, it is possible through $SU(2)_L$ transformations to set one of the vev components of the Higgs to zero. In the MSSM this can be done with one of the Higgs doublets, then we choose $H_2^+ = 0$ at the minimum. Then if we compute

$$\frac{\partial V_{scalar}}{\partial H_2^+} = \left(m_{H_2}^2 + \mu^2\right) \bar{H}_2^+ + bH_1^- + \frac{g^2}{2}\left(\bar{H}_2^+ H_1^0 + \bar{H}_2^0 H_1^-\right) \bar{H}_1^0 - \frac{g^2 + g'^2}{4}\left(|H_2^0|^2 - |H_1^0|^2 + |H_2^+|^2 - |H_1^-|^2\right) \bar{H}_2^+, \tag{IV.56}$$

so that at the minimum:

$$\frac{\partial V_{scalar}}{\partial H_2^+}|_{H_2^+=0} \quad = \quad H_1^- \left(b + \frac{g^2}{2}\bar{H}_2^0 \bar{H}_1^0\right) = 0, \tag{IV.57}$$

then we have two possibilities: if $b = -\frac{g^2}{2}\bar{H}_2^0\bar{H}_1^0$ then the b-term in Eq. [IV.55] is strictly possitive and unfavorable for SSB; if $H_1^- = 0$ at the minimum we have negative contributions from the b-term. This shows that neither H_2^+ nor H_1^- have a vev, and being charged, this feature is good in order to have a massless photon.

With vanishing vev's of the charged bosons, we focus on the terms with pure neutral interactions in the scalar potential. Moreover, the analysis can be performed by working just with the absolute values of the scalars. To see this, we note that in order to have a minimum and SSB the term involving $H_2^0 H_1^0$ must be real and positive, then their phases must be equal and opposite, but with the fact that their hypercharges are precisely equal and opposite, each total phase can be set to zero through $U(1)_Y$ transformations. Then, the potential involving the neutral fields takes the form

$$V_{scalar}^{neutral} = \left(m_{H_1}^2 + \mu^2\right)|H_1^0|^2 + \left(m_{H_2}^2 + \mu^2\right)|H_2^0|^2 - 2b|H_1^0||H_2^0| + \frac{1}{8}\left(g^2 + g'^2\right)\left(|H_2^0|^2 - |H_1^0|^2\right)^2. \tag{IV.58}$$

In the limit $H_1^0 = H_2^0$, it is readily visible that to have a potential bounded from below:

$$0 < \quad 2b \quad < 2\mu^2 + m_{H_1}^2 + m_{H_2}^2, \tag{IV.59}$$

so that $\left(m_{H_1}^2 + \mu^2\right)$ and $\left(m_{H_2}^2 + \mu^2\right)$ cannot be negative at the same time. Another constraint to the SUSY-

breaking parameters is yielded by looking to the origin in field space to be a saddle point. With

$$\left.\frac{\partial^2 V_{scalar}}{\partial {H_1^0}^2}\right|_{Origin} = 2\left(m_{H_1}^2+\mu^2\right), \qquad \left.\frac{\partial^2 V_{scalar}}{\partial H_1^0 \partial H_2^0}\right|_{Origin} = -2b, \qquad \left.\frac{\partial^2 V_{scalar}}{\partial {H_2^0}^2}\right|_{Origin} = 2\left(m_{H_2}^2+\mu^2\right), \tag{IV.60}$$

we expect the determinant of the Hessian matrix to be negative for

$$\left(m_{H_1}^2+\mu^2\right)\left(m_{H_2}^2+\mu^2\right) \quad < \quad b^2, \tag{IV.61}$$

which can be satisfied for one of $\left(m_{H_i}^2+\mu^2\right)$ being negative. With the conditions in Eq. [IV.61] and [IV.59] we see that the potential is bounded and that the origin in field space is a saddle point. Hence, the minimum of the potential can be parametrized as

$$\left\langle H_1^0 \right\rangle = \frac{v_1}{\sqrt{2}}, \qquad \left\langle H_2^0 \right\rangle = \frac{v_2}{\sqrt{2}}. \tag{IV.62}$$

Further conditions on v_1 and v_2 can be obtained. From the kinetic term of the Higgs doublets, by insertions of the vev's, it is identified

$$M_Z^2 = \frac{1}{4}\left(g^2+g'^2\right)\left(v_1^2+v_2^2\right), \qquad M_W^2 = \frac{1}{4}g^2\left(v_1^2+v_2^2\right), \tag{IV.63}$$

what is in correspondence with the SM by defining

$$\sqrt{v_1^2+v_2^2} \equiv \quad v \quad = 246\,\text{GeV}. \tag{IV.64}$$

On the other hand, let us compute at the minimum

$$\begin{aligned} \frac{\partial V_{scalar}}{\partial H_1^0} &= 2\left(m_{H_1}^2+\mu^2\right)|H_1^0| - 2b|H_2^0| + \frac{1}{2}\left(g^2+g'^2\right)\left(|H_2^0|^2-|H_1^0|^2\right)|H_1^0| = 0 \\ \Rightarrow \left.\frac{\partial V_{scalar}}{\partial H_1^0}\right|_{H_i^0=v_i/\sqrt{2}} &= \frac{2}{\sqrt{2}}\left(m_{H_1}^2+\mu^2\right)v_1 - \frac{2}{\sqrt{2}}bv_2 + \frac{1}{4\sqrt{2}}\left(g^2+g'^2\right)\left(v_1^2-v_2^2\right)v_1 = 0 \\ &\Rightarrow \left(m_{H_1}^2+\mu^2\right)v_1 = bv_2 - \frac{1}{8}\left(g^2+g'^2\right)\left(v_1^2-v_2^2\right)v_1. \end{aligned} \tag{IV.65}$$

Aanalogously for $|H_2^0|$:

$$\left(m_{H_2}^2+\mu^2\right)v_2 \quad = \quad bv_1 + \frac{1}{8}\left(g^2+g'^2\right)\left(v_1^2-v_2^2\right)v_2. \tag{IV.66}$$

Then, with the definition $\tan = \frac{v_2}{v_1}$ and the relations between vev's and gauge-boson masses, the last two

equations can be written as

$$\begin{aligned} \frac{1}{2}M_Z^2 &= \frac{m_{H_1}^2 - m_{H_2}^2 \tan^2\beta}{\tan^2\beta - 1} - \mu^2, \\ \sin(2\beta) &= \frac{2b}{m_{H_2}^2 + m_{H_1}^2 + 2\mu^2}. \end{aligned} \tag{IV.67}$$

These two equations can be used to write the parameter μ in terms of the $\tan\beta$. In order to match the MSSM with the SM, the above conditions should be satisfied.

IV.4 Supersymmetry Breaking

In the way that was introduced the MSSM, the super-partners and the known particles are in the same supermultiplet, in such a way that both of them must have the same physical properties unless their statistics. With this statement raises the question, why the super-partners were not detected so far if they are supposed to have the same mass that the known particles? With this observation, it is noted that supersymmetry must be broken at scales where the experimental observations have been performed.

In the previous section, we saw that some soft-SUSY-breaking terms were included in order to have the right SSB that allows us to match the MSSM with the physics known from the SM. In this section, we will include further explicit SUSY-breaking terms to the Lagrangian in Eq. [IV.39]. Moreover, we will see some general concepts in spontaneous supersymmetry breaking and which sources could lead to such explicit SUSY breaking terms.

IV.4.1 Soft Supersymmetry Breaking terms and full MSSM Lagrangian

Spontaneous supersymmetry breaking cannot be included in the MSSM since it leads to phenomenological complications, for instance, the super-partner should have a mass lighter than the corresponding one for the associated particle. Thus we will introduce explicit SUSY breaking with the constraint that only those terms that do not reintroduce quadratic divergences can be added. With this, the soft supersymmetry breaking terms are classified as

1. *Gaugino mass terms*: We have gauginos corresponding to each of the three vector superfields introduced for the gauge group of the SM, with these gaugino fields it is possible to construct the terms

$$M_1 \widetilde{B}\widetilde{B}, \qquad M_2 \widetilde{W}^I \widetilde{W}^I, \qquad M_3 \widetilde{G}^A \widetilde{G}^A, \tag{IV.68}$$

with $I = 1, 2, 3$ and $A = 1, \ldots, 8$.

2. *Scalar mass terms*: For every scalar coming from each chiral superfield it is possible to include a mass term of the form $m^2_{\phi_{ij}} \phi_i^* \phi_j$, where flavor violation can occur through the non-diagonal elements of the matrix $m^2_{\phi_{ij}}$. The possible mass terms are

$$m^2_{Q_{ij}} \tilde{Q}_i^\dagger \tilde{Q}_j, \quad m^2_{u_{ij}} \tilde{u}_i^{c*} \tilde{u}_j^c, \quad m^2_{d_{ij}} \tilde{d}_i^{c*} \tilde{d}_j^c, \quad m^2_{L_{ij}} \tilde{L}_i^\dagger \tilde{L}_j, \quad m^2_{e_{ij}} \tilde{e}_i^{c*} \tilde{e}_j^c, \quad m^2_{H_1} H_1^\dagger H_1, \quad m^2_{H_2} H_2^\dagger H_2, \tag{IV.69}$$

where the last two terms were already used in the previous section.

3. *Trilinear scalar couplings*: These interactions are built in the form $A_{ijk} \phi_i \phi_j \phi_k$, and with gauge symmetry of the SM we can construct three types of such interactions:

$$A^u_{ij} \tilde{Q}_i \tilde{u}_j^c H_2, \qquad A^d_{ij} \tilde{Q}_i \tilde{d}_j^c H_i, \qquad A^e_{ij} \tilde{L}_i \tilde{e}_j^c H_1, \tag{IV.70}$$

which are of the same kind that those obtained from the Yukawa couplings.

4. *Bilinear scalar couplings*: These terms correspond to the bilinear terms that already appear in the superpotential, being of the kind $B_{ij} \phi_i \phi_j$. With the gauge symmetries there is only one bilinear scalar coupling:

$$b H_1 H_2, \tag{IV.71}$$

which also was included in the scalar potential to obtain SSB of the gauge symmetry.

These terms together with the Lagrangian in Eq. [IV.39] compose the full MSSM Lagrangian:

$$\mathcal{L}_{MSSM} \;=\; \mathcal{L}^{(0)}_{MSSM} + \mathcal{L}_{Soft}. \tag{IV.72}$$

IV.4.2 Spontaneous Supersymmetry Breaking

Now, in the way the MSSM was built, it can be seen like an effective theory, where the soft SUSY breaking terms come from some hidden sector so that the dynamics of the spontaneous supersymmetry breaking happens in this hidden sector. Then, arises the question, under which conditions can be reached a spontaneous supersymmetry breaking.

From the SUSY algebra in Eq. [IV.1], we can write

$$\mathcal{H} \;=\; \frac{1}{4} \left(\bar{Q}_1 Q_1 + \bar{Q}_2 Q_2 + h.c. \right). \tag{IV.73}$$

If we want a supersymmetric vacuum it is natural to claim $Q|0\rangle = 0$, thus, a non-zero vacuum energy signals a spontaneous SUSY breaking. With the same observation, we note that from

$$\delta_\xi (field) \quad = \quad \left(\xi Q + \bar{\xi}\bar{Q}\right)(field), \tag{IV.74}$$

spontaneous SUSY breaking can happen if

$$\langle 0|\delta_\xi (field)|0\rangle \quad \neq \quad 0. \tag{IV.75}$$

By recalling the transformation of the fermionic component of the chiral superfield and for the gaugino:

$$\delta_\xi \psi = i\sqrt{2}\sigma^\mu \bar{\xi}\partial_\mu \phi + \sqrt{2}\xi F, \qquad \delta_\xi \lambda = \sigma^{\mu\nu}\xi v_{\mu\nu} + i\xi D, \tag{IV.76}$$

spontaneous SUSY breaking is reached when

$$\langle 0|F|0\rangle \neq 0, \qquad \langle 0|\delta_\xi \lambda|0\rangle \propto \langle 0|D|0\rangle \neq 0, \tag{IV.77}$$

since the only Lorentz invariants are the F- and D-terms. This fact also appears when we investigate the scalar potential. In a theory with chiral superfields Φ_i, the possible contributions to the scalar potential are of the kind

$$V_F = g_{ij}^{-1}\frac{\partial W^*}{\partial \Phi_i^*}\frac{\partial W}{\partial \Phi_j} = g_{ij}^{-1}F_i^* F_j, \qquad V_D = \frac{g^2}{2}\left(\sum_i \Phi^{\dagger i}T^a\Phi^i\right)^2, \tag{IV.78}$$

with

$$g^{ij} = \frac{\partial^2 K}{\partial\Phi_i \partial\Phi_j^*}, \qquad \text{and} \qquad F_i = \frac{\partial W}{\partial \Phi_i}, \tag{IV.79}$$

where g_{ij} is the hermitian metric of the Kähler manifold specified by the Kähler potential K. Thus, with the total scalar potential being

$$V = V_F + V_D, \tag{IV.80}$$

it is expected to have supersymmetry spontaneously broken by a non-vanishing vev for F and/or D. Hence, if does not exist a point in field space that satisfies the condition $\frac{\partial W}{\partial \Phi_i} = 0$ then SUSY is broken. Actually, here some conditions on the Kähler potential should be imposed, since V_F can vanish if g^{-1} explodes, but we will not worry about that.

In the most general fashion, to find the zeros of V in a theory with gauge interactions it is needed:

1. Finding the sub-space for which $D^a = 0$, *i.e.* the well known "D-flat directions". This sub-space is parametrized by the vev's of the chiral gauge invariants.

2. If for a sub-space of D-flat directions we also have $F_i = 0$ then the potential is zero. Such sub-space is named as "Moduli space".

With this, we look for the moduli space of a given theory, so that when this space is empty SUSY is spontaneously broken.

An example of D-flat directions is found in the $SU(N)$ gauge theory with chiral fields Q_i, in the fundamental representation, and $\bar{Q}^i$, in the anti-fundamental representation, with $i = 1, \cdots, F$. In this case, the D-flat directions are found when

$$\begin{aligned} D^a &= -g\left(Q^{*in}\left(T^a\right)_n^m Q_{im} - \bar{Q}^{in}\left(T^a\right)_n^m \bar{Q}^*_{im}\right) \\ &= -g\left(T^a\right)_n^m \left(Q^{*in}Q_{im} - \bar{Q}^{in}\bar{Q}^*_{im}\right) \end{aligned} \tag{IV.81}$$

vanishes. The generators $\left(T^a\right)_n^m$ are traceless so that the D-flat directions stand for

$$Q^{*in}Q_{im} - \bar{Q}^{in}\bar{Q}^*_{im} = c\delta^n_m, \tag{IV.82}$$

with c a constant. Each one of the fields in Eq. [IV.82] when seen as matrices have rank F, so that, with $\text{Rank}(AB) = \min\left(\text{Rank}(A), \text{Rank}(B)\right)$, the rank of the bilinears $Q^{*in}Q_{im}$ and $\bar{Q}^{in}\bar{Q}^*_{im}$ is also F. Then, such bilinears can be diagonalized through gauge transformations, where $N-F$ diagonal elements are zero for $F < N$, and

$$Q^{*in}Q_{im} = \bar{Q}^{in}\bar{Q}^*_{im}. \tag{IV.83}$$

Moreover, in this theory, there is a $SU(F)_L \times SU(F)_R$ global symmetry that allows parametrizing the D-flat directions

$$Q_{im} = \bar{Q}_{im} = v_{(i)}\delta_{im}. \tag{IV.84}$$

Another way to see if SUSY is broken is through R-symmetry. Basically, if R-symmetry is broken, then SUSY also is. This is not so difficult to be proved. Let us note that the set of equations

$$\frac{\partial W}{\partial \Phi_i} = 0, \quad i = 1, \cdots, n, \tag{IV.85}$$

are n holomorphic equations for n unknown fields. In general, this system has a solution. This no longer

stands for the situation with R-symmetry breaking. The superpotential is polynomial in the chiral superfields Φ_i $(i = 1, \cdots, n)$ with R-charge r_i. The superpotential by itself has R-charge 2. Then, at least one superfield Φ_j should have positive R-charge, which, by assumption, is taken to have non-zero vev. Now, in terms of R-neutral fields

$$X_i \quad = \quad \frac{\Phi_i}{\Phi_j^{r_i/r_j}}, \tag{IV.86}$$

the superpotential can be written as

$$W \quad = \quad \Phi_j^{2/r_j} f\left(X_i\right). \tag{IV.87}$$

R-symmetry is broken for $\langle \Phi_j \rangle \neq 0$, so that for a supersymmetric minimum the equations

$$\frac{\partial f}{\partial X_i} = 0, \qquad\qquad f\left(X_i\right) = 0, \tag{IV.88}$$

must be satisfied. This is a system of n equations for $n-1$ unknown fields, which in general does not have a solution, so that SUSY is also broken.

Then, sufficient but not necessary conditions for SUSY breaking are:

1. No flat directions.

2. A spontaneously broken global symmetry.

There are two kinds of models that present spontaneous supersymmetry breaking at tree-level: F- and D-type models. The F-type models lead to SUSY breaking by suitable superpotential so that we do not worry about the D-term coming from the gauge interactions. Let us see a variation of the canonical O'Raifeartaigh model, in which the superpotential is built out with the chiral superfields Y_i, Z_i and X $(i = 1, 2.)$:

$$W \quad = \quad X\left(Y_1 Y_2 - M^2\right) + m_1 Z_1 Y_1 + m_2 Z_2 Y_2. \tag{IV.89}$$

By looking at the F-flat directions, we must solve the system of equations

$$\begin{aligned} F_{Y_1}: \quad & XY_2 + m_1 Z_1 = 0, \qquad F_{Z_1}: \quad m_1 Y_1 = 0 \quad , \qquad F_X: \quad Y_1 Y_2 = M^2, \\ F_{Y_2}: \quad & XY_1 + m_2 Z_2 = 0, \qquad F_{Z_2}: \quad m_2 Y_2 = 0 \quad , \end{aligned} \tag{IV.90}$$

but such system cannot be solved together for m_1, m_2 and M non-zero, then supersymmetry is broken in this

model. The minimum of the potential is found to be at

$$\langle Y_1 \rangle = v_1 = \sqrt{\frac{m_2}{m_1}}\sqrt{M^2 - m_1 m_2}, \qquad Z_1 = -\frac{1}{m_1} X Y_2, \tag{IV.91}$$

for $m_1, m_2 \ll M$ and for the other fields should be made $1 \leftrightarrow 2$. In addition, here there is also an $U(1)$ symmetry under which the charges can be chosen to be $r_X = 0$, $r_{Y_1} = 1$, $r_{Y_2} = -1$, $r_{Z_1} = -1$ and $r_{Y_2} = 1$. With the minimum in Eq. [IV.91] it is found that the $U(1)$ symmetry is broken, as should be for a SUSY broken theory.

The D-type models for SUSY breaking are such that the source of the breaking comes from the D-term in the gauge interactions. The canonical example is the Fayet-Iliopulos model [50], where for the $U(1)$ gauge symmetry the vector superfield is gauge invariant by itself, so that can be included alone in the Lagrangian.

Now, a natural question is, what is $Q_\alpha |0\rangle \neq 0$ if it is not zero? As it is known from the Goldstone theorem, for every broken generator involved in a SSB must there be a Goldstone boson, then SUSY being a spontaneously global symmetry must have a Goldstone particle. The state $Q_\alpha |0\rangle$ gives the Goldstone fermion in SUSY breaking: the goldstino $\psi^G_\alpha (x)$.

With the supercurrent

$$J^\mu_\alpha \sim \sum_\phi \frac{\delta \mathcal{L}}{\delta (\partial_\mu \phi)} (\delta\phi)_\alpha \,, \tag{IV.92}$$

the goldstino comes as a massless excitation from the touch between the SUSY current and the vacuum

$$\langle 0 | J^\mu_\alpha | \psi_\beta \rangle = f (\gamma^\mu)_{\alpha\beta} \,, \tag{IV.93}$$

with f the coupling of the supercurrent to the goldstino. A term linear in the fields can only come if $(\delta\phi)_\alpha$ gets a vev. But we have already seen that the only fields that are able to develop a vev through their variations are the fermion component of a chiral superfield (ψ_α) and the gaugino (λ_α), thus

$$J^\alpha_\mu \sim \sum_i \frac{\delta \mathcal{L}}{\delta (\partial_\mu \psi_{i\alpha})} \langle F_i \rangle + \frac{1}{\sqrt{2}} \sum_a \frac{\delta \mathcal{L}}{\delta (\partial_\mu \lambda^a_\alpha)} \langle D^a \rangle \,, \tag{IV.94}$$

so that the goldstino is

$$\psi^G \sim \sum_i \langle F_i \rangle \psi_i + \sum_a \langle D^a \rangle \lambda^a. \tag{IV.95}$$

As a remark, we only mention the non-renormalization theorems, which state that the tree level superpotential is not corrected by loops effects. With this, for a supersymmetric theory with a given superpotential at tree level and with a scalar potential vanishing at some point, $V^{tree}_{scalar}|_{minimum} = 0$, the ground state energy remains zero to all orders in perturbation theory.

This fact can be understood in terms of the goldstino. If at tree level SUSY is unbroken, then there is no a massless fermion being the goldstino, so, how could it happen that through quantum corrections a massless particle arises? In the case that there were massless fermions, such particles may take the role of the goldstino, but for this to occur, such fermion should satisfy the relation [IV.93], so that f would be non-zero, this through quantum corrections. But actually f cannot obtain such non-zero value through loops corrections since it is closely related to the ground energy state:

$$E_{Vacuum} = f^2. \tag{IV.96}$$

A very instructive discussion is found in the paper published by Witten on dynamical supersymmetry breaking [49].

With this, supersymmetry can only be broken dynamically by non-perturbative effects in a theory where SUSY is conserved at tree-level. An example of such non-perturbative effects are the instantons in a $SU(N)$ theory with F fermions:

$$S_{Inst} = \frac{1}{2g^2}\int d^4x \left(F_{\mu\nu}\right)^2 \sim \frac{8\pi^2}{g^2}, \tag{IV.97}$$

which can generate the fermion-scalar interactions from the superpotential

$$W_{n-pert.} = c\left(\frac{\Lambda^{3N-F}}{\det\left(Q\cdot\bar{Q}\right)}\right)^{1/(N-F)}, \tag{IV.98}$$

with c a constant and Λ the characteristic scale of the associated gauge group.

A classic example of dynamical supersymmetry breaking given by this superpotential is the 3-2 model. In this model the superpotential in Eq. [IV.98] is determined by holomorphy and symmetries. The gauge symmetry is given by $SU(3)\times SU(2)$ and the field content is

$$Q\sim(3,2)\,,\quad \bar{Q}_A\sim(\bar{3},1)\,,\quad L\sim(1,2)\,, \tag{IV.99}$$

with $A = 1,2$. The global charges of the symmetry group $U(1)\times U(1)_R$ are assigned as $Q\sim(1/3,1)$, $\bar{Q}_1\,(-4/3,-8)$, $\bar{Q}_2\,(2/3,4)$ and $L\,(-1,-3)$.

With i and α being $SU(3)$ and $SU(2)$ indices, respectively, the renormalizable superpotential consistent with the symmetries at tree level is

$$W_{tree} = \lambda Q\cdot\bar{Q}_2\cdot L = \lambda Q_{i\alpha}\bar{Q}_2^i L_\beta\epsilon^{\alpha\beta}. \tag{IV.100}$$

It can be tested that SUSY is broken. The flat directions are found through the possible gauge and invariants

built with the field content:

$$\begin{aligned} X_A &= \epsilon^{\alpha\beta} Q_{i\alpha} \bar{Q}^i_A L_\beta, \\ Y &= \det\left(Q \cdot \bar{Q}\right) = \epsilon^{\alpha\beta}\epsilon^{AB} Q_{i\alpha}\bar{Q}^i_A Q_{j\beta}\bar{Q}^j_B \end{aligned} \tag{IV.101}$$

The equation

$$\frac{\partial W}{\partial L_\beta} = \lambda Q_{i\alpha}\bar{Q}^i_A \epsilon^{\alpha\beta} = 0, \tag{IV.102}$$

is satisfied at $X_2 = 0$. Analogously, we see that $X_1 = Y = 0$, being the origin the only supersymmetric point. This supersymmetric point is lifted when the non-perturbative effects of $W_{n-pert.}$ are included. The superpotential in Eq. [IV.98] precisely throws away of the origin the ground state found at $Y = 0$, leading to spontaneous SUSY breaking, being Λ also the scale for the dynamical supersymmetry breaking. When Y acquires a vev also ends up breaking the R-symmetry of the classical superpotential.

Not always is possible to find the superpotential expression as in the 3-2 model, but we can know that supersymmetry is broken. A good example is found in the $SU(5)$ theory with field content in the representations $T \sim 10$ and $\bar{F} \sim \bar{5}$. With this, we see that it is not possible to write a holomorphic superpotential with gauge invariant terms so that there are no flat directions. In addition to this, it can also be proved that the global symmetry $U(1) \times U(1)_R$ under which the fields have the charges $T \sim (1, 1)$ and $\bar{F} \sim (-3, -9)$ is broken by anomalous effects if this $SU(5)$ theory confines. Then, indirectly it is known that this theory presents SUSY breaking, but it is not known an expression for the superpotential.

With all these concepts in supersymmetry breaking, it is possible to construct an underlying theory that serves as a hidden sector for the soft-SUSY-terms introduced in the MSSM. One of the drawbacks of the MSSM as a phenomenological model is the number of new parameters introduced. Just the inclusion of the soft-SUSY-terms adds a lot of new parameters. The idea is that the fundamental symmetry could give an explanation for the soft-breaking parameters in terms of a few amount of parameters of the underlying theory. In some cases, it is just needed the scale Λ at which happens the dynamical supersymmetry breaking

There are many models of this kind, some of them are:

1. Gravity mediation, or mediation by Planck-suppressed higher-dimension operators.

2. Anomaly mediated supersymmetry breaking.

3. Gauge mediated supersymmetry breaking.

IV.5 Mass spectrum of the MSSM

The potential in Eq. [IV.55] shows that it is required a change in the basis of the Higgs fields in order to get the particle spectrum. At this point, it is useful to see that the 2HDM studied in the chapter [III] is related to the Higgs sector of the MSSM, so that the rotation matrices used to get the physical states are the same as in the 2HDM. The change of the basis goes as

$$\begin{pmatrix} H_2^0 \\ H_1^0 \end{pmatrix} = \begin{pmatrix} v_2 \\ v_1 \end{pmatrix} + \frac{1}{\sqrt{2}} R_1 \begin{pmatrix} h^0 \\ H^0 \end{pmatrix} + \frac{i}{\sqrt{2}} R_2 \begin{pmatrix} G^0 \\ A^0 \end{pmatrix}, \tag{IV.103}$$

for the neutral scalars, while for the charged ones

$$\begin{pmatrix} H_2^+ \\ H_1^{-*} \end{pmatrix} = R_2 \begin{pmatrix} G^+ \\ H^+ \end{pmatrix}, \tag{IV.104}$$

with

$$R_1 = \begin{pmatrix} \cos\alpha & \sin\alpha \\ -\sin\alpha & \cos\alpha \end{pmatrix}, \qquad R_2 = \begin{pmatrix} \sin\beta & -\cos\beta \\ \cos\beta & \sin\beta \end{pmatrix}. \tag{IV.105}$$

To see this, let us see that the mass term obtained from the scalar potential for the imaginary part of the neutral scalars is

$$\mathcal{L}_{Pseudo-scalar} = -\frac{1}{2} \left(\mathrm{Im}\left(H_2^0\right), \mathrm{Im}\left(H_1^0\right) \right) M_{p-s}^2 \begin{pmatrix} \mathrm{Im}\left(H_2^0\right) \\ \mathrm{Im}\left(H_1^0\right) \end{pmatrix}, \tag{IV.106}$$

with

$$M_{p-s}^2 = \begin{pmatrix} m_{H_2}^2 + \mu^2 - \frac{1}{8}\left(g^2 + g'^2\right)\left(v_1^2 - v_2^2\right) & b \\ b & m_{H_1}^2 + \mu^2 + \frac{1}{8}\left(g^2 + g'^2\right)\left(v_1^2 - v_2^2\right) \end{pmatrix}. \tag{IV.107}$$

This is simplified when we use the minimization conditions in the form of the Eq. [IV.65] and [IV.66]:

$$M_{p-s}^2 = b \begin{pmatrix} \frac{v_1}{v_2} & 1 \\ 1 & \frac{v_2}{v_1} \end{pmatrix}. \tag{IV.108}$$

Then, by diagonalizing through R_2, the physical masses are:

$$m_{G^0}^2 = 0, \qquad m_{A^0}^2 = \frac{b}{v_1 v_2}\left(v_1^2 + v_2^2\right) = \frac{2b}{\sin(2\beta)} = 2\mu^2 + m_{H_1}^2 + m_{H_2}^2, \tag{IV.109}$$

where $\tan\beta = \frac{v_2}{v_1}$, as in the 2HDM. The matrix for the charged Higgses is very similar. The diagonalized masses turn out to be

$$m^2_{G^\pm} = 0, \qquad m^2_{H^\pm} = \left(\frac{b}{v_1 v_2} + \frac{1}{4}g^2\right)\left(v_1^2 + v_2^2\right) = m^2_{A^0} + m^2_W. \tag{IV.110}$$

The computations get more difficult for the real part of the neutral Higgs bosons. The mass term for these scalars is written as

$$\mathcal{L}_{Scalars} = -\frac{1}{2}\left(\mathrm{Re}\left(H_2^0\right), \mathrm{Re}\left(H_1^0\right)\right) M_s^2 \begin{pmatrix} \mathrm{Re}\left(H_2^0\right) \\ \mathrm{Re}\left(H_1^0\right) \end{pmatrix}, \tag{IV.111}$$

where

$$M_s^2 = \begin{pmatrix} 2m^2_{H_2} + 2\mu^2 + \frac{1}{4}\left(g^2 + g'^2\right)\left(3v_2^2 - v_1^2\right) & -2b - \frac{1}{4}v_1 v_2\left(g^2 + g'^2\right) \\ -2b - \frac{1}{4}v_1 v_2\left(g^2 + g'^2\right) & 2m^2_{H_1} + 2\mu^2 + \frac{1}{4}\left(g^2 + g'^2\right)\left(3v_1^2 - v_2^2\right) \end{pmatrix}. \tag{IV.112}$$

By using the definition of the pseudoscalar A^0 and through the minimization conditions, the mass matrix is simplified as

$$M_s^2 = \begin{pmatrix} m^2_{A^0}\cos^2\beta + M_Z^2\sin\beta & -\left(m^2_{A^0} + M_Z^2\right)\sin\beta\cos\beta \\ -\left(m^2_{A^0} + M_Z^2\right)\sin\beta\cos\beta & m^2_{A^0}\sin^2\beta + M_Z^2\cos\beta \end{pmatrix}. \tag{IV.113}$$

Then, the rotation in the field space yielded by the matrix R_2 leads to the physical masses:

$$m^2_{h^0,H^0} = \frac{1}{2}\left[m^2_{A^0} + M_Z^2 \mp \sqrt{\left(m^2_{A^0} + M_Z^2\right)^2 - 4M_Z^2 m^2_{A^0}\cos^2(2\beta)}\right]. \tag{IV.114}$$

The angle used in the rotation is given by

$$\frac{\tan 2\alpha}{\tan 2\beta} = \frac{m^2_{A^0} + M_Z^2}{m^2_{A^0} - M_Z^2}. \tag{IV.115}$$

Then, the particle spectrum is as in the 2HDM: from the 8 real scalars introduced through the two Higgs doublets H_1 and H_2 we are left with 5 physical scalars, 2 neutral scalars (h^0, H^0), 1 pseudo-scalar (A^0) and two charged Higgses ($H^\pm$); while 3 of the 8 initial scalars are the would-be Nambu-Goldstone bosons (G^0, $G^\pm$), that are "eaten" by the weak bosons.

It is important to note from the Eq. [IV.114] that the mass of the lightest Higgs has an upper limit, corresponding to $m_{h^0} < M_Z$. The bound is extremized for large m_{A^0} and large $\tan\beta$. We can see that for the case of $m_{A^0} \gg M_Z$ an expansion in terms of (M_Z/m_{A^0}) leads to the tree-level relation

$$m_{h^0} < M_Z\,|\cos(2\beta)|\,. \tag{IV.116}$$

Currently, it is known that the Higgs boson is heavier than the Z-boson. This limit can be lifted by including radiative corrections or tree-level corrections.

Now, the fermionic super-partners of these scalars, or higgsinos, will be joined with the super-partners of the weak vectorial bosons, or gauginos, in order to form the *Neutralinos* and *Charginos*.

The neutral higgsinos and gauginos are arranged as $\Psi_{\tilde{N}}^T = \left(\tilde{B},\, \tilde{W}^0,\, \tilde{H}_1^0,\, \tilde{H}_2^0\right)$, so that mass terms for the neutralinos are

$$\mathcal{L}_{Mass\ Neutralinos} = -\frac{1}{2}\Psi_{\tilde{N}}^T M_{\tilde{N}} \Psi + c.c. \tag{IV.117}$$

with

$$M_{\tilde{N}} \;=\; \begin{pmatrix} M_1 & 0 & -M_Z c_\beta s_W & M_Z s_\beta s_W \\ 0 & M_2 & M_Z c_\beta c_W & -M_Z s_\beta c_W \\ -M_Z c_\beta s_W & M_Z c_\beta c_W & 0 & -\mu \\ M_Z s_\beta s_W & -M_Z s_\beta c_W & -\mu & 0 \end{pmatrix}, \tag{IV.118}$$

where $c_\beta = \cos\beta$, $c_W = \cos\theta_W$, $s_\beta = \sin\beta$ and $s_W = \sin\theta_W$. In this matrix the diagonal entries M_1 and M_2 are the coefficients introduced in Eq. [IV.68]. The μ entries come from the scalar potential in Eq. [IV.55], while the other entries come from the gauge interactions in the Kähler potential for the Higgs superfields. Actually, the matrix naturally arises in terms of the vev's and electroweak couplings, but with the formulae $\left(g^2 + g'^2\right) v^2 = 2M_Z^2$, $v_2 = v\sin\beta$ and $v_1 = v\cos\beta$ we arrive to the $M_{\tilde{N}}$ shown in Eq. [IV.118]. This matrix can also be diagonalized to get the physical neutralinos fields $\widetilde{N}_i$ by doing a rotation in the field space:

$$\widetilde{N}_i \;=\; R_{\tilde{N}ij}\Psi_{\tilde{N}j}, \tag{IV.119}$$

so that

$$R^* M_{\tilde{N}} R^{-1} \;=\; \mathrm{Diag}\left(m_{\tilde{N}_1}, m_{\tilde{N}_2}, m_{\tilde{N}_3}, m_{\tilde{N}_4}\right). \tag{IV.120}$$

For the charginos the charged gauginos and higgsinos are arranged as $\Psi^{\pm\,T}_C = \left(\widetilde{W}^+,\, \widetilde{H}_2^+,\, \widetilde{W}_1^-,\, \widetilde{H}_1^-\right)$, thus the mass term for the charginos comes to be:

$$\mathcal{L}_{Mass\ Charginos} = -\frac{1}{2}\ \Psi_C^{\pm\,T}\, M_{\tilde{C}} \Psi_C^{\pm} + c.c. \tag{IV.121}$$

where $M_{\widetilde{C}}$ is a 2×2 block matrix, given by

$$M_{\widetilde{C}} = \begin{pmatrix} 0 & X^T \\ X & 0 \end{pmatrix}, \qquad \text{and} \quad X = \begin{pmatrix} M_2 & \sqrt{2}M_W \sin\beta \\ \sqrt{2}M_W \cos\beta & \mu \end{pmatrix}. \tag{IV.122}$$

It is possible to diagonalize this non-symmetric matrix by a bi-unitary transformation in the field space. Hence, the charginos states are given by

$$\begin{pmatrix} \widetilde{C}_1^+ \\ \widetilde{C}_2^+ \end{pmatrix} = V \begin{pmatrix} \widetilde{W}^+ \\ \widetilde{H}_2^+ \end{pmatrix}, \qquad \begin{pmatrix} \widetilde{C}_1^- \\ \widetilde{C}_2^- \end{pmatrix} = U \begin{pmatrix} \widetilde{W}^- \\ \widetilde{H}_1^- \end{pmatrix}. \tag{IV.123}$$

With this, each X-block of the mass matrix is diagonalized as

$$U^* X V^\dagger = \begin{pmatrix} m_{\widetilde{C}_1} & 0 \\ 0 & m_{\widetilde{C}_2} \end{pmatrix}. \tag{IV.124}$$

The eigenvalues of the 4×4 mass matrix $M_{\widetilde{C}}^\dagger M_{\widetilde{C}}$ are degenerate, and actually just the two masses

$$m^2_{\widetilde{C}_1}, m^2_{\widetilde{C}_2} = \frac{1}{2}\left[M_2^2 + \mu^2 + 2M_W^2 \mp \sqrt{\left(M_2^2 + \mu^2 + 2M_W^2\right)^2 - 4|\mu M_2 - M_W^2 \sin(2\beta)|^2}\right] \tag{IV.125}$$

are obtained. The relevant physics comes when M_W is taken to be a perturbation, and M_2 and μ taken to be reals, so that the eigenvalues are approximately $m^2_{\widetilde{C}_1} \approx M^2$ and $m^2_{\widetilde{C}_2} \approx \mu^2$, being the former a wino-like eigenstate and the latter a higgsino-like eigenstate. By checking these conclusions it is possible to test experimentally the assumptions made on the parameters. A similar situation happens with the neutralinos.

In Eq. [IV.68] we also introduced mass terms for the gluinos. Since the gluinos form the unique color octect in the MSSM, they cannot mix with another field in order to the strong interaction does not break spontaneously. Then, the only source for mass terms associated to the gluinos is the M_3-term:

$$\begin{aligned} \mathcal{L}_{Mass\ Gluinos} &= -\frac{1}{2} M_3 \widetilde{G}^A \widetilde{G}^A + h.c. \\ &= -\frac{1}{2} M_3 \bar{\Psi}^A_{\widetilde{G}} \Psi^A_{\widetilde{G}}, \end{aligned} \tag{IV.126}$$

where in the second line we have written the Lagrangian in terms of Majorana fermions.

The only remaining physical states to be found are the sfermions. It must be recalled that we introduced soft-SUSY-breaking mass-terms for the sfermions, but in addition to them, mass-terms from the superpotential

can be yielded after electroweak SSB. In general, the mass terms for the sfermion Φ can be written as

$$\mathcal{L}_{Mass\ sfermions} = -\frac{1}{2}\Phi^{\dagger}_{sf} M^2_{sf} \Phi_{sf}, \tag{IV.127}$$

with

$$M^2_{sf} = \begin{pmatrix} m^2_{f,\,L} + m^2_f + M^2_Z \cos(2\beta)\left(T^L_3 - Q_f s^2_W\right) & m_f M^f_{LR} \\ m_f M^f_{LR} & m^2_{f,\,R} + m^2_f + M^2_Z \cos(2\beta)\, Q_f s^2_W \end{pmatrix}. \tag{IV.128}$$

In the above equation, Q_f stands for the fermion electric charge, T^L_3 is the weak isospin of the left-handed fermion and $m_{f,(R,L)}$ are the soft-SUSY breaking masses. Moreover,

$$M^f_{LR}{}^2 = \frac{1}{2} Y_f \cdot v_2 - m_f \mu \tan\beta \qquad \text{for } f = e, d \tag{IV.129}$$

$$M^f_{LR}{}^2 = \frac{1}{2} Y_f \cdot v_1 - m_f \mu \cot\beta \qquad \text{for } f = u. \tag{IV.130}$$

It is important to note that the entries of the M^2_{sf} matrix are 3×3 matrices in the flavor space, there the generation indices were omitted. In this fact resides the reason why this sector must be treated with care, here there can be non-standard sources of flavor-changing neutral currents (FCNC).

The weak basis above can be rotated in order to get the mass-eigenstates by doing

$$\widetilde{\Phi}_{sf} = R^f \Phi_{sf}, \qquad \text{with} \qquad R^f = \begin{pmatrix} \cos\theta_f & -\sin\theta_f \\ \sin\theta_f & \cos\theta_f \end{pmatrix}, \tag{IV.131}$$

so that $R^{f\,\dagger} M^2_{sf} R^f = \mathrm{diag}(m^2_{\tilde{f}_1}, m^2_{\tilde{f}_2})$. To get the diagonalized mass matrix the angle of the rotation matrix must be

$$\tan(2\theta_f) = \frac{2\ M^f_{LR}{}^2}{m^2_{f,\,L} - m^2_{f,\,R} + M^2_Z \cos(2\beta)\left(T^L_3 - 2Q_f s^2_W\right)}. \tag{IV.132}$$

It is also remarkable the fact that the mass matrix for the neutrinos is a bit different. In the construction, the right-handed neutrinos were not included so that the mass matrix is just 3×3 due to the flavors.

IV.6 Phenomenological constraints on the MSSM

In the previous sections, we have seen that too many parameters were included through soft-SUSY-breaking terms in order to make the MSSM phenomenologically consistent. These terms increased the set of independent parameters of the MSSM. The total set of parameters in the MSSM is made up of 124 parameters, where 18

of them are parameters of the SM, 1 corresponds to the QCD vacuum angle and 105 are new parameters. In these new parameters, 5 are real parameters and 3 CP-violating phases in the gaugino/higgsino sector, 21 are squark and slepton masses, 36 correspond to real mixing angles of the sfermions mass eigenstates, and 40 are CP-violating phases that may be present in sfermion interactions. In the set of 124 parameters, the non-physical quantities have already been removed through appropriate redefinitions and by writing the interactions in terms of mass eigenstates. [15]

The MSSM parameters should be additionally constrained due to the conservation of the lepton numbers L_e, L_μ and L_τ, suppression of the FCNC and consistency in the new sources of CP-violation with the experimental bounds. Experimental measures of the electric dipole moment of the neutron put bounds on the complex phases of the gaugino-mass parameters and μ. The off-diagonal matrix elements of the sfermion mass matrices get strong constraints from the non-observation of the FCNCs.

In this framework, it is expected that the high-energy structure of the theory should be much simpler than the low-energy model (MSSM). The spontaneous supersymmetry breaking should be satisfactorily explained, and many of the soft-SUSY parameters should be explained by a few number of parameters. The unification of the SM gauge couplings at very high energies (Planck scale) supports this idea.

On the other hand, the non-detection of supersymmetric partners sets bounds to their masses. The lightest supersymmetric particle (LSP), i.e. the neutralino, being a dark matter candidate gets bounds to its mass not only from accelerators experiments but also from dark matter searches. It is usually refered[15] that the masses for the lightest neutralino and chargino have the bounds

$$m_{\widetilde{N}_1} > 46\,\mathrm{GeV}, \qquad m_{\widetilde{C}_1} > 94\,\mathrm{GeV}. \tag{IV.133}$$

For the squarks, some bounds have also been found[15]. In particular, for the sbottom and for the stop:

$$m_{\tilde{b}} > 600\,\mathrm{GeV}, \qquad m_{\tilde{t}} > 240\,\mathrm{GeV}, \tag{IV.134}$$

this from hadronic accelerators. In a similar way, hadronic accelerators set bounds for the gluinos[15]. For a heavy gluino

$$m_{\tilde{g}} \quad > \quad 1150\,\mathrm{GeV}. \tag{IV.135}$$

For the extra Higgs bosons at 95% of C.L. it is known that[15]

$$m_{H^\pm} > 80\ \mathrm{GeV}, \qquad \text{and} \quad m_{A^0} > 93.4\ \mathrm{GeV} \quad \text{for } \tan\beta > 0.4. \tag{IV.136}$$

Chapter V

Higgs physics

In the chapter I we saw the way the Standard Model is built and, at the end, it was commented that it is possible to do some predictions from known parameters. In the present chapter we want to discuss some of those predictions in the Higgs sector.

The Higgs mass measured directly and the VEV, known through electroweak boson masses, allow us to discover the numeric value for λ in the Eq. [I.15]. Then a forecast for the trilinear and the quartic Higgs boson self-interaction can be made.

New proposals for linear colliders have been made, such as the ILC and CLIC projects [16][17], where TeV-collisions will be reached through e^+e^- and $\gamma\gamma$ scattering. These projects manifest a remarkable advantage: a clean environment in the measurements, unlike the situation at an hadronic machine such as the LHC. It is expected that these new linear colliders provide better measurements of the couplings of the Higgs boson with quarks, leptons and gauge bosons, as well as the self-couplings of the Higgs boson, supporting the SM predictions or giving different signs for new physics. This motivates the study of Higgs production from e^+e^- scattering in extensions of the SM, such as the Two Higgs Doublet Model (2HDM) or the Minimal Supersymmetric Standard Model (MSSM). It is also interesting to parametrize the new physics effects in the aforementioned experiments in a model independent, which is done with the Standard Model Effective Field Theory (SMEFT).

Precisely, through the use of computational tools such as FeynArts (FA)[52], FormCalc (FC) and LoopTools (LT)[53] we shall present, in the next chapter [VI], enhancemnts in the Higgs pair production cross-section through pair annihilation in the 2HDM, MSSM and SMEFT . In this chapter we focus on some computations related to the Higgs boson in the SM, checking our results with the computational tools already mentioned.

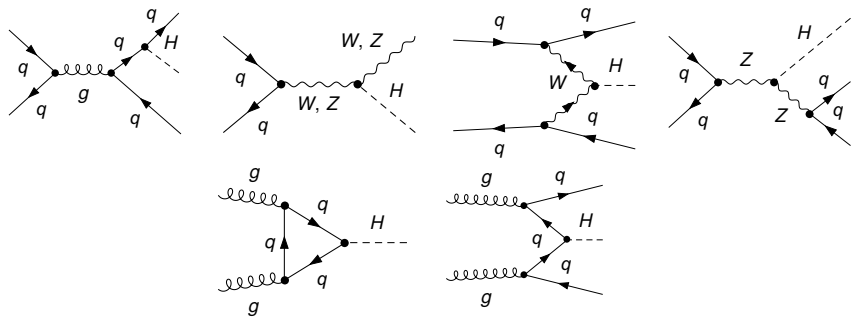

Figure V.1: Main production processes for the Higgs boson in hadronic collisions.

V.1 Channels of production

We can start by revisiting some remarkable SM-processes for Higgs production. The channel of production and detection through which the Higgs boson was discovered in 2012 is the well-known gluon fussion process, $gg \to h$ (Fifth diagram in the Fig. [V.1]). This process take advantage of the top loop wich involves the top mass. Although the gluon-fussion process took the important role in the discovering of the Higgs, there are other relevant processes. In hadronic colliders the posibilities shown in Fig. [V.1] are relevant in Higgs production.

Before the detection of the Higgs, the proton-antiproton collider Tevatron had the important possible channel $\bar{q}q \to WH$. This process has the advantage of presenting just two final particles, what means, bigger factors coming from the phase space than those coming from processes with three or more final particles. The proton-proton collider LHC also considered the processes involving electroweak vector boson fusion, where couplings of the kind W^+W^-H are exploited, the disadvantage with respect to the former process is the three final particle's phase space.

On the other hand, the electron-positron colliders offer cleaner results than those yielded by hadron colliders. For this reason, the processes that are observable in e^+e^- colliders are of special interest in high precision physics. The main reactions in such colliders are similar to those through hadronic collisions. They are shown in the figure [V.2].

The second process in Fig. [V.2] is usually named as Higgsstrahlung, and in leptonic colliders dominates the Higgs production modes below $\sqrt{s} = 450\,\text{GeV}$, where the weak-boson fusion takes tha main role (Third Feynman diagram in Fig. [V.2]). The maximum of the cross-section for the process $e^+e^- \to hZ$ is close to $\sqrt{s} = 250\,\text{GeV}$. Let us note that it could happen that the decay $Z \to \nu\bar{\nu}$ so that $e^+e^- \to hZ \to h\nu\bar{\nu}$, which actually, concerning the final particles, seems the same as the weak-boson fusion mode $e^+e^- \to W^+W^-\nu\bar{\nu} \to h\nu\bar{\nu}$ (Fourth Feynman diagram in Fig. [V.2]), thus these two modes are complementary. Precise measurementes on these processes are important to get separate constraints on the parameters of the effective operators that could contribute on

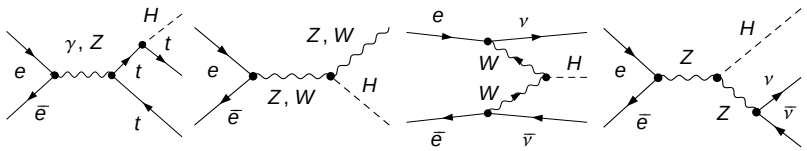

Figure V.2: Main production processes for the Higgs boson in e^+e^- colliders.

each of them[65].

At the LEP, the most relevant process in Higgs production is $e^+e^- \to ZH$, the trouble presented in this accelerator in order to measure the Higgs boson was that it did not have enough energy to produce a 125 GeV boson.

The weak-boson fusion has the feature of a cross-section that always grows with the energy, thus it is better measured above of $\sqrt{s} = 350\,\text{GeV}$, since at this point it is possible to separate its contribution from the corresponding of the Higgstrahlung. On the other hand, the process $e^+e^- \to t\bar{t}h$ requires a large center-of-mass energy, which only can be achieved at linear colliders. The main contribution for this process comes from the first diagram in Fig. [V.2], involving the top-Yukawa coupling. Thus, physics BSM that involves such coupling can be studied through the $e^+e^- \to t\bar{t}h$ process.

Before the detection of the Higgs boson it was considered the existence of a strongly interacting Higgs sector. This possibility arises when we write the quartic self-coupling λ in terms of the Higgs mass:

$$\lambda = \frac{1}{2}\frac{m_h^2}{v^2}, \tag{V.1}$$

hence the coupling λ grows with the square of the Higgs mass. Currently, we know the exact value of the quartic coupling, but at the time when the Higgs boson remained undetected, a strongly interacting sector was an option for high enough Higgs mass, i.e. the Higgs boson could self-interact strongly if $m_h \gg v$.

A way in looking for this situation was going to massive electroweak bosons. Due to the "screening" theorem [63], the low-energy observables are protected to big contributions coming from a large Higgs mass, and so, coming from a strong interacting sector. Hence, a remaining way to see the strong effects was through the "closest" sector to the Higgs doublet: the longitudinal modes for the weak gauge bosons. "Closest" in the sense that precisely three would-be Goldstone bosons become such longitudinal modes. This fact can be seen from the equivalence theorem, which implies that the amplitudes involving longitudinal gauge bosons are equal to those involving unphysical scalars coming from the Higgs doublet plus corrections of order $\mathcal{O}(M_W/E)$, i.e.

$$T(W_L^+, W_L^-, Z_L, \dots) = T(\varphi^+, \varphi^-, \varphi_Z, \dots) + \mathcal{O}\left(\frac{M_W}{E}\right), \tag{V.2}$$

this with the parametrization of Eq. [I.26]. The equivalence theorem for this situation can be checked through simple decay channels of the Higgs boson. This is better discussed in the chapter 15 of [64].

V.2 Software implementation

Before getting results in the Higgs pair production cross-sections with FA, FC, and LT, we would like to check the accuracy of our implementations. Thus, some known results are reproduced in this section.

V.2.1 $e^+e^- \to \mu^+\mu^-$

For this process the total cross section at tree-level in QED is given by

$$\sigma = \frac{4\pi\alpha^2}{3E}\sqrt{1-\frac{4m_\mu^2}{E^2}}\left(1+\frac{1}{2}\frac{4m_\mu^2}{E^2}\right), \tag{V.3}$$

with E the energy of the center of mass. When we load the packages in Mathematica a result for the total cross-section can be obtained through a procedure as the following:

```
<<Feynarts
<<FormCalc
<<LoopTools

(** Calling the Model **)
InitializeModel[SM];
(** Generation of the Feynman diagrams **)
top = CreateTopologies[0, 2 -> 2];
AA = InsertFields[
        top, {F[2, {1}], -F[2, {1}]} -> {F[2, {2}], -F[2, {2}]},
     InsertionLevel -> {Classes}, ExcludeParticles -> {V[2], S}];
(** Getting and Simplifying the Amplitude **)
amp = CreateFeynAmp[AA];
ClearProcess[];
res = CalcFeynAmp[amp, FermionChains -> VA];
(** Squaring the Amplitude **)
_Hel = 0;
MatrixElement = 4*SquaredME[res] //. HelicityME[res];
(** Replacement of Numerical Values and Kinematical Quantities **)
VALUES := {
```

```
  Den[p2_, m2_] :> 1/(p2 - m2),
  ME -> 0, ME2 -> 0,
  MM -> 0.105658371500000, MM2 -> 0.105658371500000^2,
  Alfa -> 1/128, Alfa2 -> 1/128^2}
SQAmpValues[EN_, \[Theta]_] :=
 MatrixElement //. Subexpr[] //.
   Join[VALUES, {S -> EN^2,
     T -> -(1/
        2) (EN^2 - 2 MM2 - Cos[\[Theta]] EN Sqrt[EN^2 - 4 MM2 ]),
     U -> -(1/
        2) (EN^2 - 2 MM2 + Cos[\[Theta]] EN Sqrt[EN^2 - 4 MM2 ])}] //
  Simplify
(** Differential and Total Cross-Section **)
d\[Sigma][EN_, \[Theta]_] :=
    1/(32 Pi^2 EN^3) Sqrt[EN^2/4 - 0.105658^2] SQAmpValues[EN, \[Theta]]
\[Sigma][EN_?NumericQ] :=
    2 Pi*NIntegrate[{Sin[\[Theta]]*
     Re[d\[Sigma][EN, \[Theta]]]}, {\[Theta], 0, Pi},
      PrecisionGoal -> 1]
```

Through this, the plot (a) of the figure [V.3] is obtained, which could be compared with the Figure 5.1 in [54]. When the ratio between the theoretical value in Eq. [V.3] and the cross-section obtained numerically is analyzed it is possible to observe deviations of order 0.999994 nearby the threshold, which rapidly goes to 1 when the energy increases. So, the packages implemented are in good agreement with the expected values.

Another good result obtained through the packages is the resonance of the Z-boson, for which its full propagator must be implemented. For this sake, it was used the width $\Gamma_Z = 2.4952\,\text{GeV}$. The result is shown in figure (b) [V.3], which also is in good agreement with Figure 1 in the ref. [66].

V.3 $h \to \gamma\gamma$

Now, let us move on towards a more interesting process: the Higgs decay into two photons. We want to reproduce with FA, FC and LT the width of this decay mode. The cross-section for the Higgs production via $\gamma\gamma$ is determined by this decay rate. Another remark on this decay comes from the effective coupling $\gamma\gamma H$, which is mediated by all charged particles. This is a window to see the effects of particles with masses much bigger than the Higgs through the coupling of the Higgs boson to those heavy particles. Such fact happens in

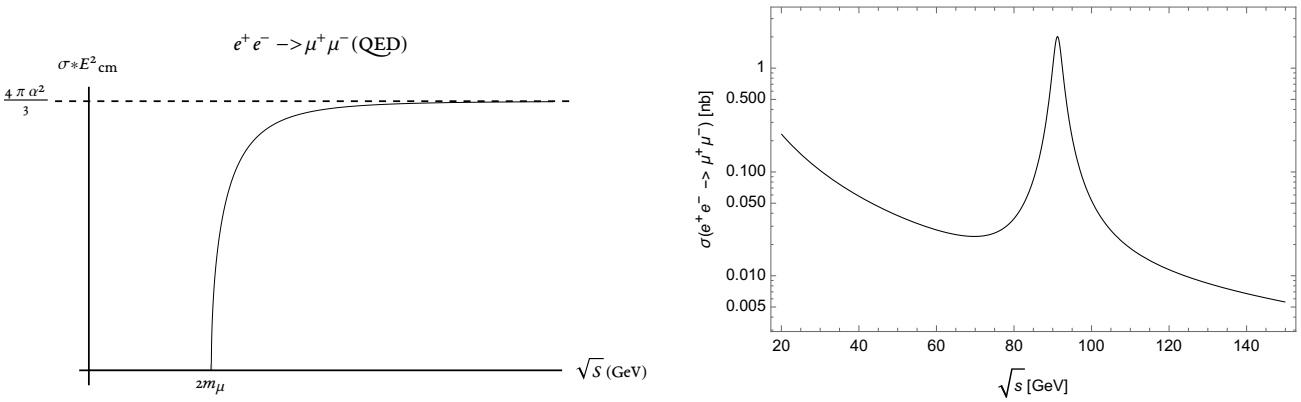

(a) (b)

Figure V.3: Cross-section for the process $e^+e^- \to \mu^+\mu^-$ (Compare to Fig. 5.1 in [54]) a) in QED, b) in the Glashow-Weinberg-Salam model with the full Z-boson propagar (Compare to Fig. 1 in [66]).

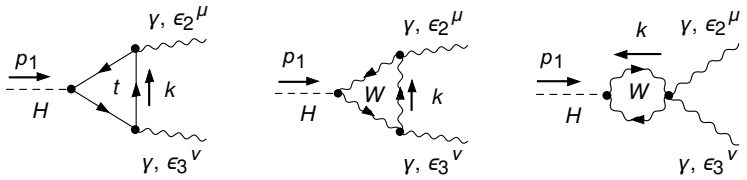

Figure V.4: Feynman diagrams in the unitary gauge for the Higgs decay into two photons, with $\epsilon_2^\mu = \epsilon^\mu(p_2)$ and $\epsilon_3^\nu = \epsilon^\nu(p_3)$, and where the crossed diagrams have been omitted.

the framework that the new masses are obtained via Higgs mechanism.

The process runs through loops involving quarks, charged leptons and the W boson, and in general the charged ghosts and Goldstone bosons. The amplitude for this Higgs decay is computed in renormalizable and unitary gauges in [51], so that ghosts and Goldstone bosons do not appear. There it is deduced the decay rate:

$$\Gamma(H \to \gamma\gamma) = |F|^2 \left(\frac{\alpha}{4\pi}\right)^2 \frac{G_F m_H^3}{8\sqrt{2}\pi}, \tag{V.4}$$

with

$$F = F_W(\beta_W) + \sum_f N_c Q_f^2 F_f(\beta_f), \tag{V.5}$$

where $\beta_W = \frac{4m_W^2}{m_H^2}$, $\beta_f = \frac{4m_f^2}{m_H^2}$, and

$$F_W(\beta) = 2 + 3\beta + 3\beta(2-\beta) f(\beta), \tag{V.6}$$

$$F_f(\beta) = -2\beta[1 + (1-\beta) f(\beta)], \tag{V.7}$$

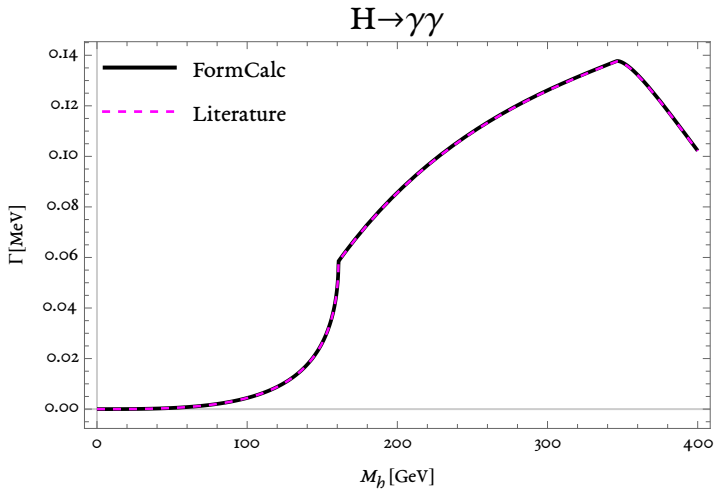

Figure V.5: Width for the decay $H \to \gamma\gamma$ computed theoretically (Black) and by FormCalc implementation (Magenta).

and

$$f(\beta) = \begin{cases} \arcsin^2\left(\sqrt{\frac{1}{\beta}}\right) & for \quad \beta \geq 1, \\ -\frac{1}{4}\left[\log\frac{1+\sqrt{1-\beta}}{1-\sqrt{1-\beta}} - i\pi\right]^2 & for \quad \beta < 1. \end{cases} \tag{V.8}$$

The contribution of the fermion loops depends on the quark masses through the Yukawa couplings between them and the Higgs, thus the main contribution from these loops comes from the top loop. As an interesting computation we study a fermion loop contribution. The amplitude for the first diagram in Fig. [V.4] is given by

$$\begin{aligned} i\mathcal{M}_1 &= -N_c\left(\frac{-im_f}{v}\right)(-iQ_f e)^2 \int \frac{d^4k}{(2\pi)^4} \frac{(-i)\,\mathrm{Tr}\left[(\not{k}+\not{p}_2+m_f)\,\gamma^\mu\,(\not{k}+m_f)\,\gamma^\nu\,(\not{k}-\not{p}_3+m_f)\right]}{\left[(k+p_2)^2-m_f^2\right]\left[k^2-m_f^2\right]\left[(k-p_3)^2-m_f^2\right]} \cdot \epsilon_\mu^2 \epsilon_\nu^3 \\ &= -e^2 N_c Q_f^2 \frac{m_f}{v}\epsilon_\mu^2\epsilon_\nu^3 \int \frac{d^4k}{(2\pi)^4} \frac{\mathrm{Tr}\left[(\not{k}+\not{p}_2+m_f)\,\gamma^\mu\,(\not{k}+m_f)\,\gamma^\nu\,(\not{k}-\not{p}_3+m_f)\right]}{\left[(k+p_2)^2-m_f^2\right]\left[k^2-m_f^2\right]\left[(k-p_3)^2-m_f^2\right]}, \end{aligned} \tag{V.9}$$

where the term $+i\epsilon$ in the propagators have been omitted, the N_c is a color factor, the q stands for the charge of the fermion in the loop and a minus sign appears since the fermionic character of the loop. The trace in the numerator, named by $N^{\mu\nu}$ can be simplified by the usual properties of the trace of gamma matrices, so that dropping terms proportional to k, which vanishes by parity symmetry of the integral, we simplified

$$\begin{aligned} N^{\mu\nu} &\equiv m_f \mathrm{Tr}\left[(\not{k}+\not{p}_2)\,\gamma^\mu\not{k}\gamma^\nu + (\not{k}+\not{p}_2)\,\gamma^\mu\gamma^\nu\,(\not{k}-\not{p}_3) + \gamma^\mu\not{k}\gamma^\nu\,(\not{k}-\not{p}_3) + m_f^2\gamma^\mu\gamma^\nu\right] \\ &\to m_f \mathrm{Tr}\left[2\not{k}\gamma^\mu\not{k}\gamma^\nu + \not{k}\gamma^\mu\gamma^\nu\not{k} - \not{p}_2\gamma^\mu\gamma^\nu\not{p}_3 + m_f^2\gamma^\mu\gamma^\nu\right] \\ &= 4m_f^2\left[4k^\mu k^\nu - k^2 g^{\mu\nu} - p_2^\mu p_3^\nu + p_2^\nu p_3^\mu - p_2\cdot p_3 g^{\mu\nu} + m_f^2 g^{\mu\nu}\right]. \end{aligned} \tag{V.10}$$

The longitudinal polarization of the photon is no-physical, then we recall $\epsilon_\mu (p_2)\, p_2^\mu = 0$ and $\epsilon_\nu (p_3)\, p_3^\nu = 0$, which leads us to

$$N^{\mu\nu} \;\; \to \;\; 4m_f \left[4k^\mu k^\nu - k^2 g^{\mu\nu} + p_2^\nu p_3^\mu + \left(m_f^2 - p_2 \cdot p_3\right) g^{\mu\nu}\right]. \tag{V.11}$$

Now, we use the Feynman parametrization to compute the integral. After introducing the Feynman parameters x, y and z, the denominator D of the integral reduces to

$$\begin{aligned} D &\equiv x\left[k^2 - m_f^2\right] + y\left[(k+p_2)^2 - m_f^2\right] + z\left[(k-p_3)^2 - m_f^2\right] + i\epsilon \\ &= k^2 + 2yk\cdot p_2 - 2zk\cdot p_3 - m_f^2 + i\epsilon \\ &= (k + yp_2 - zp_3)^2 + 2yzp_2\cdot p_3 - m_f^2 + i\epsilon \\ &= \ell^2 - \Delta + i\epsilon, \end{aligned} \tag{V.12}$$

with $\ell = k + yp_2 - zp_3$ and $\Delta = m_f^2 - 2yzp_2\cdot p_3$. With the shift made in the momentum the numerator also changes, so that dropping terms of order ℓ,

$$\begin{aligned} N^{\mu\nu} &= 4m_f\left[4\left(\ell - yp_2 + zp_3\right)^\mu \left(\ell - yp_2 + zp_3\right)^\nu - \left(\ell - yp_2 + zp_3\right)^2 g^{\mu\nu} + p_2^\nu p_3^\mu + \left(m_f^2 - p_2\cdot p_3\right) g^{\mu\nu}\right] \\ &\to 4m_f\Big(4\ell^\mu\ell^\nu + 4\left(-yp_2 + zp_3\right)^\mu \left(-yp_2 + zp_3\right)^\nu - \ell^2 g^{\mu\nu} - \left(-yp_2 + zp_3\right)^2 g^{\mu\nu} \\ &\qquad + p_2^\nu p_3^\mu + \left(m_f^2 - p_2\cdot p_3\right) g^{\mu\nu}\Big) \\ &= 4m_f\left(4\ell^\mu\ell^\nu - \ell^2 g^{\mu\nu} + (1-4yz)\, p_3^\mu p_2^\nu + \left[m_f^2 + (2yz-1)\, p_2\cdot p_3\right] g^{\mu\nu}\right) \\ &= 4m_f\left(N_1^{\mu\nu} + N_2^{\mu\nu}\right) \end{aligned} \tag{V.13}$$

with $N_1^{\mu\nu} \equiv 4\ell^\mu\ell^\nu - \ell^2 g^{\mu\nu}$ and $N_2^{\mu\nu} \equiv (1-4yz)\, p_3^\mu p_2^\nu + \left[m_f^2 + (2yz-1)\, p_2\cdot p_3\right] g^{\mu\nu}$. Now, we are able to evaluate the integrations in the momentum, which are well known integrals. Naively, the integral of $N_1^{\mu\nu}$ seems logarithmic divergent, then we used dimensional regularization to get,

$$\begin{aligned} \int \frac{d^d\ell}{(2\pi)^d} \frac{4\ell^\mu\ell^\nu - \ell^2 g^{\mu\nu}}{\left[\ell^2 - \Delta\right]^3} &= \left(\frac{4}{d} - 1\right) \int \frac{d^d\ell}{(2\pi)^d} \frac{\ell^2 g^{\mu\nu}}{\left[\ell^2 - \Delta\right]^3} \\ &= \frac{ig^{\mu\nu}}{(4\pi)^{d/2}} \left(2 - \frac{d}{2}\right) \frac{\Gamma\left(2 - d/2\right)}{2} \left(\frac{1}{\Delta}\right)^{2-d/2}. \end{aligned} \tag{V.14}$$

The integral of $N_2^{\mu\nu}$ is readily computable, being finite. By recalling the identity $\Gamma\left(3 - d/2\right) = \left(2 - \frac{d}{2}\right)\Gamma\left(2 - d/2\right)$, we write

$$N_2^{\mu\nu} \cdot \int \frac{d^d\ell}{(2\pi)^d} \frac{1}{\left[\ell^2 - \Delta\right]^3} = \frac{-iN_2^{\mu\nu}}{(4\pi)^{d/2}} \left(2 - \frac{d}{2}\right) \frac{\Gamma\left(2 - d/2\right)}{2} \left(\frac{1}{\Delta}\right)^{3-d/2}. \tag{V.15}$$

Hence, the full integral in the momentum is evaluated to

$$\int \frac{d^d\ell}{(2\pi)^d}\frac{N_1^{\mu\nu}+N_2^{\mu\nu}}{D^3} = \frac{i}{2}\frac{\Gamma(2-d/2)}{(4\pi)^{d/2}}\left(\frac{1}{\Delta}\right)^{2-d/2}\left(2-\frac{d}{2}\right)\left(\frac{\Delta g^{\mu\nu}-N_2^{\mu\nu}}{\Delta}\right). \tag{V.16}$$

By taking $d=4-\epsilon$ and expanding around $\epsilon=0$,

$$\frac{\Gamma(2-d/2)}{(4\pi)^{d/2}}\left(\frac{1}{\Delta}\right)^{2-d/2} = \frac{1}{(4\pi)^2}\left(\frac{2}{\epsilon}-\log\Delta-\gamma+\log(4\pi)+\mathcal{O}(\epsilon)\right), \tag{V.17}$$

moreover, $2-d/2=\epsilon/2$. By multiplying these factors, in the end, the divergences cancel out. Also, with the definition of Δ, it is found the factor

$$\begin{aligned}\Delta g^{\mu\nu}-N_2^{\mu\nu} &= \left(m_f^2-2p_2\cdot p_3yz\right)g^{\mu\nu}-(1-4yz)\,p_3^\mu p_2^\nu-\left[m_f^2+(2yz-1)\,p_2\cdot p_3\right]g^{\mu\nu}\\ &= (1-4yz)\left(p_2\cdot p_3 g^{\mu\nu}-p_3^\mu p_2^\nu\right),\end{aligned} \tag{V.18}$$

where the gauge invariance can be seen manifested. Then, we have found

$$\begin{aligned}\int \frac{d^d\ell}{(2\pi)^d}\frac{N_1^{\mu\nu}+N_2^{\mu\nu}}{D^3} &= \frac{i}{2}\frac{1}{(4\pi)^2}\frac{1-4yz}{m_t^2-2p_2\cdot p_3yz}\left(p_2\cdot p_3g^{\mu\nu}-p_3^\mu p_2^\nu\right)\\ &= \frac{i}{16\pi^2}\frac{1}{p_2\cdot p_3}\frac{1-4yz}{\beta-4yz}\left(p_2\cdot p_3g^{\mu\nu}-p_3^\mu p_2^\nu\right),\end{aligned} \tag{V.19}$$

where, and from now on, we use $\beta_f\equiv\frac{2m_f^2}{p_2\cdot p_3}$, so that by momentum conservation $p_1^2=m_H^2=(p_2+p_3)^2=2p_2\cdot p_3$, $\beta_f=\frac{4m_f^2}{m_H^2}$. All these pieces can be joined together in order to get the amplitude

$$\begin{aligned}i\mathcal{M}_1 &= -e^2N_cQ_f^2\frac{m_f}{v}\epsilon_\mu(p_2)\,\epsilon_\nu(p_3)\\ &\qquad\cdot 4m_f\frac{i}{16\pi^2}\frac{1}{p_2\cdot p_3}\left(p_2\cdot p_3g^{\mu\nu}-p_3^\mu p_2^\nu\right)\int_0^1 dx\,dy\,dz\,2\delta(x+y+z-1)\frac{1-4yz}{\beta_f-4yz}\\ &= \frac{-i}{16\pi^2}N_cQ_f^2\frac{ge^2}{2M_W}\epsilon_\mu(p_2)\,\epsilon_\nu(p_3)\,\frac{4m_f^2}{p_2\cdot p_3}\left(p_2\cdot p_3g^{\mu\nu}-p_3^\mu p_2^\nu\right)\int_0^1 dy\int_0^{1-y}dz\,2\frac{1-4yz}{\beta_f-4yz}\\ &= \frac{i}{32\pi^2}\frac{ge^2}{M_W}\epsilon_\mu(p_2)\,\epsilon_\nu(p_3)\left(p_2\cdot p_3g^{\mu\nu}-p_3^\mu p_2^\nu\right)F,\end{aligned} \tag{V.20}$$

since the formula $M_W=gv/2$, and with the definition

$$F=\sum_f N_cQ_f^2F_f(\beta_f), \tag{V.21}$$

being

$$\begin{aligned} F_f\left(\beta_f\right) &\equiv -4\beta_f \int_0^1 dy \int_0^{1-y} dz \, \frac{1-4yz}{\beta_f - 4yz} \\ &= -4\beta_f \int_0^1 dy \int_0^{1-y} dz \, \frac{1-4yz}{\beta_f - 4yz} \\ &= -2\beta_f \left(1 + \frac{1}{2}\left(1-\beta_f\right)\left[\mathrm{Li}_2\left(\frac{2}{a_-}\right) + \mathrm{Li}_2\left(\frac{2}{a_+}\right)\right]\right), \end{aligned} \tag{V.22}$$

where $a_\pm \equiv 1 \pm \sqrt{1-\beta_f}$ and $\beta_f \geq 1$, so that from now on we focus on the region for such β_f. One can show that these di-logarithms can be written in a suitable way. For this, let us note that

$$1 + \frac{a_-}{a_+} = \frac{2}{a_+}, \qquad 1 + \frac{a_+}{a_-} = \frac{2}{a_-} \tag{V.23}$$

thus, by using the identities

$$\mathrm{Li}_2\left(\frac{1}{z}\right) = -\mathrm{Li}_2\left(z\right) - \frac{\pi^2}{6} - \frac{1}{2}\log^2\left(-z\right), \tag{V.24}$$

$$\mathrm{Li}_2\left(1-z\right) = -\mathrm{Li}_2\left(z\right) + \frac{\pi^2}{6} - \log\left(z\right)\log\left(1-z\right), \tag{V.25}$$

we can write the dilogarithms in terms of usual logarithms. Then, by recalling that $\log(-1) = (2n+1)i\pi$ $(n = 0, \pm 1, \dots)$, we can have two branches, where the positive one

$$\begin{aligned} \mathrm{Li}_2\left(\frac{2}{a_-}\right) + \mathrm{Li}_2\left(\frac{2}{a_+}\right) &= \frac{\pi^2}{2} + \frac{1}{2}\log^2\left(\frac{a_-}{a_+}\right) - \log\left(-\frac{a_-}{a_+}\right)\left[\log\left(\frac{2}{a_+}\right) - \log\left(\frac{2}{a_-}\right)\right] \\ &= \frac{\pi^2}{2} - \frac{1}{2}\log\left(\frac{a_-}{a_+}\right)\left[\log\left(\frac{a_-}{a_+}\right) + 2i\pi\right] \\ &= -\frac{1}{2}\left(\log\left(\frac{a_-}{a_+}\right) + i\pi\right)^2. \end{aligned} \tag{V.26}$$

Now, with the relation $\beta_f/(1-\sqrt{1-\beta_f}) = 1 + \sqrt{1-\beta_f}$,

$$-\frac{1}{2}\left(\log\left(\frac{a_-}{a_+}\right) + i\pi\right)^2 = -\frac{1}{2}\left(\log\left(-\left(1-\sqrt{1-\beta_f}\right)\frac{1-\sqrt{1-\beta_f}}{\beta_f}\right)\right)^2 \tag{V.27}$$

$$= -\frac{1}{2}\left(\log\left(\frac{i}{\sqrt{\beta_f}}\left(1-\sqrt{1-\beta_f}\right)\right)^2\right)^2 \tag{V.28}$$

$$= -2\left(\log\left(\frac{i}{\sqrt{\beta_f}}\left(1-\sqrt{1-\beta_f}\right)\right)\right)^2, \tag{V.29}$$

and, finally, with the the identity (for $x > 0$)

$$\log(x) = i\text{ArcSin}\left(\frac{x^2-1}{2ix}\right), \tag{V.30}$$

we find that in our case,

$$\text{Li}_2\left(\frac{2}{a_-}\right) + \text{Li}_2\left(\frac{2}{a_+}\right) = 2\left(\text{ArcSin}\left(\sqrt{\frac{1}{\beta_f}}\right)\right)^2. \tag{V.31}$$

Hence, the amplitude for the first diagram including the contributions of all the charged fermions turns out to be [V.20], where

$$F_f(\beta) = -2\beta_f\left[1 + (1-\beta_f) f(\beta_f)\right], \tag{V.32}$$

and for $\beta \geq 1$, with

$$f(\beta) = \left(\text{ArcSin}\left(\sqrt{\frac{1}{\beta}}\right)\right)^2. \tag{V.33}$$

The case for $\beta_f < 1$ can be done through complex extension, so that from Eq. [V.26] we have

$$f(\beta) = -\frac{1}{4}\left(\log\left(\frac{a_+}{a_-}\right) - i\pi\right)^2. \tag{V.34}$$

The total amplitude for the fermion loops contributions is twice $i\mathcal{M}_1$, since the crossed diagrams leads to the same expressions that we have already studied. Thus

$$i\mathcal{M} = \frac{i}{16\pi^2}\frac{ge^2}{M_W}\epsilon_\mu(p_2)\,\epsilon_\nu(p_3)\,(p_2\cdot p_3 g^{\mu\nu} - p_3^\mu p_2^\nu)\,F. \tag{V.35}$$

Therefore, we have reproduced the amplitude for contributions coming from fermion loops, as can be seen in [51]. Now, the partial decay rate can be computed. First, we recall that the final state correspond to two identical particles, thus the phase-space factor should have a 1/2 factor, then this factor is $\int D_2 = \frac{1}{16\pi}$. Also, by recalling that for photons $\sum_\pm \epsilon_\mu(k)\epsilon_\nu^*(k) \to -g_{\mu\nu}$,

$$\sum_\pm \epsilon_\mu(p_2)\,\epsilon_\nu(p_3)\,\epsilon_\rho^*(p_2)\,\epsilon_\sigma^*(p_3)\,(p_2\cdot p_3 g^{\mu\nu} - p_3^\mu p_2^\nu)\,(p_2\cdot p_3 g^{\rho\sigma} - p_3^\rho p_2^\sigma) = 2(p_2\cdot p_3)^2 = \frac{1}{2}m_H^4. \tag{V.36}$$

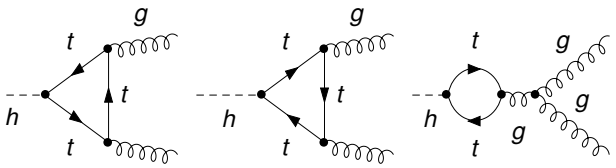

Figure V.6: Feynman diagrams for the Higgs decay into two gluons.

Thus, finally we find the partial width for Higgs into two photons.

$$\begin{aligned}\Gamma^{CM} &= \frac{1}{2m_H}\int D_2|\mathcal{M}\left(h\to\gamma\gamma\right)|^2 \\ &= \frac{1}{2m_H}\cdot\frac{1}{16\pi}\cdot\frac{1}{2}m_H^4|\frac{e^2}{4\pi}\frac{g}{4\pi M_W}F|^2 \\ &= \left(\frac{\alpha}{4\pi}\right)^2\frac{G_F m_H^3}{8\sqrt{2}\pi}|F|^2 \end{aligned} \tag{V.37}$$

The values of the Eq. [V.4] can be reproduced with the use of FC and LT. When we do so the plot of the figure [V.5] is obtained, where actually there are two curves, one given by Eq. [V.4] and the other represent the result of the Mathematica packages. It is shown a perfect agreement between the procedures.

The amplitude for $H \to \gamma\gamma$ is real when the Higgs mass is smaller than the thresholds for the WW and quark-antiquark pairs, while above such thresholds it becomes complex. From the plot of Fig. [V.5] we can see for $2m_W < m_H < 2m_t$ that the W loops dominate over the quark loops, while above $2m_t$ there is a destructive interference between the W and quark loops.

V.4 $h \to gg$

Similar to the Higgs decay into two photons, the decay mode into two gluons is also possible, mediated through quark loops. This process was first considered in 1977 by Wilczek[56]. The $H \to gg$ decay is of special importance since it determines the cross-section for the Higgs production through gluon fusion to leading order. It also gives a chance to see into colored particles heavier than the top quark, in analogy to the case of the previous section.

We can also see the timing between software and the theoretical computations for this Higgs decay, in which enter the diagrams that are shown in Figure [V.6]. Here the bubble contribution actually vanishes because of the colorless structure of the Higgs, the same reason applies for the lack of loops involving W and Z bosons. The theoretical computation involves the solution of an integral over the three propagators of the top loop. The

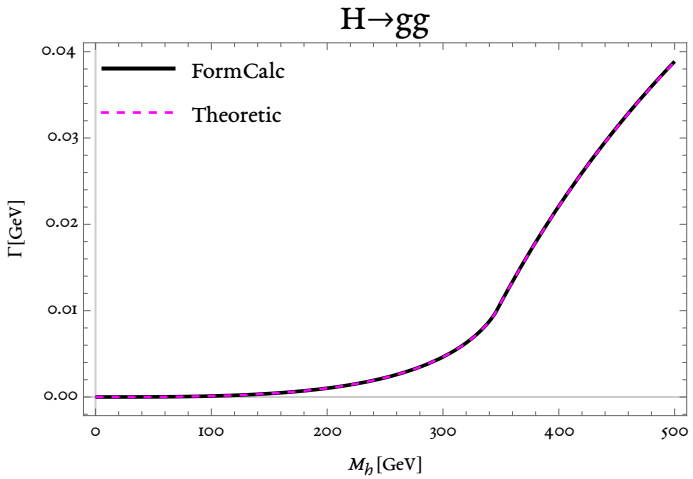

Figure V.7: Width for the decay $H \to gg$ given by FormCalc (Black) and theoretical computations from [15] (Magenta).

well-known result can be found in [55] or [15]. From the latter, its equation (49.33) reads

$$\Gamma\left(H \to gg\right) = \frac{G_F \alpha_s^2}{36\sqrt{2}\pi^3} m_H^3 \left| \sum_Q I\left(\frac{m_Q^2}{m_H^2}\right) \right|^2 , \tag{V.38}$$

with

$$I\left(t\right) = 3\left[2t + 2t\left(1-4t\right)\left(\arcsin\frac{1}{2\sqrt{t}}\right)^2\right] . \tag{V.39}$$

where the index Q denotes the quark in the loop. As was already said, the biggest contribution comes from the top loop, so the summation over Q shrinks to just the contribution from the top mass. In the figure [V.7] we can see a perfect agreement between the results from FC and the PDG's formula. It is interesting to see the growth in $\Gamma\left(H \to gg\right)$ for a Higgs mass bigger than $2m_t$, where the top quarks can be produced on-shell.

V.5 Branching ratios and decay widths of the Higgs boson

In the previous sections, we computed some of the contributions that enter in the decay of the Higgs boson into massless vectorial bosons. We saw that the leading order is found at 1-loop. Now, we want to see other decay widths of the Higgs boson and, in particular, we can see some remarks on the Branching Ratios (BR) of the Higgs in terms of its mass. This was very useful before the discovery of the Higgs in 2012, and still nowadays the Higgs decay widths are essential for the understanding and interpretation of the experimental results.

We start by computing the decay width of the Higgs boson into the electroweak bosons. Thus, we start with

the amplitude at tree-level,

$$\begin{aligned} i\mathcal{M}\left(h \to W^+W^-\right) &= \epsilon_\mu^{r*}\left(k_1\right)\left(igM_W\eta^{\mu\nu}\right)\epsilon_\nu^{s*}\left(k_2\right) \\ &= igM_W\epsilon_\mu^{r*}\left(k_1\right)\epsilon^{\mu s*}\left(k_2\right), \end{aligned} \tag{V.40}$$

from which it follows that the squared amplitude is

$$\left|\mathcal{M}\left(h \to W^+W^-\right)\right|^2 = g^2M_W^2\epsilon_\mu^{r*}\left(k_1\right)\epsilon^{\mu s*}\left(k_2\right)\epsilon_\nu^{r}\left(k_1\right)\epsilon^{\nu s}\left(k_2\right), \tag{V.41}$$

so that the unpolarized squared amplitude is found through $\sum_{r=1}^{3}\epsilon_\mu^{r*}\left(k\right)\epsilon_\nu^{r}\left(k\right) = \eta_{\mu\nu} + \frac{k_\mu k_\nu}{M_W^2}$:

$$\begin{aligned} \overline{\left|\mathcal{M}\left(h \to W^+W^-\right)\right|^2} &= g^2M_W^2\cdot\sum_r\epsilon_\mu^{r*}\left(k_1\right)\epsilon_\nu^{r}\left(k_1\right)\cdot\sum_s\epsilon^{\mu s*}\left(k_2\right)\epsilon^{\nu s}\left(k_2\right) \\ &= g^2M_W^2\left(-\eta_{\mu\nu} + \frac{k_{1\mu}k_{1\nu}}{M_W^2}\right)\left(-\eta^{\mu\nu} + \frac{k_2^\mu k_2^\nu}{M_W^2}\right) \\ &= g^2M_W^2\left(4 - \frac{k_2^2}{M_W^2} - \frac{k_1^2}{M_W^2} + \frac{\left(k_1\cdot k_2\right)^2}{M_W^4}\right) \\ &= \frac{g^2}{M_W^2}\left(2M_W^4 + \left(k_1\cdot k_2\right)^2\right). \end{aligned} \tag{V.42}$$

Now, we note that in the rest frame of the Higgs boson, by means of conservation of 4-momentum, it is possible to set

$$p^\mu = \left(m_h,\,\mathbf{0}\right), \qquad k_1^\mu = \left(E,\,\mathbf{k}\right), \qquad k_2^\mu = \left(E,\,-\mathbf{k}\right), \tag{V.43}$$

thus

$$k_1\cdot k_2 = E^2 + \mathbf{k}^2 = 2E^2 - M_W^2 \qquad \Rightarrow \quad \begin{aligned}\left(k_1\cdot k_2\right)^2 &= \left(2E^2 - M_W^2\right)^2 \\ &= 4E^4 - 4M_W^2E^2 + M_W^4.\end{aligned}$$

Moreover, by energy conservation $m_h = 2E$, hence

$$\begin{aligned} \overline{\left|\mathcal{M}\left(h \to W^+W^-\right)\right|^2} &= \frac{g^2}{M_W^2}\left(\frac{1}{4}m_h^4 - M_W^2m_h^2 + 3M_W^4\right) \\ &= \frac{g^2m_h^4}{4M_W^2}\left(1 - 4\frac{M_W^2}{m_h^2} + 12\left(\frac{M_W^2}{m_h^2}\right)^2\right). \end{aligned} \tag{V.44}$$

Now, the unpolarized square amplitude in terms of the ratio $x_W \equiv M_W^2/m_h^2$ is

$$\overline{\left|\mathcal{M}\left(h \to W^+W^-\right)\right|^2} = \frac{g^2m_h^4}{4M_W^2}\left(1 - 4x_W + 12x_W^2\right). \tag{V.45}$$

For a $1 \to 2$ decay process, the differential width is

$$d\Gamma\left(h \to final\right) = \frac{1}{2m_h}\frac{d^3k_1}{\left(2\pi\right)^3}\frac{d^3k_2}{\left(2\pi\right)^3}\frac{1}{4E_1E_2}\overline{\left|\mathcal{M}\left(h \to final\right)\right|^2}\left(2\pi\right)^4\delta^4\left(p - k_1 - k_2\right). \tag{V.46}$$

By considering the Dirac delta in the 3-momenta $\delta^3\left(-\mathbf{k}_1 - \mathbf{k}_2\right)$, it is possible to evaluate the k_2-momentum integral so that we put $\mathbf{k}_1 = -\mathbf{k}_2 = \mathbf{k}$, then

$$d\Gamma\left(h \to W^+W^-\right) = \frac{1}{2m_h}\frac{d^3k}{\left(2\pi\right)^2}\frac{1}{4E^2}\overline{\left|\mathcal{M}\left(h \to W^+W^-\right)\right|^2}\delta\left(m_h - 2E\right), \tag{V.47}$$

where it has been noted that the energies E_1 and E_2 are equal if the momenta are also equal. Now, with k_0 the root (positive) of the argument of the Dirac delta in Eq. [V.47] and $|\mathbf{k}| = k$:

$$\begin{aligned}\delta\left(m_h - 2E\right) &= \frac{\delta\left(k - k_0\right)}{2\,\frac{dE}{dk}\big|_{k=k_0}} \\ &= \left.\frac{E}{2k}\right|_{k=k_0}\delta\left(k - k_0\right).\end{aligned} \tag{V.48}$$

Thus, if we recall that $m_h = 2E$, the differential width can be simplified to

$$d\Gamma\left(h \to W^+W^-\right) = \frac{1}{8m_h^2\left(2\pi\right)^2}d\Omega\; k\,\overline{\left|\mathcal{M}\left(h \to W^+W^-\right)\right|^2}, \tag{V.49}$$

where k is such that the energy and momentum are conserved, i.e. $k = \frac{1}{2}\sqrt{m_h^2 - 4M_W^2}$. Hence, we have that by inserting the Eq. [V.45] in the above formula and evaluating the integral over the solid angle the total width is

$$\begin{aligned}\Gamma\left(h \to W^+W^-\right) &= \frac{1}{32\pi^2m_h^2}\cdot\frac{g^2m_h^4}{4M_W^2}\left(1 - 4x_W + 12x_W^2\right)\cdot 4\pi\cdot\frac{1}{2}\sqrt{m_h^2 - 4M_W^2} \\ &= \frac{g^2m_h^3}{64\pi M_W^2}\sqrt{1 - 4x_W}\left(1 - 4x_W + 12x_W^2\right),\end{aligned} \tag{V.50}$$

where we have used the fact that the amplitude has spherical symmetry, due to the scalar nature of the Higgs boson. Finally, we remember that $\frac{G_F}{\sqrt{2}} = \frac{g^2}{8M_W^2}$, therefore

$$\Gamma\left(h \to W^+W^-\right) = \frac{G_Fm_h^3}{8\sqrt{2}\pi}\sqrt{1 - 4x_W}\left(1 - 4x_W + 12x_W^2\right). \tag{V.51}$$

From this result, it is easily computable the width for the process $h \to ZZ$. To afford this, we just need to do $M_W \to M_Z$ in the formula [V.51], taking care of the Fermi constant. The Fermi constant factor arises from the

dynamic of the problem and it can be reduced as follows:

$$\begin{aligned}\frac{g_Z^2}{8M_Z^2} &= \frac{g_Z^2}{8M_W^2}\cos^2\theta_W \\ &= \frac{g^2+g'^2}{8M_W^2}\frac{g^2}{g^2+g'^2} \\ &= \frac{G_F}{\sqrt{2}},\end{aligned} \tag{V.52}$$

thus, the differences between the couplings of the Higgs boson and the electroweak bosons do not lead to differences in the final width. There is another issue that actually has effect on the width of the process $h \to ZZ$, which comes from the global $SU(2)$ custodial symmetry that remains after applying the vev. The result in Eq. [V.51] can be seen as

$$\Gamma\left(h \to W^+W^-\right) = \Gamma\left(h \to W^1W^1\right) + \Gamma\left(h \to W^2W^2\right), \tag{V.53}$$

which is equivalent to say that the Eq. [V.51] has a factor of two compared to the width of $h \to ZZ$. With all these, we have

$$\Gamma\left(h \to ZZ\right) = \frac{G_F m_h^3}{16\sqrt{2}\pi}\sqrt{1-4x_Z}\left(1-4x_Z+12x_Z^2\right). \tag{V.54}$$

Finally, we compute the decay width of the Higgs boson into fermions. Thus, we start with the amplitude at tree-level

$$\mathcal{M}\left(h \to \psi\bar{\psi}\right) = \bar{u}\left(p_\psi\right)\left(-i\frac{m_\phi}{v}\right)v\left(p_{\bar{\psi}}\right). \tag{V.55}$$

Then, by squaring and summing over the polarizations, we have

$$\begin{aligned}\overline{\left|\mathcal{M}\left(h \to \psi\bar{\psi}\right)\right|}^2 &= \left(\frac{m_\psi}{v}\right)^2 \mathrm{Tr}\left[\left(\not{p}_\psi + m_\psi\right)\left(\not{p}_{\bar{\psi}} - m_\psi\right)\right] \\ &= 4\left(\frac{m_\psi}{v}\right)^2\left(p_\psi \cdot p_{\bar{\psi}} - m_\psi^2\right).\end{aligned} \tag{V.56}$$

This can be written in a suitable way through $m_h^2 = \left(p_\psi + p_{\bar{\psi}}\right)^2 = 2m_\psi^2 + 2p_\psi \cdot p_{\bar{\psi}}$, thus

$$\overline{\left|\mathcal{M}\left(h \to \psi\bar{\psi}\right)\right|}^2 = 2\left(\frac{m_\psi}{v}\right)^2\left(m_h^2 - 4m_\psi^2\right). \tag{V.57}$$

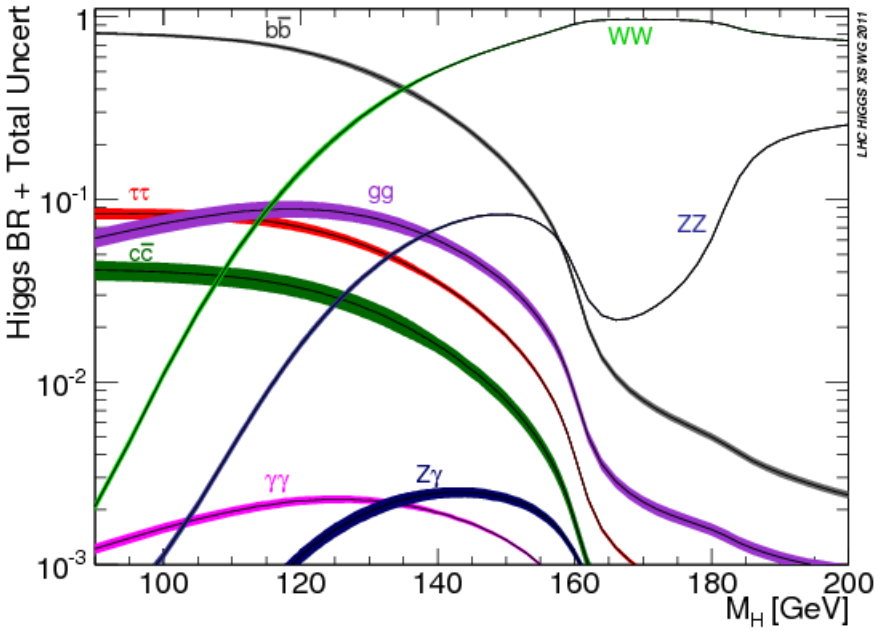

Figure V.8: Branching ratios and their uncertainties of the Higgs boson as a function of its mass.[67]

We recall the formula [V.46] and the computation of the phase-space integral, which leads to the result

$$\begin{aligned}\Gamma\left(h\to\psi\bar{\psi}\right) &= \frac{1}{2m_h}\cdot 2\left(\frac{m_\psi}{v}\right)^2 m_h^2\left(1-4x_\psi\right)\cdot\frac{1}{8\pi}\left(1-4x_\psi\right)^{1/2}\\ &= \frac{m_h}{8\pi}\left(\frac{m_\psi}{v}\right)^2\left(1-4x_\psi\right)^{3/2}. \end{aligned} \tag{V.58}$$

When this formula is applied to the case of quarks, we must take care of a color factor of 3. Thus, the decay width of the Higgs boson into quarks q and $\bar{q}$ is

$$\begin{aligned}\Gamma\left(h\to q\bar{q}\right) &= 3\cdot\frac{m_h}{8\pi}\left(\frac{m_q}{v}\right)^2\left(1-4x_\psi\right)^{3/2}\\ &= \frac{3G_F m_q^2 m_h}{4\pi\sqrt{2}}\left(1-4x_\psi\right)^{3/2}, \end{aligned} \tag{V.59}$$

while the decay width into leptons is

$$\Gamma\left(h\to\ell\bar{\ell}\right) = \frac{G_F m_\ell^2 m_h}{4\pi\sqrt{2}}\left(1-4x_\ell\right)^{3/2}. \tag{V.60}$$

With all this, we are able to see the BR of the Higgs boson:

$$\mathrm{BR}\left(h\to W^+W^-\right) = \frac{\Gamma\left(h\to final\right)}{\Gamma_h}. \tag{V.61}$$

In the Fig. [V.8] can be seen that there is a significant probability for the Higgs boson decay to W^+W^- below the threshold energy $\sqrt{s}\sim 160\,\mathrm{GeV}$ of the charged electroweak bosons. The same happens in the $h\to ZZ$

decay. This is possible due to the off-shell production of one of the electroweak bosons, which could decay into fermions. For a heavy Higgs boson, the decays would be mostly to WW and ZZ (and some $t\bar{t}$):

$$\mathrm{BR}\left(h \to W^+W^-\right) \approx \frac{\Gamma\left(h \to W^+W^-\right)}{\Gamma\left(h \to W^+W^-\right) + \Gamma\left(h \to ZZ\right)} \approx \frac{2}{3}. \tag{V.62}$$

For low Higgs mass ($m_h \leq 135\,\mathrm{GeV}$), decays into fermions dominate. The most important channel, in this case, is that for the heaviest fermion that is kinematically allowed, i.e. the bottom quark. Indeed, it is known that for $m_h \leq 100\,\mathrm{GeV}$ then $\mathrm{BR}\left(h \to b\bar{b}\right) \approx 0.8$.

From the decay widths of Higgs boson into fermions, it is noted that, with the masses of the charm quark $m_c = 1.27\,\mathrm{GeV}$ and the τ-lepton $m_\tau = 1.77\,\mathrm{GeV}$, the ratio

$$\frac{\Gamma\left(h \to \tau\bar{\tau}\right)}{\Gamma\left(h \to c\bar{c}\right)} \approx \frac{m_\tau^2}{3m_c^2} \approx 0.64, \tag{V.63}$$

suggests that the Higgs boson would decay more into the charm quark than into the τ-lepton. This observation does not match with the curves shown in the Fig. [V.8]. This happens because in the estimates made previously we have not taken the appropriate masses. We should take the running masses at the scale $\mu \sim m_h$. To leading order, the QCD corrections to the charm quark mass are given by

$$m_c\left(\mu\right) = \left[\frac{\alpha_s\left(\mu\right)}{\alpha_s\left(m_c^0\right)}\right]^{\gamma/2b} \cdot m_c\left(m_c^0\right), \tag{V.64}$$

where m_c^0 represents the charm mass at the QCD scale, the γ is the quark anomalous dimension, and b is the β-function coefficient at one-loop for the QCD coupling constant. The b expression is given by the number of colors and the number of flavors which at the scale that we are interested are just five (the top quark mass is bigger than the scale treated here) so that, in the end, $b = 23/3$, while $\gamma = 8$. Moreover, the QCD coupling is given at different energies by $\alpha_s\left(m_c^0\right) \approx 0,36$ and $\alpha_s\left(100\,\mathrm{GeV}\right)$. With this, the charm mass near the measured Higgs mass is

$$m_c\left(100\,\mathrm{GeV}\right) \approx 0.68\,\mathrm{GeV}. \tag{V.65}$$

We can neglect the running of the τ-mass, which is due only to the weak interactions. With this, it turns out that

$$\frac{\Gamma\left(h \to \tau\bar{\tau}\right)}{\Gamma\left(h \to c\bar{c}\right)} \approx \frac{m_\tau^2}{3\left(m_c\left(100\,\mathrm{GeV}\right)\right)^2} \approx 2.3, \tag{V.66}$$

which explains why $\mathrm{BR}\left(h \to \tau\bar{\tau}\right) \approx 2\mathrm{BR}\left(h \to c\bar{c}\right)$ in the Fig. [V.8].

Decay Channel	Branching Ratio
$h \to \gamma\gamma$	2.27×10^{-3}
$h \to ZZ$	2.62×10^{-2}
$h \to W^+W^-$	2.14×10^{-1}
$h \to \tau^+\tau^-$	6.27×10^{-2}
$h \to b\bar{b}$	5.84×10^{-1}
$h \to Z\gamma$	1.53×10^{-3}
$h \to \mu^+\mu^-$	2.18×10^{-4}

Table V.1: The Branching Ratios for a Higgs boson with $m_h = 125\,\text{GeV}$.[15]

Now, with a Higgs mass of 125 GeV, we can see from Fig. [V.8] that the dominant decay modes, from preferred to less preferred, are $h \to b\bar{b}$, $h \to WW^*$, $h \to gg$, followed by $h \to \tau\bar{\tau}$, $h \to c\bar{c}$, and $h \to ZZ^*$. The total width of the SM Higgs boson is $\Gamma_h = 4.07 \times 10^{-3}\,\text{GeV}$, with uncertainties $(+4.0\% - -3.9\%)$ [15]. Here, the uncertainties include the missing higher-order corrections in the theoretical calculations and the errors in the SM input parameters. Some BR are listed in the table [V.1].

Chapter VI

Double Higgs production via electron-positron annihilation

It is strongly believed since the already discussed phenomenological and theoretical reasons that the electroweak symmetry breaking of the SM is not fully characterized, and so, that there should be a deeper mechanism for such symmetry breaking. With this motivation, a whole description of the Higgs sector is required, as well as a direct measurement with high precision of the parameters of the Higgs potential. Higgs production processes can yield relevant information about the details of the Higgs sector.

The triple Higgs boson production tells us the way this kind of processes give hints about the UV completions of the SM. Specifically, the processes

$$e^+e^- \to H^+H^-h_i, \qquad e^+e^- \to h^0H^0A^0, \qquad e^+e^- \to h_ih_iA^0,$$

with $h_i = h^0, H^0, A^0$, have been studied at tree level in the 2HDM and MSSM frames giving substantial differences between the cross-sections. In the 2HDM type I and II the above processes have $\sigma \sim 0.01 - 1$ pb, while the MSSM counterparts have $\sigma \sim 10^{-6}$ pb [58].

In the same fashion, the processes $e^+e^- \to 2h$, with $2h_i = h^0A^0, H^0A^0$, present unmatched results for the cross-sections between the 2HDM and MSSM at 1-loop. Thus a detailed analysis here allows a phenomenological distinction between the above two mentioned extensions of the Standard Model. The main difference comes from the tree-level coupling A^0h^0Z, since in the MSSM it presents a suppression as $\tan\beta$ and M_{A^0} grow. At $\sqrt{s} = 500\,\text{GeV}$ and with $M_{A^0} = 300\,GeV$ the cross-section for double Higgs production is $\sim 0.01\,\text{fb}$ for the MSSM, while for the 2HDM it is obtained a prediction of order $\sim 10\,\text{fb}$. A complete analysis of the production

of the scalar - pseudo-scalar can be found in [59].

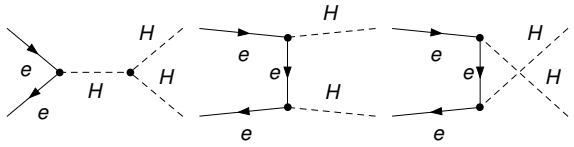

Figure VI.1: Feynman diagrams at tree-level for $e^+e^- \to hh$.

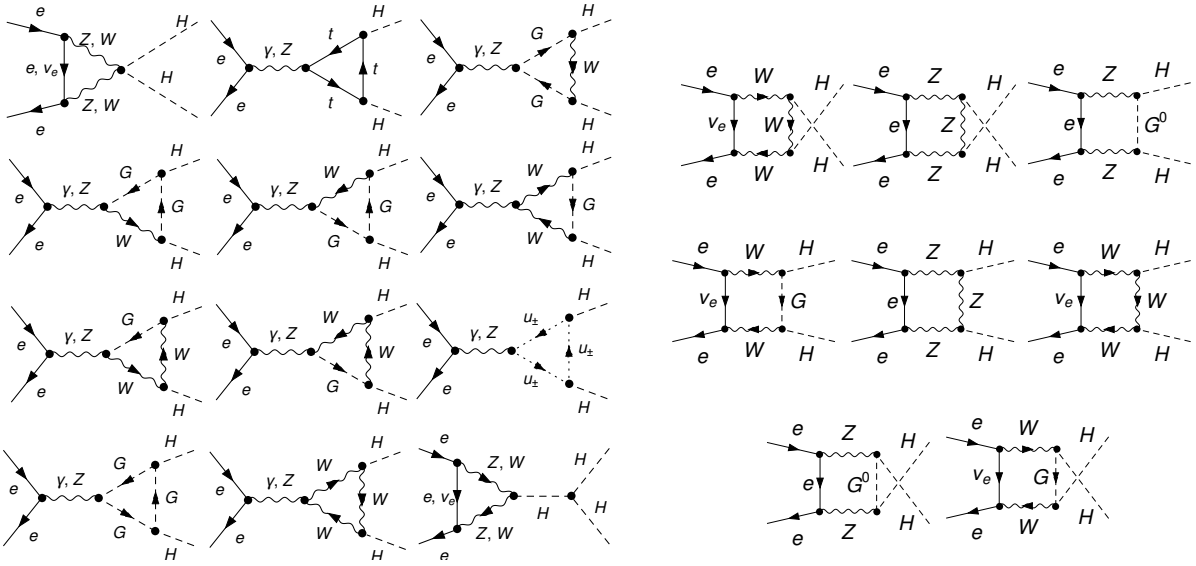

Figure VI.2: (a) Triangle and (b) Box topologies at 1-loop for $e^+e^- \to hh$.

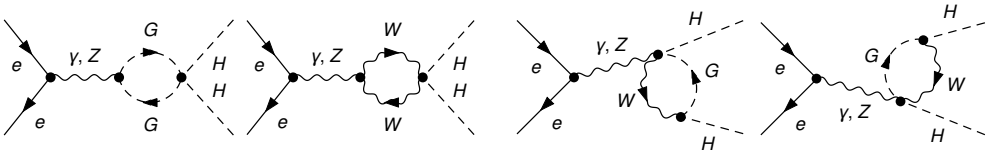

Figure VI.3: Bubble topologies at 1-loop for $e^+e^- \to hh$.

Also remarkable is the fact that, in the SM, the process $e^+e^- \to hh$ is highly suppressed. The tree-level amplitude is very small, while at one-loop the cross-section is of order 10^{-2} fb, as it is known from the work [60] presented in 1984. Thus a detection of this process at the order of 1 fb or above is a strong sign of new physics.

Now, we focus on the double Higgs production through e^+e^- annihilation, then it is discussed in this section that these processes will give us hints about new physics in the forthcoming accelerators.

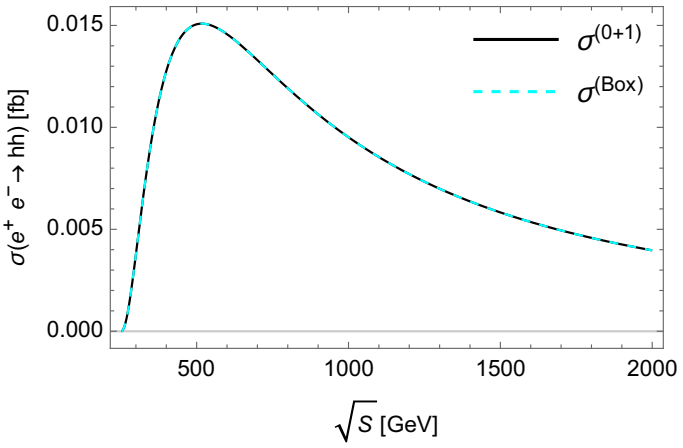

Figure VI.4: Total cross-section and box contribution for the process $e^+e^- \to hh$ in the SM, where it is shown that only the box topologies do contribute substantially. Here $\sigma^{(0+1)}$ stands for the total cross-section at NLO and $\sigma^{(Box)}$ for the cross-section coming just from the Box diagrams.

VI.1 Double Higgs production in the SM ($e^+e^- \to hh$)

This subsection is dedicated to this basic process. This process is computed at tree-level through 3 diagrams, while 68 diagrams can be found that contribute at 1-loop, this in the Feynman gauge. At tree-level, we get a process that is suppressed from the Yukawa couplings of the electron-positron to the Higgs, i.e. suppressed from the smallness of the electron mass.

In particular, the production of a Higgs boson pair in the SM is weakly dependent on the triangle and bubble topologies of the loops (Fig. [VI.3 and [VI.2](a)]), as can be seen in the plot [VI.4], i.e. the biggest contribution comes from the boxes (Fig. [VI.2](b)). Although in this process there are top loops involved, as it is presented in the figure [VI.2], they are manifestly zero.

Usually, the diagrams with top loops represent some of the biggest contributions for a given process. In our particular process, the diagrams with a top loop cancel out between them. For example, there are two diagrams with a Z-boson propagator and a top loop, which are almost the same, except for the direction of the fermionic flow in the loop. These two diagrams cancel out. The same happens with a γ-boson propagator.

The whole contribution of the triangle topologies represent a contribution to the 1-loop cross-section of order $\sim 10^{-14}$ fb. This process is weakly dependent on the trilinear coupling of the Higgs. To see it, let us analyze the diagram in the figure [VI.6]. When we see the terms $h(\bar{e}_L e_R + \bar{e}_R e_L)$ in the Lagrangian of the SM, it is noted that such structure must be preserved in the loop mediated between the Higgs and the pair electron-positron. Thus, the non-vanishing combinations of helicities are those in which the electron and the positron have opposite helicities. Hence, to get a non-vanishing contribution a mass insertion should appear, such that this contribution is proportional to the electron mass. The hhh-interaction is also presented in the diagrams at

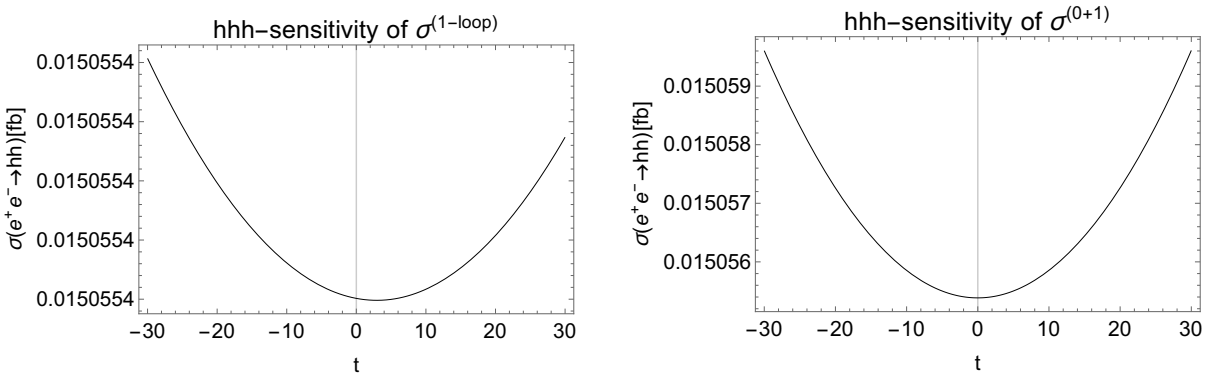

(a) (b)

Figure VI.5: Dependence on the trilinear Higgs coupling of the cross-section for $e^+e^- \to hh$ just for the 1-loop contribution (Left), and of the total cross section at NLO (Right).

tree-level, which are also proportional to the electron mass. Hence, the dependence on these Higgs interactions is suppressed by the small electron mass.

The dependence on the trilinear Higgs coupling can also be seen by a naive parametrization of such coupling by changing $\mu^2 \to t\mu^2$, so that the Standard Model result can be found at $t = 1$. From the Feynman diagrams, we can expect a quadratic sensitivity of the cross-sections at tree level and 1-loop. Precisely, this is what is obtained, as is shown in Fig. VI.5. The 1-loop contribution has as a minimum near $t = 3$ and the SM situation is very close to such minimum, which evidences the fact that the 1-loop contribution is non-sensitive to the trilinear Higgs coupling. A different situation happens to the total cross-section at NLO, which presents a stronger sensitivity to the trilinear Higgs coupling than the case with just 1-loop, and in this case, the SM gets closer to the minimum of the contribution of this coupling.

A well-known fact in Higgs physics is the vanishing of amplitudes involving multiple scalars near the threshold energy. This can be reached through cancellation of classes of Feynman diagrams. In our case, this property is satisfied, as it is shown through the plot in Fig. [VI.7], where it is clear the suppression of the amplitude when we approach $\sqrt{s} = 250\,\text{GeV}$.

Such suppression near the threshold of the production of multiple Higgses has been highly featured in other cases. In particular, in the double Higgs production through gluon fusion, low-energy theorems can easily

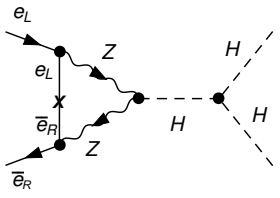

Figure VI.6: Example of the helicity structure for diagrams involving the trilinear Higgs interaction.

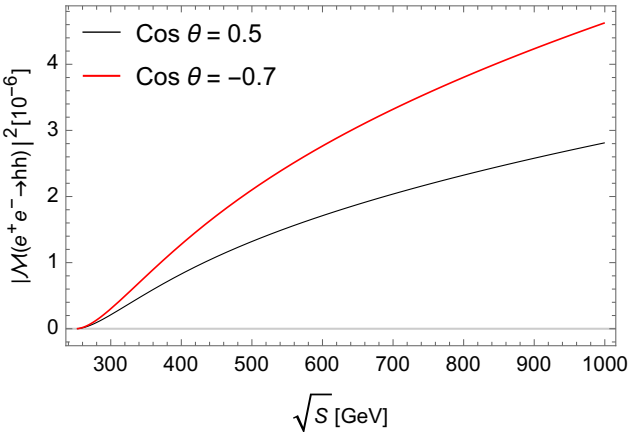

Figure VI.7: Vanishing amplitude for the process $e^+e^- \to hh$ near threshold, where it has been fixed randomly two collision angles in order to present that the suppression is not due to such fixing.

show that the box contributions are of the same order of the triangle contributions so that near the threshold both contributions cancel out[57]. Such cancellations between diagrams arising from different topologies cannot happen in our electron-positron annihilation, due to the fact that the triangles topologies are highly suppressed.

VI.2 Enhancement of $e^+e^- \to hh$ via Effective operators

From the last section, it is known that the triangle topologies do not contribute substantially to the total cross-section of the process $e^+e^- \to hh$. However, it could happen that new physics changes the above situation so that the total cross-section is enhanced due to different triangle contributions. The first sign of such new contributions can be found through effective operators, then, in this section, it is studied in a model-independent fashion the way to get an enhancement of $\sigma(e^+e^- \to hh)$ from the effective operators discussed in the section [II.2].

The coupling between the top quark and the Higgs field usually leads to big contributions, since it is proportional to the top mass, then if new physical particles can interact with fermions and quarks it is expected that the top-Yukawa coupling could yield a good enhancement. Following this idea, we start by inspecting the interaction

$$\mathcal{L}_{et} = \frac{C_1}{\Lambda^2}(\bar{e}e)(\bar{t}t), \tag{VI.1}$$

which does not respect the SM gauge symmetry, but that may give us a hint of which kind of effective operators could provide the discussed cross-section with a big enhancement. The implementation of this effective contribution can be done through FeynRules[61], so that the model file can be used by FeynArts and FormCalc.

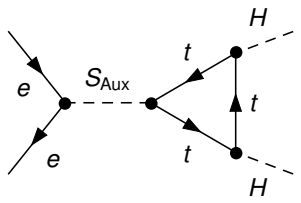

Figure VI.8: Feynman Diagram of an effective contribution that reproduces a Fermi-like interaction.

At this step, it arises an annoying situation: FormCalc does not work well with Fermi-like interactions. This can be managed with an auxiliary scalar as a mediator of the interaction between electrons and top quarks so that the propagator shrinks to a point when we take a huge mass for the fictitious scalar. Hence, we consider a scalar with the interaction

$$\mathcal{L}^{Aux} = \frac{1}{2}(\partial\phi)^2 + \frac{1}{2}m_\phi^2\phi^2 + Y_\phi\phi\bar{e}e + Y_\phi\phi\bar{t}t, \tag{VI.2}$$

then, from the Feynman rules, it is readily identified

$$\frac{C_1}{\Lambda^2} = \frac{Y_\phi^2}{m_\phi^2}. \tag{VI.3}$$

This relation can be easily checked. By implementing the model with the auxiliary scalar it is found

$$\overline{|\mathcal{M}^{FA}\left(e^+e^- \to \bar{t}t\right)|^2} \;=\; 3\frac{Y_\phi^4}{m_\phi^4}\, s\left(s - 4m_t^2\right), \tag{VI.4}$$

while, if we use the four-point interaction coming from the Lagrangian [VI.2], it is obtained the Feynman rule for the four fermions $i\frac{C_{et}}{\Lambda^2}\delta^{ab}$, with a, b being color indices. With this it is easy to compute the analogous of Eq. [VI.4]:

$$\begin{aligned}
\overline{|\mathcal{M}^{4-fermion}\left(e^+e^- \to \bar{t}t\right)|^2} &= \frac{C_1^2}{\Lambda^4}\cdot 3\cdot\frac{1}{4}\sum_{r,\,r',s,\,s'}\left(v_b^r(p)\bar{v}_a^r(p)\right)\left(u_a^{r'}(p')\bar{u}_b^{r'}(p')\right)\left(u_d^s(q)\bar{u}_c^s(q)\right)\left(v_c^{s'}(q')\bar{v}_d^{s'}(q')\right)\\
&= \frac{3}{4}\frac{C_1^2}{\Lambda^4}\mathrm{Tr}[\not{p}\not{p}']\mathrm{Tr}[(\not{q}+m_t)(\not{q}'-m_t)]\\
&= \frac{3}{4}\frac{C_1^2}{\Lambda^4}\left(4p\cdot p'\right)\left(4q\cdot q' - 4m_t^2\right)\\
&= 3\frac{C_1^2}{\Lambda^4}\, s\left(s - 4m_t^2\right)
\end{aligned} \tag{VI.5}$$

with the electron massless and $s = (p+p')^2 = 2p\cdot p'$ or $s = (q+q')^2 = 2m_t^2 + 2q\cdot q'$. In the first line, the factor 3 comes as a color factor. Thus, we can see that Eq. [VI.3] is truthful.

This approach allows the implementation in FeynArts and FormCalc of Fermi-like interactions. The new

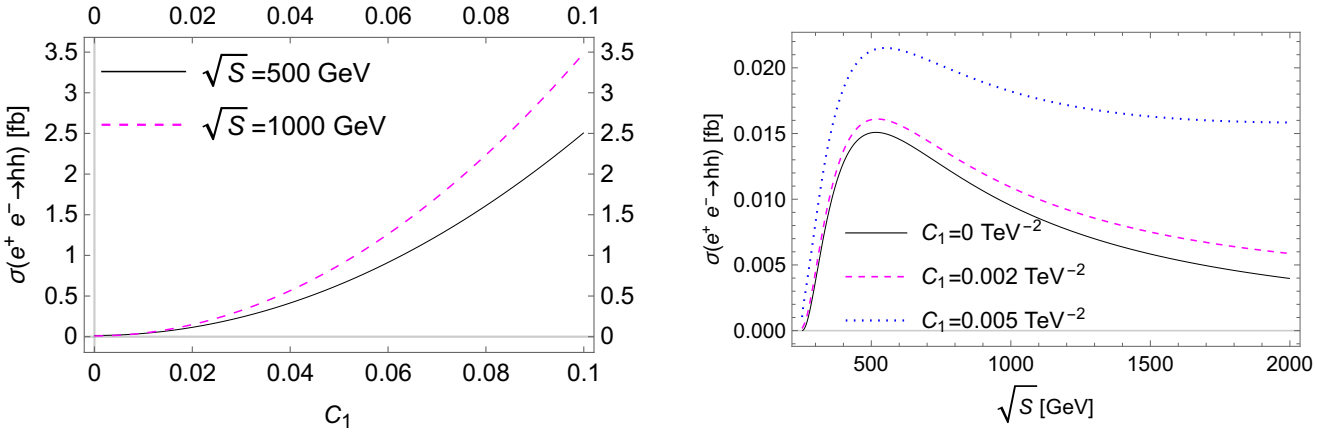

(a) (b)

Figure VI.9: Sensitivity (Left) and enhancement (Right) of the cross-section $\sigma\left(e^+e^- \to hh\right)$ due to variations of the Wilson coefficient C_1 that appears in Eq. [VI.1].

contributions to the process of interest come from the triangle diagram shown in Fig. [VI.8] and the analogous crossed one. These contributions lead to the enhancement presented in the plots in Fig. [VI.9]. Now that we have seen that four-fermion interactions between the electron and the top quark succeeds in increasing the cross section for the process $e^+e^- \to hh$, we are able to move on towards more complex operators that do respect the gauge symmetries of the SM. Thus we seek operators in the basis shown in section [II.2] that can contain the electron-top interactions. In this direction, we can find several possibilities. By using the Warsaw basis published in [62] we pick up some operators

$$\begin{aligned} Q_{lq}^{(1)} &= \frac{C_{lq}}{\Lambda^2}\left(\bar{L}_e\gamma_\mu L_e\right)\left(\bar{Q}_t\gamma^\mu Q_t\right), \quad Q_{eu} = \frac{C_{eu}}{\Lambda^2}\left(\bar{E}_e\gamma_\mu E_e\right)\left(\bar{U}_t\gamma^\mu U_t\right), \quad Q_{lq}^{(3)} = \frac{C'_{lq}}{\Lambda^2}\left(\bar{L}_e\gamma_\mu\tau^I L_e\right)\left(\bar{Q}_t\gamma^\mu\tau^I Q_t\right) \\ Q_{lu} &= \frac{C_{lu}}{\Lambda^2}\left(\bar{L}_e\gamma_\mu L_e\right)\left(\bar{U}_t\gamma^\mu U_t\right), \quad Q_{qe} = \frac{C_{qe}}{\Lambda^2}\left(\bar{Q}_t\gamma_\mu Q_t\right)\left(\bar{E}_e\gamma^\mu E_e\right), \quad Q_{lequ}^{(1)} = \frac{C_{et}}{\Lambda^2}\epsilon_{ij}\left(\bar{L}_e^i E_e\right)\left(\bar{Q}_t^j U_t\right), \end{aligned} \tag{VI.6}$$

where the notation of the chapter [I] was used. Here, the trick of including an auxiliary mediator between the electronic and top currents again may be used. For the first five operators in Eq. [VI.6] instead of a scalar operator, it should be introduced an auxiliary vectorial boson. With this in mind, the possible new diagrams have a vectorial propagator together with a top loop. This is the same situation that we had with the Z- and γ-bosons, which vanished. In effect, the trick of inserting a vectorial boson in between the two fermionic currents leads to vanishing contributions.

The remaining operator in Eq. [VI.6] that could contribute to the process $e^+e^- \to hh$ is $Q_{lequ}^{(1)}$. Such operator can be implemented in FeynArts through an auxiliary $SU(2)_L$ scalar doublet, with the Lagrangian

$$\mathcal{L} \;=\; \left(\partial_\mu\Phi\right)^2 + m_\Phi^2\Phi^2 + Y_\Phi\left(\bar{L}_e^j E_e\right)\Phi_j + Y_\Phi\epsilon_{jk}\left(\bar{Q}_t^j U_t\right)\Phi^{*k}, \tag{VI.7}$$

where

$$\Phi \;=\; \begin{pmatrix} -i\phi^{+} \\ \frac{\phi_0+i\phi_1}{\sqrt{2}} \end{pmatrix}. \tag{VI.8}$$

Then, a match between this auxiliary model and the four-fermion interaction is needed. Through the auxiliary model and FeynArts, it is found that

$$\overline{|\mathcal{M}^{FA}\left(e^{+}e^{-}\to\bar{t}t\right)|^{2}} \;=\; \frac{3}{2}\frac{Y_{\phi}^{4}}{m_{\Phi}^{4}}\, s\left(s-2m_{t}^{2}\right). \tag{VI.9}$$

On the other hand, the vertex of the operator with four fermions is

$$-\,i\frac{C_{et}}{\Lambda^{2}}\left(\left(P_{-}\right)_{ab}\left(P_{-}\right)_{cd}+\left(P_{+}\right)_{ab}\left(P_{+}\right)_{cd}\right) \tag{VI.10}$$

with $P_{\pm} = (1 \pm \gamma_5)/2$. With this, the amplitude involving electron and top fields through the Fermi-like interaction takes the form

$$i\mathcal{M}\left(e^{+}e^{-}\to\bar{t}t\right) = -i\frac{C_{et}}{\Lambda^{2}}\left(\bar{v}^{r}(p)P_{-}u^{r'}(p')\bar{u}^{s}(q)P_{-}v^{s'}(q')+\bar{v}^{r}(p)P_{+}u^{r'}(p')\bar{u}^{s}(q)P_{+}v^{s'}(q')\right). \tag{VI.11}$$

Thus, the unpolarized square of the amplitude only have the non-vanishing crossed terms

$$\begin{aligned}
\overline{|\mathcal{M}|^{2}} \;&=\; \frac{C_{et}^{2}}{\Lambda^{4}}\cdot 3\cdot\frac{1}{4}\left\{\left(P_{+}\right)_{ab}\left(P_{-}\right)_{ef}\left(P_{+}\right)_{cd}\left(P_{-}\right)_{gh}+\left(P_{-}\right)_{ab}\left(P_{+}\right)_{ef}\left(P_{-}\right)_{cd}\left(P_{+}\right)_{gh}\right\} \\
&\qquad\times\left(\sum_{r}v_{f}^{r}(p)\bar{v}_{a}^{r}(p)\right)\left(\sum_{r'}u_{b}^{r'}(p')\bar{u}_{e}^{r'}(p')\right)\left(\sum_{s}u_{h}^{s}(q)\bar{u}_{c}^{s}(q)\right)\left(\sum_{s'}v_{d}^{s'}(q')\bar{v}_{g}^{s'}(q')\right) \\
&=\; \frac{3}{4}\frac{C_{et}^{2}}{\Lambda^{4}}\left\{\mathrm{Tr}[\not{p}P_{+}\not{p}'P_{-}]\mathrm{Tr}[(\not{q}+m_{t})\,P_{+}\,(\not{q}'-m_{t})\,P_{-}]\;+\;\mathrm{Tr}[\not{p}P_{-}\not{p}'P_{+}]\mathrm{Tr}[(\not{q}+m_{t})\,P_{-}\,(\not{q}'-m_{t})\,P_{+}]\right\} \\
&=\; \frac{3}{4}\frac{C_{et}^{2}}{\Lambda^{4}}\cdot\frac{1}{16}\left[2\times\left(2\mathrm{Tr}[\not{p}\not{p}']\right)\left(2\mathrm{Tr}[\not{q}\not{q}']\right)\right] \\
&=\; 3\frac{C_{et}^{2}}{\Lambda^{4}}\cdot\frac{1}{16}\left[2\times 4p\cdot p'\times 4q\cdot q'\right] \\
&=\; 3\frac{C_{et}^{2}}{\Lambda^{4}}\cdot\frac{1}{16}\left[2\times 2s\times 2(s-2m_{t}^{2})\right] \\
&=\; \frac{3}{2}\frac{C_{et}^{2}}{\Lambda^{4}}\cdot s(s-2m_{t}^{2}).
\end{aligned} \tag{VI.12}$$

Then, by matching the Eq. [VI.9] and [VI.12], it is found the relation

$$\frac{C_{et}}{\Lambda^{2}} = -\frac{Y_{\phi}}{m_{\Phi}^{2}}, \tag{VI.13}$$

where the minus sign does not appear before in the computations since we compare equations at the squared amplitude level, but that should be there in the implementation in FormCalc.

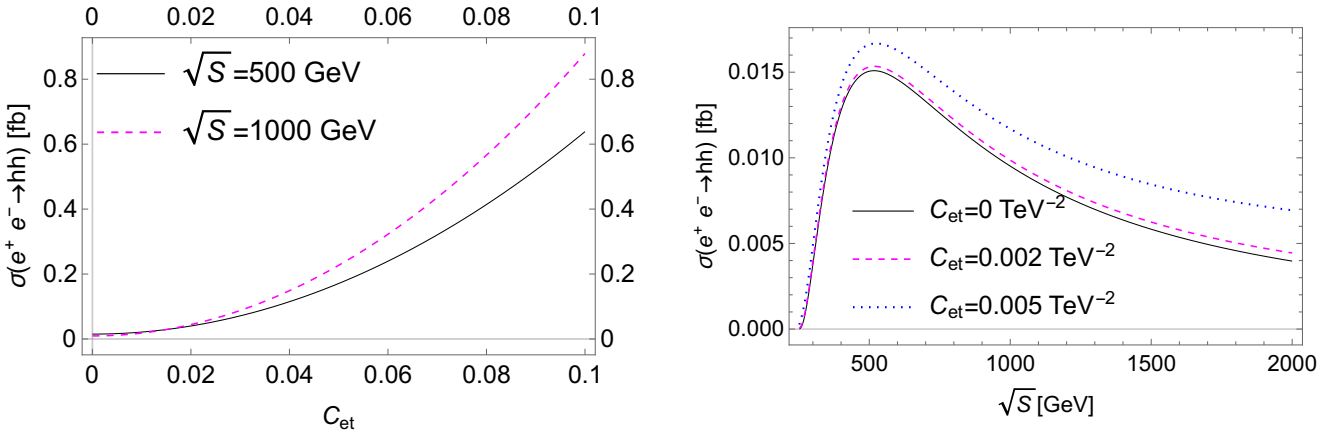

(a) (b)

Figure VI.10: Sensitivity (Left) and enhancement (Right) of the cross-section $\sigma\left(e^+e^- \to hh\right)$ due to variations of the Wilson coefficient C_{et} introduced in the Lagrangian of Eq. [VI.15].

For the Higgs production, just the interaction between electrons and tops contained in $Q^{(1)}_{lequ}$ contributes, while the interaction involving the bottom quark and electronic neutrino does not affect the cross-section at 1-loop. After the computations through FormCalc, it is found the enhanced cross-section shown in Fig. [VI.10].

In addition, we can think about other interactions that could enhance the double Higgs production. In this analysis, we take effective operators with less-constrained Wilson operators in the literature[69]. An additional operator is considered: the modification to the Yukawa coupling of the electron:

$$Q_{eH} = \frac{C_{eH}}{\Lambda^2}\left(H^\dagger H - \frac{v^2}{2}\right)\bar{L}_e H E_e. \tag{VI.14}$$

Hence, we consider the enhancement coming from the Lagrangian

$$\mathcal{L}^{eff} = \mathcal{L}_{SM} + \left(\frac{C_{eH}}{\Lambda^2}\left(H^\dagger H - \frac{v^2}{2}\right)\bar{L}_e H E_e + \frac{C_{et}}{\Lambda^2}\epsilon_{ij}\left(\bar{L}^i_e E_e\right)\left(\bar{Q}^j_t U_t\right) + h.c.\right). \tag{VI.15}$$

The operator Q_{eH} has been defined in such a way that the identification of the electron mass in terms of the Yukawa coupling remains as in the SM. This last fact can be seen explicitly. In the unitary gauge

$$\begin{aligned}
\mathcal{L}^{eff} &\supset -y_e \bar{L}_e H E_e + \frac{C_{eH}}{\Lambda^2}\left(H^\dagger H - \frac{v^2}{2}\right)\bar{L}_e H E_e + h.c. \\
&\to -y_e \cdot \frac{1}{\sqrt{2}}(v+h)\,\bar{e}_L e_R + \frac{C_{eH}}{\Lambda^2}\left(\frac{1}{2}(v+h)^2 - \frac{v^2}{2}\right)\cdot\frac{1}{\sqrt{2}}(v+h)\,\bar{e}_L e_R + h.c. \\
&= -y_e \frac{v}{\sqrt{2}}\bar{e}_L e_R - \left(\frac{y_e}{\sqrt{2}} - \frac{C_{eH}}{\Lambda^2}\cdot\frac{v^2}{\sqrt{2}}\right) h\bar{e}_L e_R + h.c. + \ldots,
\end{aligned} \tag{VI.16}$$

so that the mass term of the electron is as in the SM, while the Yukawa interaction gets a modification.

In addition to the 68 1-loop Feynman diagrams that appear in the SM, there is 1 additional tree-level diagram

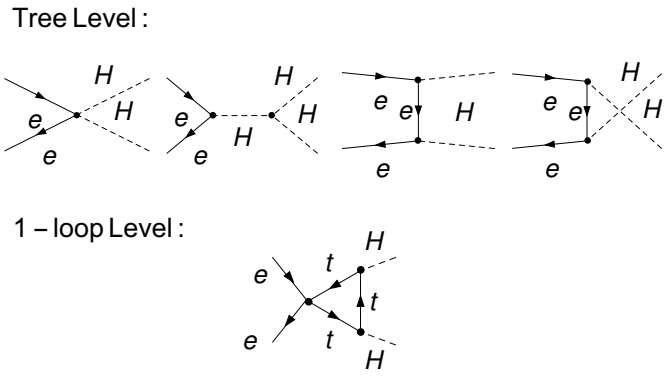

Figure VI.11: Chosen Feynman diagrams that introduces the effective interactions effects from Eq. [VI.15] into the cross-section $\sigma\left(e^+e^- \to hh\right)$.

coming from the modified Yukawa interaction and 1 additional 1-loop diagram that comes from the four-fermion interaction. In the figure [VI.11] are shown the chosen diagrams that are sensitive to the effective interactions. It is remarkable the fact that the first two diagrams at tree-level in Fig. [VI.11] are of order $\mathcal{O}\left(C_{eH}\right)$, while the last two diagrams can reach the order $\mathcal{O}\left(C_{eH}^2\right)$. It is also noted that the modified Yukawa interaction could contribute through numerous diagrams at 1-loop, but such contributions were not taken into account in this analysis. The total number of Feynman diagrams studied is $4^{(tree)} + 69^{(1-loop)} = 73$, where the 68 diagrams at 1-loop are the 68 from the SM and the 1 diagram from the four-fermion interaction.

The cross-section has been taken to be of order

$$\sigma\left(e^+e^- \to hh\right) \sim \mathcal{O}\left(C_{eH}^2\right) + \mathcal{O}\left(C_{eH}C_{et}\right) + \mathcal{O}\left(C_{et}^2\right), \tag{VI.17}$$

then, the quartic contributions in the coefficient C_{eH} that could come from the tree-level diagrams have been neglected. Moreover, we note that the contributions $\mathcal{O}\left(C_{eH}C_{et}\right)$ come from interference between the tree-level and the 1-loop diagrams.

Now, the goal is to put bounds to the Wilson coefficients that appear in Eq. [VI.15] by assuming that its effects have been unveiled to the current experimental precision. To do this, it is needed a statistical analysis. The usual measure to test a hypothesis is the χ^2 distribution. Then, we want to see the possible values of our coefficients that leave the enhanced cross-section near to the SM values, allowed by a given statistical confidence. We take the χ^2 distribution for one degree of freedom, given by the SM values:

$$\chi^2\left(C_i\right) \quad = \quad \frac{\left(\sigma\left(C_i\right) - \sigma_{SM}\right)^2}{\delta\sigma_{SM}^2}, \tag{VI.18}$$

with the $\delta\sigma_{SM}^2$ the expected deviations due to statistical and systematic uncertainties, while the numerator is

the usual measure of the deviations of the enhanced cross-section from the SM values. Then we want to put bounds to the Wilson coefficients by excluding values that lead to significant deviations, in particular, for

$$\chi^2(C_i) \quad > \quad 3.841, \tag{VI.19}$$

we exclude C_i values at 95% of confidence level. The relation [VI.18] can be written in a suitable way. We follow by knowing that the total number of events (N) is related to the cross-section through a fixed integrated luminosity $\mathcal{L}$:

$$N \quad = \quad \mathcal{L}\,\sigma. \tag{VI.20}$$

It is also well known that there can be statistic and systematic uncertainties so that the total uncertainty of the number of events and the cross-section can be taken to be

$$\frac{\delta N}{N} \quad = \quad \sqrt{\left(\frac{\delta N}{N}\right)^2_{Stat} + \left(\frac{\delta N}{N}\right)^2_{Sys}}, \qquad \frac{\delta\sigma}{\sigma} = \sqrt{\left(\frac{\delta\sigma}{\sigma}\right)^2_{Stat} + \left(\frac{\delta\sigma}{\sigma}\right)^2_{Sys}}. \tag{VI.21}$$

Moreover,

$$\left(\frac{\delta\sigma}{\sigma}\right)_{Stat} = \left(\frac{\delta N}{N}\right)_{Stat} \quad = \quad \frac{1}{\sqrt{N}}, \tag{VI.22}$$

so that by Eq. [VI.20]:

$$\delta\sigma_{Stat} \quad = \quad \frac{\sigma}{\sqrt{N}} = \sqrt{\frac{\sigma}{\mathcal{L}}}. \tag{VI.23}$$

On the other hand, the systematic uncertainties are parametrized as

$$\left(\frac{\delta\sigma}{\sigma}\right)_{Sys} = \left(\frac{\delta N}{N}\right)_{Sys} \quad = \quad \alpha. \tag{VI.24}$$

With all this, we write

$$\chi^2(C_i) \quad = \quad \frac{\mathcal{L}}{\sigma_{SM}} \frac{\left(\sigma(C_i) - \sigma_{SM}\right)^2}{1 + \alpha^2 \sigma_{SM} \mathcal{L}}. \tag{VI.25}$$

By studying the sensitivity in $\sigma(e^+e^- \to hh)$ to the operators in Eq. [VI.15], the bounds plotted in the figures [VI.12] and [VI.13] are obtained. This was done through the formula [VI.25] to construct a χ^2-distribution depending on the coefficients C_{eH} and C_{et}. To get such bounds, some benchmark values were used, listed in the table [VI.1] taken from [65], where $\alpha = 0.01$. It can be seen that the bounds to modified Yukawa interaction are stronger than those for the four-fermion interaction.

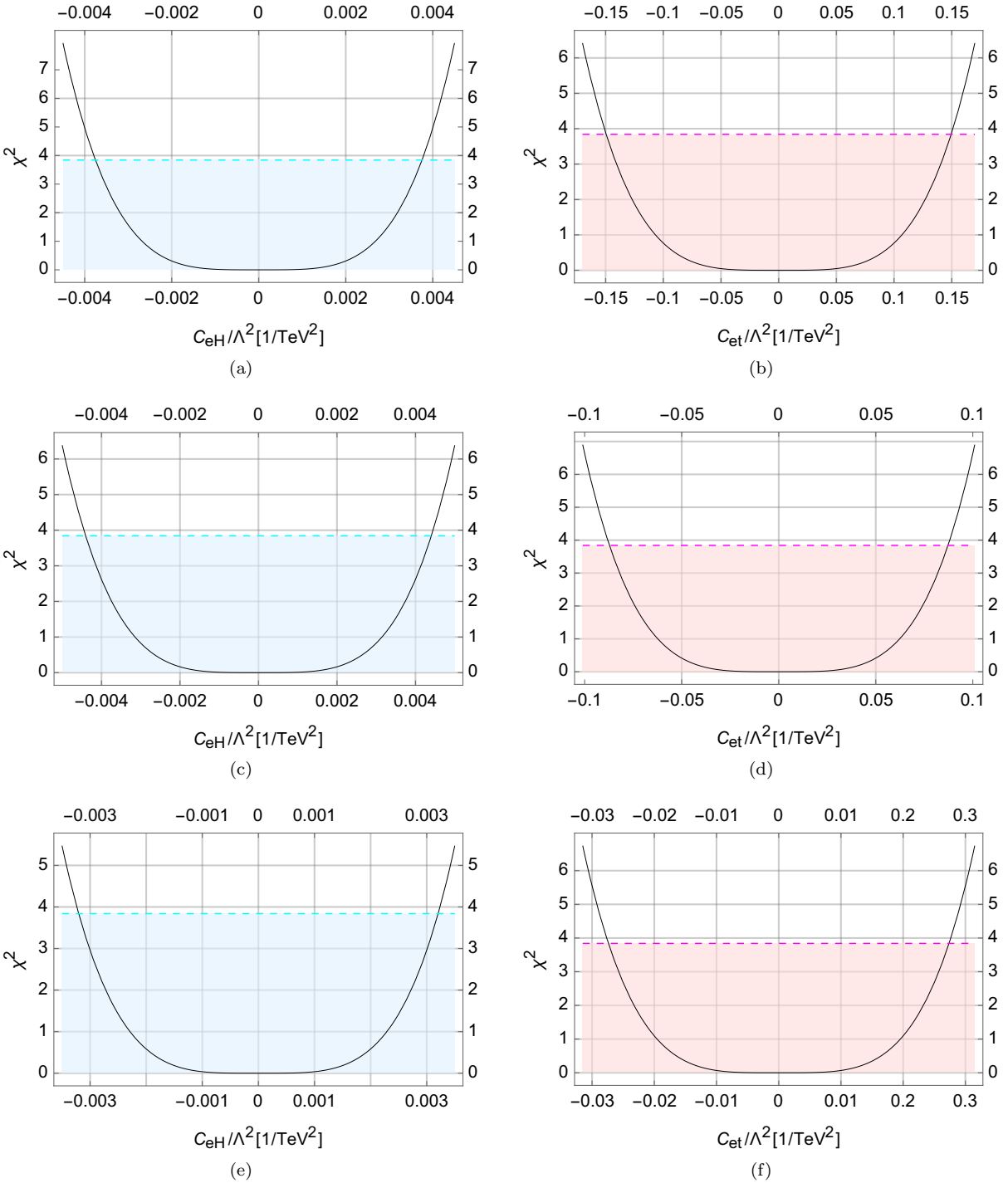

Figure VI.12: χ^2-distribution for the Wilson coefficients C_{eH} (left) and C_{et} (right) from the cross-section of the double Higgs production via electron-positron annihilation. Here the horizontal lines stand for the limit of 95% of confidence level from a χ^2 distribution with 1 degree of freedom. The bounds a)-b) are expected for $\mathcal{L} = 2.6\,\text{ab}^{-1}$ at 350 GeV, benchmark values of the FCC-ee Project. The bounds c)-d) are expected for $\mathcal{L} = 4\,\text{ab}^{-1}$ at 500 GeV, benchmark values of the ILC Project. The bounds e)-f) are expected for $\mathcal{L} = 1.5\,\text{ab}^{-1}$ at 1.5 TeV, benchmark values of the CLIC Project.

FCC-ee	CLIC	ILC
2.6 ab^{-1}@ 350 GeV	500 fb^{-1}@ 380 GeV	4 ab^{-1}@ 500 GeV
	1.5 ab^{-1}@ 1,5 TeV	
	3 ab^{-1}@ 3 TeV	

Table VI.1: Benchmark luminosities and energies for different future experiments.[65]

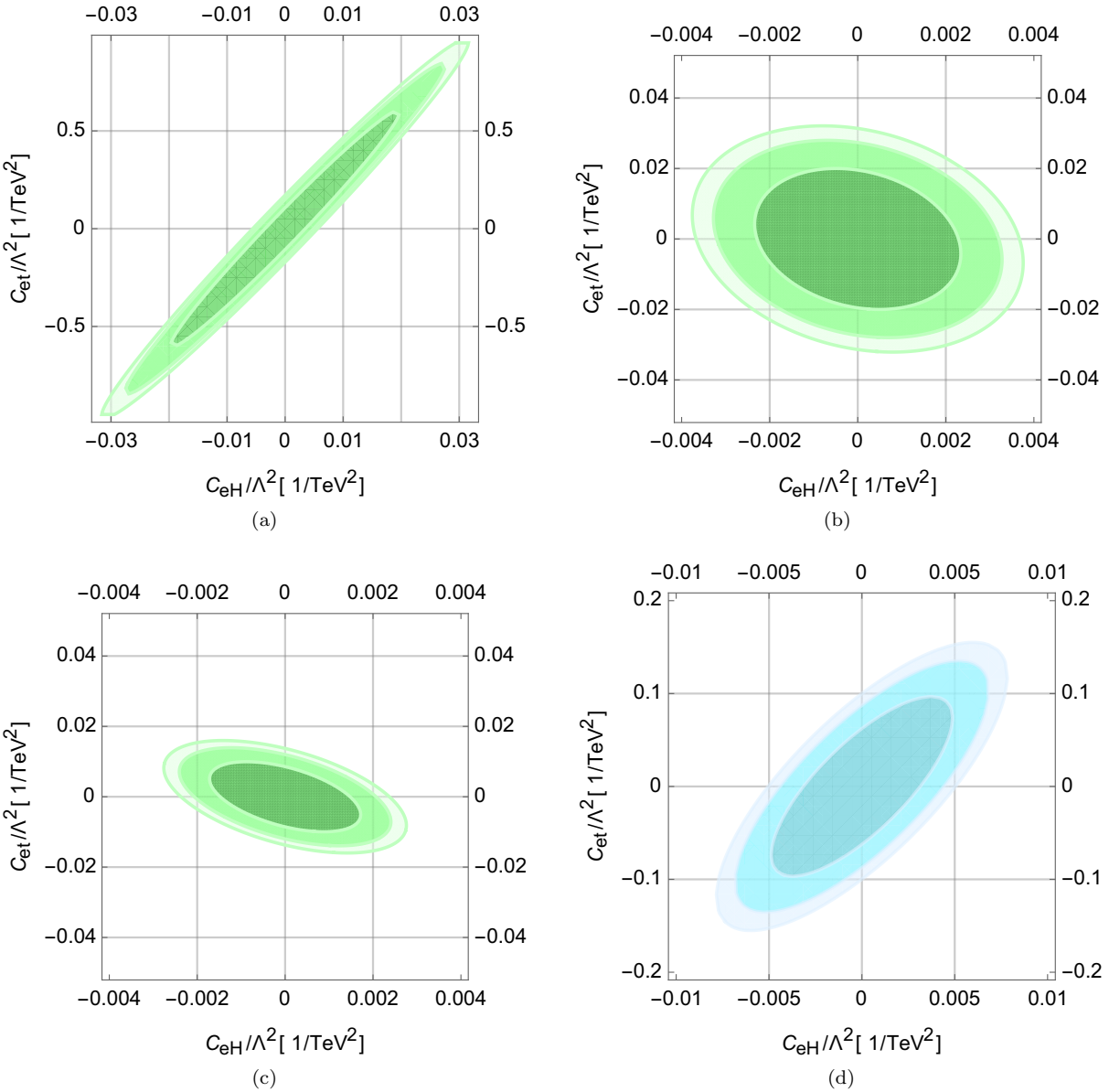

Figure VI.13: χ^2-distribution for the Wilson coefficients C_{eH} and C_{et} from the cross-section of the double Higgs production via electron-positron annihilation. It is presented, from inner to outer, the 68.5%, 95% and 99% confidence regions for 1 degree of freedom for the mentioned Wilson coefficients. These bounds are expected for (a) $\mathcal{L} = 500\,\text{fb}^{-1}$ at 380 GeV, (b) $\mathcal{L} = 1.5\,\text{ab}^{-1}$ at 1.5 TeV, (c) $\mathcal{L} = 3\,\text{ab}^{-1}$ at 3 TeV, benchmark values of the CLIC project; and (d) $\mathcal{L} = 4\,\text{ab}^{-1}$ at 500 GeV, benchmark values of the ILC projects (arXiv: 1704.02333v2).

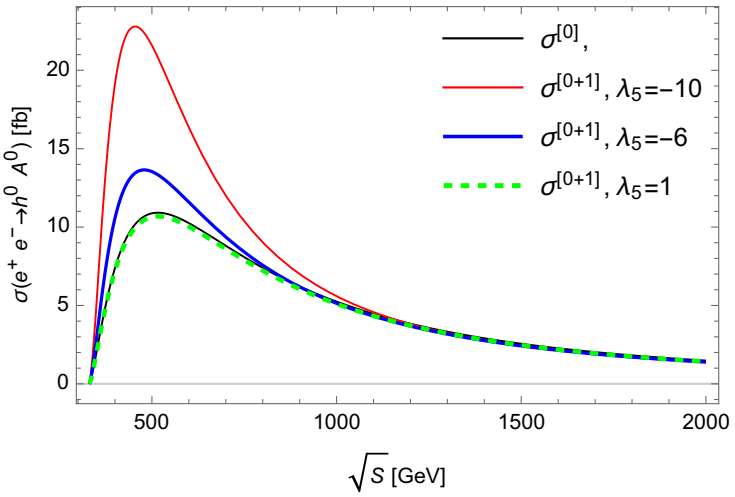

Figure VI.14: Total cross-section of the process $e^+e^- \to A^0h^0$ in the 2HDM for $\tan\beta = 1$ and $\sin\alpha = 1$, at tree level and at 1-loop with different values for λ_5.

VI.3 $e^+e^- \to h^0A^0$ (2HDM)

We can now see that the production of a CP-even Higgs together with the pseudoscalar A^0 through pair annihilation is enhanced in the 2HDM by loop effects. We shall compare our procedure with some results from [59] by using FC and LT. With this in mind, we will not take into account a diagram that yields a QED infrared divergence, coming from the vertex correction e^+e^-Z. It is possible to compute the contribution of such diagram to the amplitude in the regions of the parameter space where the trilinear Higgs couplings are dominant in order to check that the dropped diagram is comparatively negligible.

We can focus on the fermiophobic limit for type I 2HDM given by $\sin\alpha = 1$ and $\tan\beta = 1$, where the h^0 boson is completely decoupled from the fermionic sector. Following the analysis in [59], the best enhancement for the cross-section with scalars masses set to

$$M_{h^0} = 130\,\text{GeV},\ M_{H^0} = 150\,\text{GeV},\quad M_{A^0} = 200\,\text{GeV},\quad M_{H^\pm} = 160\,\text{GeV},$$

is given for $\lambda = -10$, and the most disfavoravel situation is with $\lambda = 0$. When our procedure is applied to the mentioned configuration, such behavior is observed, as it is shown in the Fig. [VI.14]. There can be seen that for $\lambda_5 = 1$ the enhancement due to quantum effects is very small, while the highest enhancement is found for $\lambda_5 = -10$ nearby $\sqrt{s} = 500\,\text{GeV}$. At tree-level we can see a good agreement between our results and those in fig. (8) of [59], since we find that at $\sqrt{s} = 500\,\text{GeV}$ the tree-level cross-section is $\sigma^0(e^+e^- \to h^0A^0) = 10.88\,\text{fb}$, while in the literature $\sigma^0_{lit}(e^+e^- \to h^0A^0) = 10.17\,\text{fb}$. The discrepancy is expected to come from the numerical inputs.

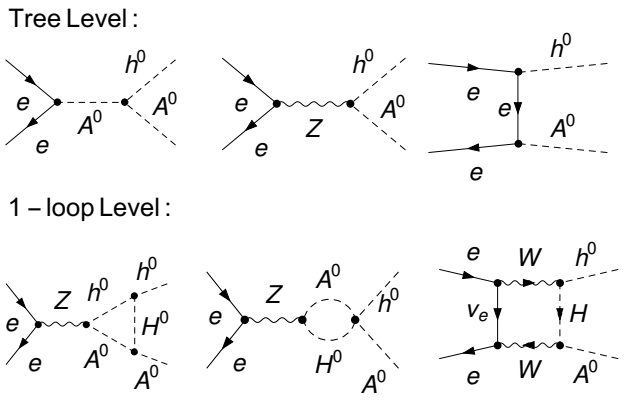

Figure VI.15: Some examples of the Feynman diagrams that enter in the the process $e^+e^- \to A^0h^0$ in the 2HDM and in the MSSM.

It is important to make clear that our results do not include the corrections for the h^0-leg. Then our total amplitude is of the form

$$\mathcal{M}\left(e^+e^- \to h^0A^0\right) \;=\; \mathcal{M}^{(0)}\left(e^+e^- \to h^0A^0\right) + \mathcal{M}^{(1)}\left(e^+e^- \to h^0A^0\right) + \delta\mathcal{M}^{(1)}\left(e^+e^- \to h^0A^0\right) \quad \text{(VI.26)}$$

instead of that presented in eq. (63) of [59]. This fact may explain why our enhancement is bigger than the obtained in the literature. We find that the total cross-section at NLO is $\sigma^{(0+1)}(e^+e^- \to A^0h^0) = 21.59\,\text{fb}$, which is in contrast to $\sigma^{(0+1)}_{lit}(e^+e^- \to A^0h^0) = 13.10\,\text{fb}$. Despite the differences, we find a good agreement in the behaviour of the cross-sections with respect to the parameter space.

VI.4 $e^+e^- \to \{h^0A^0,\ H^0A^0\}$ (MSSM)

With the computation of the cross-section for this processes, we want to see that in the MSSM the enhancement is not so big as that shown in the previous section in the 2HDM. This situation corresponds to the freedom of the coupling of the triple and quartic Higgs self-interaction in the 2HDM, which might grow independently, while in the MSSM such couplings are restrained by the gauge couplings. Remarkably, the differences between the cross-sections in the aforementioned models come from quantum effects, when 1-loop diagrams are taken into account in the 2HDM.

The tree-level cross-section for the process $e^+e^- \to h^0A^0$ is the same as that shown at the same perturbative order in the Fig. [VI.14]. Thus, the loop effects in the 2HDM can allow an experimental distinction with the MSSM.

In other processes for double Higgs production, the cross-sections obtained are considerable big. Following the

paper [70], we can find the cross-section at tree-level for $e^+e^- \to H^0A^0$, where $\sigma^0(e^+e^- \to H^0A^0) = 21.8126\,\text{fb}$ at $\sqrt{s} = 500\,\text{GeV}$ with $m_{A^0} = 200\,\text{GeV}$ and $\cos(\alpha - \beta) = 0$ (See Fig. [VI.16]). The Feynman diagrams for this process are as in the figure [VI.15], there must only be replaced h^0 by H^0

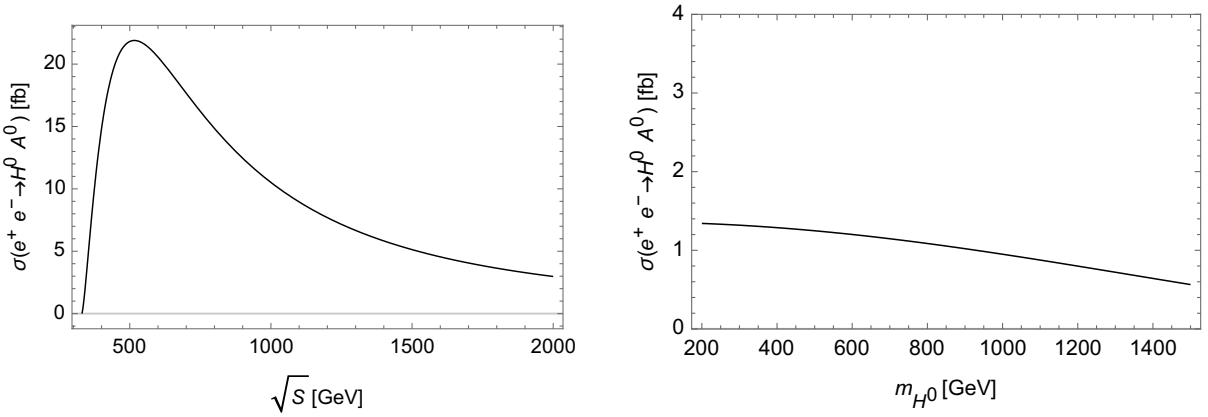

(a) (b)

Figure VI.16: Cross-sections at tree-level for the Higgs boson production $e^+e^- \to H^0A^0$ in the MSSM a) as a function of the energy ($m_{A^0} = 200\,\text{GeV}$), and b) as a function of the mass of the CP-even neutral Higgs boson H_0 ($\sqrt{s} = 3\,\text{TeV}$). Compare the above results with [70].

VI.5 Sommerfeld enhancement

At last, in this section, we want to discuss the way the $e^+e^- \to hh$ can be enhanced by the non-perturbative Sommerfeld effect, due to a hidden sector. Such effect is broadly exploted in dark matter analysis[71] for calculating the thermal relic densities and recently it was also computed in the SM above threshold [72][73].

VI.5.1 Remarks on Sommerfeld effect

It is well-known that the probability of transition is proportional to $|\psi_k^0(\mathbf{0})|^2$, with

$$\psi_i^0(\mathbf{r}) = e^{i\mathbf{k}_i\cdot\mathbf{r}}, \qquad \psi_f^0(\mathbf{r}) = e^{i\mathbf{k}_f\cdot\mathbf{r}}, \tag{VI.27}$$

the initial and final wavefunctions, respectively. Let us consider the situation where the particle is under the effects of a central potential, and that, near the origin, has a small velocity. Then, it could happen that, even though the potential is treated perturbatively, the wavefunction suffers strong distortions due to the small velocity. Thus, we focus on non-relativistic final states. Such effects can modify the scattering amplitude. For

instance, in the s-channel for a 2-2 scattering, we can have

$$\mathcal{M}_s \quad = \quad \mathcal{M}_s^{pert.} \cdot \frac{\psi_i\left(\mathbf{0}\right)\psi_f^*\left(\mathbf{0}\right)}{\psi_i^0\left(\mathbf{0}\right)\psi_f^{0*}\left(\mathbf{0}\right)}, \tag{VI.28}$$

with $\mathcal{M}_s^{pert.}$ the amplitude computed perturbatively. This new factor gives corrections to the usual planar-wave in the perturbative amplitude. Hence,

$$|\mathcal{M}|^2 = |\mathcal{M}_s^{pert.}|^2 |\psi_f\left(\mathbf{0}\right)|^2, \qquad \text{or,} \qquad \sigma = \sigma^{pert} S_k, \tag{VI.29}$$

where the corrections to the amplitude come from the factor $S_k \equiv |\psi_f\left(\mathbf{0}\right)|$. The above wavefunction obey the Schrödinger equation

$$-\nabla^2\psi_f + 2mV\left(r\right)\psi_f \quad = \quad k^2\psi_f. \tag{VI.30}$$

Under the central potential, we can expand in partial waves

$$\psi_f \quad = \quad \frac{1}{2k}\sum_{l=0}^{\infty} i^l\left(2l+1\right)e^{i\delta_l}P_l\left(\cos\theta\right)R_{kl}\left(r\right), \tag{VI.31}$$

where the real radial functions are normalized as

$$\int_0^\infty R_{k'l}R_{kl}r^2\,dr = 2\pi\delta\left(k'-k\right). \tag{VI.32}$$

We recall that the partial wave expantion is useful in the low-energy regime. Then, for sufficient low-energies, we can take just the s-wave contribution ($l=0$). Therefore, in this regime,

$$S_k \quad = \quad \left|\frac{R_{k0}\left(0\right)}{2k}\right|^2 = \left|\frac{\phi_k\left(r\right)}{2kr}\right|^2_{r\to 0}, \tag{VI.33}$$

where $\phi_k\left(r\right) \equiv rR_{k0}\left(r\right)$. With this definition, the function $\phi_k\left(r\right)$ satisfies the equation

$$-\frac{d^2\phi_k\left(r\right)}{dr^2} + mV\left(r\right)\phi_k\left(r\right) \quad = \quad \left(mv\right)^2\phi_k\left(r\right), \tag{VI.34}$$

with boundary conditions

$$\phi_k\left(r\right) \to 0 \quad \text{as} \quad r\to 0, \qquad \text{and,} \qquad \phi_k\left(r\right) \to 2\sin\left(kr+\delta_0\right) \quad \text{as} \quad r\to\infty. \tag{VI.35}$$

Some analytical Sommerfeld factors are known for a few potentials. For example, for the Coulomb case, where

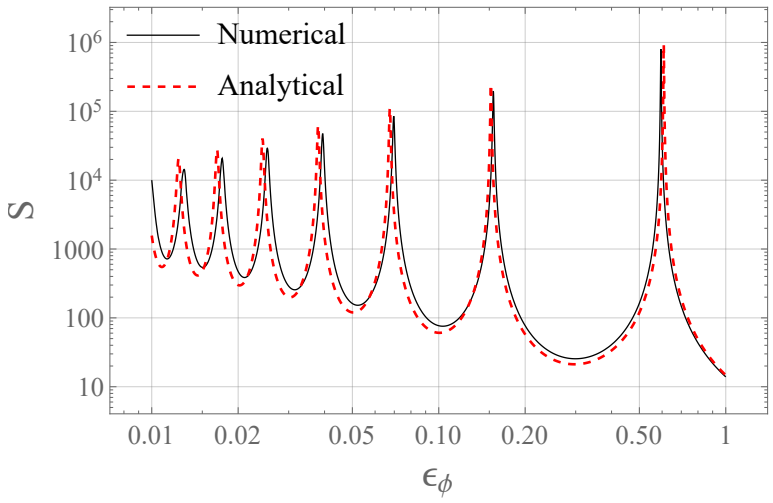

Figure VI.17: Sommerfeld Factor (S) as a function of ϵ_ϕ with the fixed value $\epsilon_v = 10^{-3}$. Here the black solid curve represent the numerical solution of the Schrödinger equation while the red dashed curve stands for analytical solution with the approximation taking the Hulthen potential.

the force carrier is massless, and the potential is $V_C(r) = -\alpha/(2r)$, the Sommerfeld factor is:

$$S = \left| \frac{\frac{\pi}{\epsilon_v}}{1 - e^{-\frac{\pi}{\epsilon_v}}} \right|, \tag{VI.36}$$

with $\epsilon_v \equiv v/\alpha$.

In the Ref. [74], the Sommerfeld effect in a model with dark matter particle X is discussed, coupled to a force carrier ϕ, with coupling given by α_X. Then, to see the enhancement in the process $XX \to \phi\phi$, the Yukawa potential used is:

$$V(r) = -\alpha_X \frac{e^{-m_\phi r}}{r}. \tag{VI.37}$$

To solve the Eq. [VI.34] analytically, we can approximate the Yukawa potential in a suitable way. In the Ref. [75], the author takes the Hulthén potential:

$$V_H = -\alpha_X \frac{\delta e^{-\delta r}}{1 - e^{-\delta r}}, \tag{VI.38}$$

with $\delta = \pi^2 m_\phi/6$ as an approximation to the Yukawa potential. For this potential, the Sommerfeld factor found is

$$S = \frac{\pi}{\epsilon_v} \frac{\sinh\left(\frac{2\pi\epsilon_v}{\pi^2\epsilon_\phi/6}\right)}{\cosh\left(\frac{2\pi\epsilon_v}{\pi^2\epsilon_\phi/6}\right) - \cos\left(2\pi\sqrt{\frac{1}{\pi^2\epsilon_\phi/6} - \frac{\epsilon_v^2}{\left(\pi^2\epsilon_\phi/6\right)^2}}\right)}, \tag{VI.39}$$

where $\epsilon_v \equiv v/\alpha_X$ and $\epsilon_\phi \equiv m_\phi/(\alpha_X m_X)$. In the Fig. [VI.17], the Sommerfeld factor as a function of ϵ_ϕ is shown, given by the formula [VI.39] and the numerical solution with the Yukawa potential. There, a good agreement between the two approaches can be inferred. From Eq. [VI.39], it is noted that the location of the resonances in terms of the energy depends on the masses of the particles (m_ϕ, m_X), but not on the coupling α_X. Moreover, for $\epsilon_v \ll \epsilon_\phi$, the S factor presents resonances at

$$m_\phi \simeq \frac{6\alpha_X m_X}{\pi^2 n^2}, \qquad n = 1, 2, 3\ldots \tag{VI.40}$$

VI.5.2 Sommerfeld effect from ladder approximation applied to the $e^+e^- \to hh$ process

The discussion of the previous subsection can be completely inferred from non-perturbative methods, which, in a deeper way, solve the Bethe-Salpeter equation. In this section, we will see that such deeper analysis applies to the $e^+e^- \to hh$ process. We follow the method developed by Strassler and Peskin[77].

Here, the non-perturbative effects come from the fact that near threshold the Higgs bosons can behave in a non-relativistic way. Thus, it could happen that, a hidden scalar ϕ, coupled to the Higgs boson, acts like a force mediator between the Higgses, binding them. This can be seen as a ladder of infinite hidden scalars, being exchanged between the Higgs bosons. Thus, a bound-state made up of Higgses could be formed through quantum tunneling, where the energy of such bound-state would be negative, leading to the appearance of resonances below the threshold energy ($\sqrt{s} = 250\,\text{GeV}$). This analysis takes relevance, since it has been revealed that the ILC project will operate at a center-of-mass energy of 250 GeV, so that the threshold behavior of the cross-section of double Higgs production is needed[76].

In addition to the SM Lagrangian, we take new interactions coming from

$$\mathcal{L} = \mathcal{L}_{SM} + \frac{1}{2}(\partial_\mu \phi)^2 - \frac{1}{2}m_\phi^2 \phi^2 + guhh\phi, \tag{VI.41}$$

where ϕ is the hidden scalar field, m_ϕ is the mass of such scalar, g is the dimensionless coupling between the Higgs and the hidden scalar, and u is a characteristic energy scale of the new sector.

To find the non-perturbative effects below threshold, we can compute the amplitude of the $e^+e^- \to hh$ process through the optical theorem:

$$\sigma\left(e^+e^- \to hh\right) = \frac{1}{s}\text{Im}\mathcal{M}\left(e^+e^- \underset{hh}{\longrightarrow} e^+e^-\right), \tag{VI.42}$$

where the amplitude in the right-hand side stands just for the contributions that involve loops with two Higgs

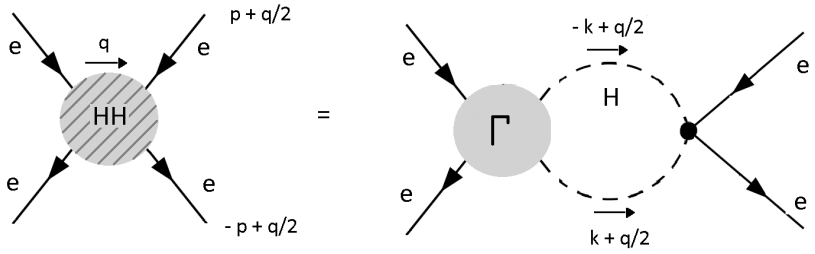

Figure VI.18: Relation that defines the amplitude of the process $e^+e^- \to e^+e^-$ mediated by Higgs bosons in terms of $\Gamma(q,p)$.

bosons. Such amplitude can be found through the ladder approximation. To get started, the amplitude $\mathcal{M}\left(e^+e^- \underset{hh}{\longrightarrow} e^+e^-\right)$ can be computed through the equation in the figure [VI.18], which is equivalent to

$$\mathcal{M}\left(e^+e^- \to e^+e^-\right) = \quad \Gamma^{(0)}(E) \int \frac{d^4k}{(2\pi)^4} \frac{i}{\left(\frac{q}{2}+k\right)^2 - m_h^2 + im_h\Gamma_h} \frac{i}{\left(\frac{q}{2}-k\right)^2 - m_h^2 + im_h\Gamma_h} \Gamma(q,k)\,. \quad \text{(VI.43)}$$

Here, it is of importance to note that we are taking $\Gamma^{(0)}(E)$ to be an effective vertex, which gives information of the $e^+e^- \to hh$ process without the effects of the hidden scalar ϕ. Such effective interaction is taken to be related to a s-wave dominated process, thus we do not include any momentum dependence.

Near the threshold, we take $q = (2m_h + E, \mathbf{0})$, so that E represents the binding energy of the bound state, satisfying $m_h \gg |E|$. The scalar propagators can be approximated to their non-relativistic form, so that the tree-momentum is small. Then, we obtain $q^2 \approx 4m_h^2 + 4m_hE$ and $q \cdot k = (2m_h + E)\,k^0 \approx 2m_hk^0$. Moreover, $k^2 \approx -\mathbf{k}^2$, hence the propagators for the scalar fields are reduced to

$$\frac{i}{\left(\frac{q}{2} \pm k\right)^2 - m_h^2 + im_h\Gamma_h} \quad \longrightarrow \quad \frac{i}{2m_h\left(\frac{E}{2} \pm k^0 - \frac{\mathbf{k}^2}{2m_h} + i\frac{\Gamma_h}{2}\right)}. \quad \text{(VI.44)}$$

Inserting this into Eq. [VI.43]:

$$\mathcal{M}\left(e^+e^- \to e^+e^-\right) = -\frac{\Gamma^{(0)}(E)}{4m_h^2} \int \frac{d^3k}{(2\pi)^3} \int \frac{dk^0}{2\pi} \frac{1}{\left(k^0 + \frac{E}{2} - \frac{\mathbf{k}^2}{2m_h} + i\frac{\Gamma_h}{2}\right)\left(k^0 - \frac{E}{2} + \frac{\mathbf{k}^2}{2m_h} - i\frac{\Gamma_h}{2}\right)} \Gamma(E,\mathbf{k})\,. \quad \text{(VI.45)}$$

The integral in k^0 can be performed by complex extension. We note that the integrand has two poles, one in the upper complex half-plane and the other in the lower complex half-plane. Then, the integral is computed along the curve C, composed of a semi-circle C', with radius going to infinit, and the real axis. The integrand

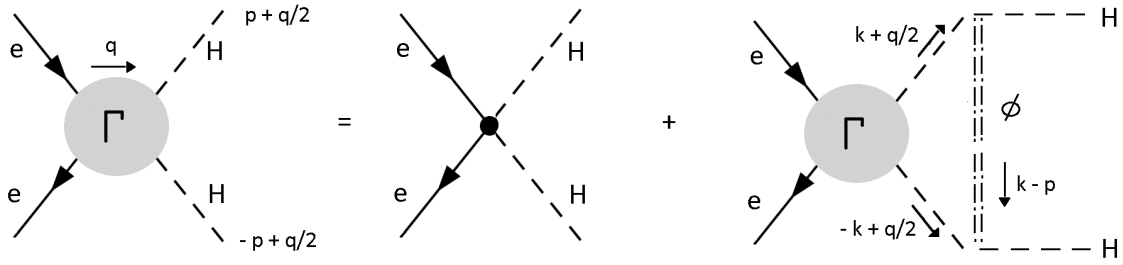

Figure VI.19: Relation that must be satisfied by Γ in the ladder approximation.

vanishes in C'. Let us define $k' \equiv \frac{E}{2} - \frac{\mathbf{k}^2}{2m_h} + i\frac{\Gamma_h}{2}$, so that we have

$$\begin{aligned}\oint_C dk^0 \frac{1}{(k^0+k')(k^0-k')} &= \int_{-\infty}^{\infty} dk^0 \frac{1}{(k^0+k')(k^0-k')} + \int_{C'} dk^0 \frac{1}{(k^0+k')(k^0-k')} \\ &= \int_{-\infty}^{\infty} dk^0 \frac{1}{(k^0+k')(k^0-k')} \\ &= 2\pi i \,\mathrm{Res}\left(\frac{1}{(k^0+k')(k^0-k')};\ k^0 = k'\right) \\ &= 2\pi i \,\frac{1}{2k'}. \end{aligned} \tag{VI.46}$$

With this, the relation [VI.45] takes the form

$$\mathcal{M}\left(e^+e^- \to e^+e^-\right) = -\frac{\left(\Gamma^{(0)}(E)\right)^2}{4m_h^2} \int \frac{d^3k}{(2\pi)^3} \frac{i}{E - \frac{\mathbf{k}^2}{m_h} + i\Gamma_h} \frac{\Gamma(E,\mathbf{k})}{\Gamma^{(0)}(E)}. \tag{VI.47}$$

We can define $S(q,p) = \Gamma(q,p)/\Gamma^{(0)}(q)$ and the Green's function as

$$\widetilde{G}(\mathbf{p}, E + i\Gamma_h) = -\frac{1}{E + i\Gamma_h - \frac{\mathbf{p}^2}{m_h}} S(\mathbf{p}, E), \tag{VI.48}$$

so that

$$\begin{aligned}\mathcal{M}\left(e^+e^- \to e^+e^-\right) &= i\frac{\left(\Gamma^{(0)}(E)\right)^2}{4m_h^2} \int \frac{d^3k}{(2\pi)^3} \widetilde{G}(\mathbf{k}, E + i\Gamma_h) \\ &= i\frac{\left(\Gamma^{(0)}(E)\right)^2}{4m_h^2} \int \frac{d^3k}{(2\pi)^3} \int d^3r G(\mathbf{r}, E + i\Gamma_h)\, e^{i\mathbf{k}\cdot\mathbf{r}} \\ &= i\frac{\left(\Gamma^{(0)}(E)\right)^2}{4m_h^2} G(0, E + i\Gamma_h). \end{aligned} \tag{VI.49}$$

Now, we must find the equation that gives the Green's function defined above. For this, we use the equation

shown in the figure [VI.19]. Explicitly:

$$\Gamma\left(q,p\right)=\Gamma^{(0)}\left(q\right)+\left(2igu\right)^{2}\int\frac{d^{4}k}{\left(2\pi\right)^{4}}\frac{i}{\left(p-k\right)^{2}-m_{\phi}^{2}}\frac{i}{\left(\frac{q}{2}+k\right)^{2}-m_{h}^{2}+im_{h}\Gamma_{h}}\frac{i}{\left(\frac{q}{2}-k\right)^{2}-m_{h}^{2}+im_{h}\Gamma_{h}}\Gamma\left(q,k\right), \tag{VI.50}$$

which in terms of $S(q,p)$, and in the non-relativistic limit, is

$$S\left(q,p\right)=1-\frac{ig^{2}u^{2}}{m_{h}^{2}}\int\frac{d^{4}k}{\left(2\pi\right)^{4}}\frac{1}{\left(\mathbf{p}-\mathbf{k}\right)^{2}+m_{\phi}^{2}}\frac{1}{\left(k^{0}+\frac{E}{2}-\frac{\mathbf{k}^{2}}{2m_{h}}+i\frac{\Gamma_{h}}{2}\right)\left(\frac{E}{2}-k^{0}-\frac{\mathbf{k}^{2}}{2m_{h}}-i\frac{\Gamma_{h}}{2}\right)}S\left(q,k\right), \tag{VI.51}$$

where it was used that

$$\frac{ig^{2}u^{2}}{\left(p-k\right)^{2}-m_{\phi}^{2}}\quad=\quad\frac{ig^{2}u^{2}}{\left(p^{0}-k^{0}\right)^{2}-\left(\mathbf{p}-\mathbf{k}\right)^{2}-m_{\phi}^{2}}\longrightarrow\frac{-ig^{2}u^{2}}{\left(\mathbf{p}-\mathbf{k}\right)^{2}+m_{\phi}^{2}}. \tag{VI.52}$$

Here we identify the potential

$$\widetilde{V}\left(\mathbf{p}-\mathbf{k}\right)\quad=\quad-\frac{g^{2}u^{2}}{m_{h}^{2}}\frac{1}{\left(\mathbf{p}-\mathbf{k}\right)^{2}+m_{\phi}^{2}}. \tag{VI.53}$$

Performing the integral in k^0, as it was discussed previously, we arrive to the integral equation

$$S\left(q,p\right)=1+\int\frac{d^{3}k}{\left(2\pi\right)^{3}}\widetilde{V}\left(\mathbf{p}-\mathbf{k}\right)\frac{1}{E-\frac{\mathbf{k}^{2}}{m_{h}}+i\Gamma_{h}}S\left(q,k\right). \tag{VI.54}$$

With the definition in equation [VI.48], we can do Fourier transform to write this integral equation in its differential form. Thus, it appears the Schrödinger equation

$$\left[-\frac{\nabla^{2}}{m_{h}}-E-i\Gamma_{h}+V\left(\mathbf{r}\right)\right]G\left(\mathbf{r},E+i\Gamma_{h}\right)\quad=\quad\delta^{3}\left(\mathbf{r}\right), \tag{VI.55}$$

with the potential in space coordinates given by

$$V\left(r\right)\quad=\quad-\frac{g^{2}u^{2}}{4\pi m_{h}^{2}}\frac{e^{-m_{\phi}r}}{r}. \tag{VI.56}$$

Hence, we recognize the Green's function $G\left(\mathbf{r},E+i\Gamma_{h}\right)$ as the standard Green's function $G\left(\mathbf{r},\mathbf{r}';E+i\Gamma_{h}\right)$ of the Schrödinger equation.

By using the equation [VI.42], and combining the results in the relations [VI.49], we obtain

$$\sigma\left(e^{+}e^{-}\rightarrow hh\right)\quad=\quad\sigma_{0}\left(e^{+}e^{-}\rightarrow hh\right)R\left(E\right), \tag{VI.57}$$

where the Sommerfeld factor is given by

$$R(E) = \frac{\operatorname{Im} G(0,0;E)}{\operatorname{Im} G_0(0,0;E)}. \tag{VI.58}$$

The Green's function $G_0(r,r';E)$ correspond to the Schrödinger equation with zero potential. It is known that for $r < r'$, such Green's function is given by

$$G_0(r,r';E+i\Gamma_h) = -\frac{m_h}{4\pi}\frac{\sin\lambda r}{\lambda r}\frac{e^{i\lambda r'}}{r'}, \tag{VI.59}$$

where $\lambda = [m_h(E+i\Gamma_h)]^{1/2}$.

VI.5.3 Solution to the Schrödinger equation

Now, we want to find the imaginary part of the Green's function, which solves the Schrödinger equation

$$\left[-\frac{\nabla^2}{m_h} - E - i\Gamma_h + V(\mathbf{r})\right] G(\mathbf{r},\mathbf{r}';E+i\Gamma_h) = \delta^3(\mathbf{r}-\mathbf{r}'). \tag{VI.60}$$

We note that for this scattering, the s-wave represents the biggest contribution, which means spherical symmetry in the Schrödinger equation, thus we shall focus on its radial part. For this, we start by doing the change of variables

$$G(r,r') = \frac{g(r,r')}{rr'}, \tag{VI.61}$$

which leads to the ordinary differential equation

$$\left[\frac{d^2}{dr^2} + m_h(E+i\Gamma_h - V(r))\right] g(r,r') = \frac{m_h}{4\pi}\delta(r-r'), \tag{VI.62}$$

The solution of this equation has the form

$$g(r,r') = \begin{cases} Ag_a(r)\,g_b(r') & \text{for } 0 < r < r' < \infty, \\ Ag_a(r')\,g_b(r) & \text{for } 0 < r' < r < \infty, \end{cases} \tag{VI.63}$$

where the $g_{a,b}$ are homogeneous solutions to the differential equation, and A is a normalization constant. The normalization constant is chosen in order to give the correct coefficient to the Dirac delta. We can also remember that the solutions in the equation [VI.63] are such that $g(r,r')$ is regular as $r \to 0$ and $r \to \infty$.

We can get more information about Im $G(0,0;E+i\Gamma_h)$ through the definition of a regular $g_0(r)$ and an irregular

solution $g_1(r)$ as $r \to 0$, satisfying

$$g_0(r) = r + \dots \text{ as } r \to 0, \tag{VI.64}$$

$$g_1(r) = 1 + \dots \text{ as } r \to 0. \tag{VI.65}$$

The definition of $g_0(r)$ is justified in the fact that the Green's function should be regular at the origin, and by the equation [VI.61] $g(r, r')$ must vanish as $r \to 0$. In this definition, there could be an arbitrary admixture of g_0 in g_1. To avoid this, it can be imposed that

$$\text{Im}\left(\frac{d}{dr} g_1(r)\right) \to 0 \text{ as } r \to 0, \tag{VI.66}$$

so that $g_1(r)$ can be chosen arbitrarly satisfying the above condition. Now, we can identify $g_a(r)$ with $g_0(r)$, since both of them should vanish at the origin. Then, we write

$$g_a(r) = g_0(r), \tag{VI.67}$$

$$g_b(r) = g_1(r) + B g_0(r), \tag{VI.68}$$

where the second solution must vanish as $r \to \infty$, which sets

$$B = \lim_{r\to\infty}\left(-\frac{g_1(r)}{g_0(r)}\right). \tag{VI.69}$$

By computing the wronskian, it is easily identified $A = -m_h/4\pi$. Hence, with the equations VI.61 and VI.63, it is found that

$$G(0,0) = -\frac{m_h}{4\pi}\lim_{r'\to 0}\left(\frac{g_1(r')}{r'} + B\right), \tag{VI.70}$$

so that the imaginary part of the Green's function can be simplified to

$$\text{Im}\, G(0,0) = -\frac{m_h}{4\pi}\text{Im}\, B. \tag{VI.71}$$

VI.5.4 Sommerfeld enhancement of $e^+e^- \to hh$

The process $e^+e^- \to hh$ in the SM is p-wave dominated. Then, the above analysis should be modified. With the Peskin and Strassler method, used before, instead of working with the Eq. [VI.62], we would have an inhomogeneous radial Schrödinger equation, where the inhomogeneous term is related to the cross-section in

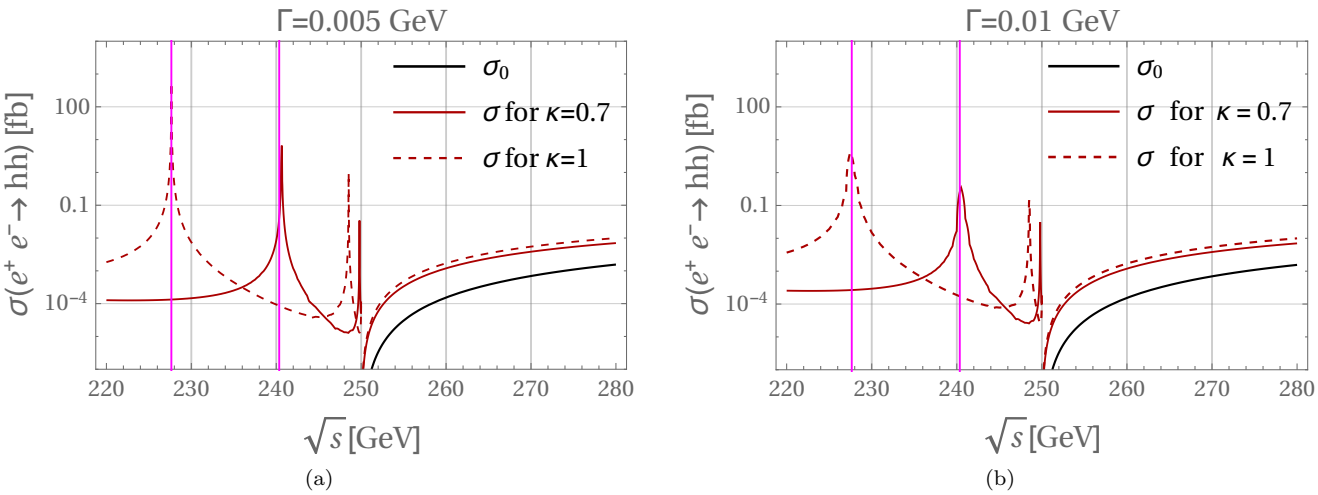

Figure VI.20: Behavior around threshold of the cross-sections for the double Higgs production when the Sommerfeld effects of a hidden scalars ϕ with $m_\phi = 10\,\text{GeV}$ are taken into account. The left plot corresponds to the Higgs boson with a width of $\Gamma_h = 0.005\,\text{GeV}$ as in the SM, while the left plot corresponds to $\Gamma_h = 0.01\,\text{GeV}$. The black solid curve represents the SM cross-section σ_0. The vertical lines in magenta represent the energies $\sqrt{s} = 227.65\,\text{GeV}$ and $\sqrt{s} = 240.35\,\text{GeV}$ of the $\ell = 0$ bound-state from the formulas [VI.78].

the SM. This equation is much harder to be solved than the one that we treated previously. However, just for illustration of the change that the Sommerfeld effect could induce in our process, we show here the results of the Peskin-Strassler method applied to the $e^+e^- \to hh$.

With this, it is possible to see the behavior of the $\sigma\left(e^+e^- \to hh\right)$ around the threshold energy. It can be solved, numerically, the homogeneous Schrödinger equation in [VI.62] for $g_0\left(r\right)$ and $g_1\left(r\right)$, with boundaries conditions which come from the relations [VI.64] and [VI.65]:

$$g_0 \to 0 \quad \text{as} \quad r \to 0, \qquad g_0' \to 1 \quad \text{as} \quad r \to 0, \tag{VI.72}$$

$$g_1 \to 1 \quad \text{as} \quad r \to 0, \qquad g_1' \to 0 \quad \text{as} \quad r \to 0. \tag{VI.73}$$

On the other hand, the perturbative cross-section for the process $e^+e^- \to hh$ has the form

$$\sigma_0\left(e^+e^- \to hh\right) = \frac{1}{64\pi s}\sqrt{1 - \frac{4m_h^2}{s}}\overline{|\mathcal{M}\left(e^+e^- \to hh\right)|^2}, \tag{VI.74}$$

where the symmetry factor for identical particles in the final state has been included. On the other hand, from equation [VI.59], we have that

$$\begin{aligned} \text{Im}\, G_0\left(0, E\right) &= -\frac{m_h}{4\pi}\lim_{r,r'\to 0}\left(\frac{\sin\lambda r}{\lambda r}\frac{e^{i\lambda r'}}{r'}\right) \\ &= -\frac{m_h}{4\pi}\sqrt{m_h E} \\ &= -\frac{m_h}{4\pi}\sqrt{m_h\left(\sqrt{s} - 2m_h\right)}. \end{aligned} \tag{VI.75}$$

Thus, by inserting the relations [VI.71], [VI.74], and [VI.75] into [VI.57] we have that

$$\begin{aligned}\sigma\left(e^+e^-\to hh\right) &= \frac{1}{64\pi s}\sqrt{\left(1-\frac{2m_h}{\sqrt{s}}\right)\left(1+\frac{2m_h}{\sqrt{s}}\right)}\overline{|\mathcal{M}\left(e^+e^-\to hh\right)|^2}\times\frac{\mathrm{Im}B}{\sqrt{m_h\left(\sqrt{s}-2m_h\right)}}\\ &= \frac{1}{64\pi s}\sqrt{1+\frac{2m_h}{\sqrt{s}}}\overline{|\mathcal{M}\left(e^+e^-\to hh\right)|^2}\times\frac{\mathrm{Im}B}{\sqrt{m_h\sqrt{s}}}.\end{aligned}\tag{VI.76}$$

The numerical solutions with the total cross-section can be seen in the Fig. [VI.20] for $m_\phi = 10\,\mathrm{GeV}$ and with different values of the coupling parameter

$$\kappa \equiv \frac{g^2u^2}{4\pi m_h^2}.\tag{VI.77}$$

In Fig. [VI.20] can be seen that the location of the resonances remains the same as the width of the Higgs boson changes, while the enhancement factor decreases as Γ_h increases, a well-known feature for these kind of resonances. It is also remarkable that the enhancement factor and the location of the peaks depend on the coupling. Even though, in these plots the mass of the hidden scalar is the same, it was checked that the binding energy for the $\ell = 0$ bound-state increases as m_ϕ decreases, and it is noted that more resonances appear.

The location of the resonances in the Fig. [VI.20] can be checked. It is known that, through variational methods [78], the energy for the $\ell = 0$ bound-state with a Yukawa potential is given by

$$E = -\kappa m_\phi\frac{p^3\left(p-1\right)}{4\left(p+1\right)^3},\qquad \text{where } p \text{ solves}\qquad \kappa\frac{m_h}{m_\phi} = \frac{\left(p+1\right)^3}{p\left(p+3\right)}.\tag{VI.78}$$

By applying this to our system, for $\kappa = 1$ and with $m_\phi = 10\,\mathrm{GeV}$, then $p = 12.2986$, which leads to $E_{\ell=0} = -22.3416$, so that this resonance should be located at $\sqrt{s} = 227.65\,\mathrm{GeV}$. Similarly, for $\kappa = 0.7$, it is found $p = 8.47836$, which leads to $E_{\ell=0} = -9.36657$, so that this resonance should be located at $\sqrt{s} = 240.35\,\mathrm{GeV}$. These values are in good agreement with the numerical solutions shown in Fig. [VI.20].

Chapter VII

Conclusion

In this dissertation, it was shown some new results regarding the double Higgs production through e^+e^--pair annihilation. Through an EFT analysis, in the section [VI.2], bounds to the Wilson coefficients C_{eH} and C_{et} were found. The case studied where the bounds are strongest correspond to the CLIC project, where $-0.003\,\mathrm{TeV}^{-2} \lesssim C_{eH}/\Lambda^2 \lesssim 0.003\,\mathrm{TeV}^{-2}$ and $-0.03\,\mathrm{TeV}^{-2} \lesssim C_{et}/\Lambda^2 \lesssim 0.03\,\mathrm{TeV}^{-2}$. These coefficients are less constrained in the literature, making useful the presented results. In the future, it would be of matter the way some of these Wilson coefficients are bounded in a LHC environment.

In the section [VI.5.4], it was also presented the Sommerfeld enhancement below and above the threshold energy $\sqrt{s} = 250\,\mathrm{GeV}$ in the double Higgs boson production due to the effects of a Hidden sector. Remarkably, it was found the $\ell = 0$ bound-states for two different coupling-parameter values, assuming that the process $e^+e^- \to hh$ is s-wave dominated. This could happen in cases where the leading contribution comes from effective operators, for instance. The SM situation correspond to a p-wave dominated process. For $\kappa = 1$, and with a hidden-scalar mass $m_\phi = 10\,\mathrm{GeV}$, it was found that the energy at which a $\ell = 0$ bound-state made up of Higgs bosons would be $\sqrt{s} \approx 227.65\,\mathrm{GeV}$, while for $\kappa = 0.7$ and same hidden-scalar mass the energy for the $\ell = 0$ bound-state would be $\sqrt{s} \approx 240.35\,\mathrm{GeV}$. Other resonances corresponding to other excited states were also found. This analysis was done by taking two different widths of the Higgs, finding that enhancement factors are bigger for smaller widths.

The study of the cross-section of the process $e^+e^- \to hh$ around of threshold is of relevance since it was revealed that the ILC project will operate at energies $\sqrt{s} = 250\,\mathrm{GeV}$ in the center-of-mass reference. It could also be of importance the study of the Sommerfeld enhancement of this process due to other kind of interactions, as well as definite value of the Higgs boson width.

Bibliography

[1] S. L. Glashow, *Partial-Symmetries of Weak Interactions*, Nucl. Phys. 22(1961) p. 579.

[2] S. Weinberg, *A Model of Leptons*, Phys. Rev. Lett. 19(1967) p. 1264.

[3] A. Salam, *Elementary Particle Physics: Relativistic Groups and Analyticity*, 8th Nobel Symp.: Almquvist and Wiksell (1968) p. 367.

[4] F. Englert et al., *Broken Symmetry and the Mass of Gauge Vector Mesons*, Phys. Rev. Lett. 13(1964) p. 321.

[5] P. Higgs, *Broken Symmetries and the masses of Gauge Bosons*, Phys. Rev. Lett. 13(1964) p. 508.

[6] G. S. Guralnik et al., *Global Conservation Laws and Massless Particles*, Phys. Rev. Lett. 13(1964) p. 585.

[7] M. Gell-Mann, *Symmetries of Baryons and Mesons*, Phys. Rev. 125(1962) p. 1067.

[8] H. Fritzsch, M. Gell-Mann, and H. Leutwyler, *Advantages of the Color Octet Gluon Picture*, Phys. Lett. 47b(1973) p. 365.

[9] G. 't Hooft and M. Veltman, *Regularization and renormalization of gauge fields*, Nucl. Phys. B 44(1972) p. 189.

[10] D. Gross and F. Wilczek, *Ultraviolet Behavior of Non-Abelian Gauge Theories*, Phys. Rev. Lett. 30(1973) p. 1343.

[11] H. D. Politzer, *Reliable Perturbative Results for Strong Interactions?*, Phys. Rev. Lett. 30(1973) p. 1346.

[12] ATLAS Collaboration, *Observation of a new particle in the search for the Standard Model Higgs boson with the ATLAS detector at the LHC*, Phys. Lett. B 716(2012) p. 1.

[13] CMS Collaboration, *Observation of a new boson at a mass of 125 GeV with the CMS experiment at the LHC*, Phys. Lett. B 716(2012) p. 30.

[14] G. 't Hooft, *Naturalness, chiral symmetry, and spontaneous chiral symmetry breaking*, NATO Sci. Ser. B, 50(1980) p. 135.

[15] C. Patrignani et al. (Particle Data Group), Chin. Phys. C, 40, 100001 (2016).

[16] `https://www.linearcollider.org/ILC`

[17] `http://clic-study.web.cern.ch/`

[18] P. Langacker and J. Erler, *Review of particle properties*, Phys. Rev. D 50(1994) p. 1304.

[19] P. Langacker, *The Standard Model and beyond*, CRC press (2010).

[20] J. F. Donoghue, *General relativity as an effective field theory: The leading quantum corrections*, Phys. Rev. D 50(1994) p. 3874.

[21] P. A. R. Ade et al., *Planck 2015 results. XIII. Cosmological parameters*, Astron. Astrophys. 594(2016) p. A13.

[22] S. Weinberg, *The cosmological constant problem*, Rev. Mod. Phys. 61(1989) p. 1.

[23] G. Bertone, D. Hooper, and J. Silk *Particle dark matter: evidence, candidates and constraints*, Phys. Rep. 405(2005) p. 279.

[24] R. Mohapatra and G. Senjanović, *Neutrino mass and spontaneous parity nonconservation*, Phys. Rev. Lett. 44(1980) p. 912.

[25] C. Giganti, S. Lavignac, and M. Zito, *Neutrino oscillations: the rise of the PMNS paradigm*, arXiv: hep-ph/1710.00715.

[26] R. Mohapatra and R. E. Marshak, *Local B-L Symmetry of Electroweak Interactions, Majorana Neutrinos and Neutron Oscillations*, Phys. Rev. Lett. 44(1980) p. 1316.

[27] R. Mohapatra and G. Senjanović, *Neutrino masses and mixings in gauge models with spontaneous parity violation*, Phys. Rev. D 23(1981) p. 165.

[28] C. Degrande, N. Greiner, W. Kilian, O. Mattelaer, H. Mebane, T. Stelzer, S. Willenbrock, and C. Zhang, *Effective field theory: A modern approach to anomalous couplings*, Annals of Physics 335(2013) p. 21.

[29] W. Buchmüller and D. Wyler, *Effective lagrangian analysis of new interactions and flavour conservation*, Nucl. Phys. B 268(1986) p. 621.

[30] B. Grzadkowski, Z. Hioki, K. Ohkuma, and J. Wudka, *Probing anomalous top quark couplings induced by dimension-six operators at photon colliders*, Nucl. Phys. B 689(2004) p. 108.

[31] K. Hagiwara, S. Ishihara, R. Szalapski, and D. Zeppenfeld, *Low energy effects of new interactions in the electroweak boson sector*, Phys. Rev. D 48(1993) p. 2182.

[32] R. Contino, M. Ghezzi, C. Grojean, M. Muhlleitner, and M. Spira, *Effective Lagrangian for a light Higgs-like scalar* JHEP 7(2013) p. 35.

[33] G. Giudice, C. Grojean, A. Pomarol, and R. Rattazzi, *The Strongly-Interacting Light Higgs*, Nucl. Phys. B 703(2007) p. 127.

[34] R. Diaz and R. Martinez, *The Custodial symmetry*, Rev. Mex. Fis. 47(2001) p. 489.

[35] S. L. Glashow and S. Weinberg, *Natural Conservation Laws for Neutral Currents*, Phys. Rev. D15(1976) p. 316.

[36] E. A. Paschos, *Diagonal neutral currents*, Phys. Rev. D 15(1977) p. 1966.

[37] G. C. Branco, P. M. Ferreira, L. Lavoura, M. N. Rebelo, M. Sher, and J. Silva, *Theory and phenomenology of two-Higgs-doublet models*, arXiv: hep-ph/1106.0034.

[38] M. Misiak et al., *The First Estimate of* $\mathcal{B}\left(\bar{B} \to X_s\gamma\right)$ *at* $\mathcal{O}\left(\alpha_s^2\right)$, Phys. Rev. Lett. 98(2007) p. 022002.

[39] X. Xu, *Tree-level vacuum stability of two-Higgs-doublet models and new constraints on the scalar potential*, Phys. Rev. D 95(2017), p. 115019.

[40] E. Kaffas, A. Wahab, P. Osland, and O. M. Ogreid, *CP Violation, Stability and Unitarity of the Two Higgs Doublet Model*, Nonlin. Phenom. Complex Syst. 10(2007) p. 347.

[41] G. Ridolfi, *An Introduction to the Standard Model of Electroweak Interactions*, `https://www.ge.infn.it/~ridolfi/notes/smcom.ps`

[42] G. Bhattacharyya and D. Das, *Scalar Sector of Two-Higgs-Doublet Models: A minireview*, Pranama 87(2016) p. 40.

[43] M.Aoki, S. Kanemura, K. Tsumura, and K. Yagyu, *Models of Yukawa interaction in the two Higgs doublet model, and their collider phenomenology*, arXiv: hep-ph/0902.4665

[44] S. P. Martin, *A Supersymmetry Primer*, arXiv: hep-ph/9709356

[45] S. K. Vempati, *Introduction to the MSSM*, arXiv: hep-ph/1201.0334v1

[46] M. Dine and J. D. Mason, *Supersymmetry and Its Dynamical Breaking*, arXiv: hep-th/1012.2836

[47] Y. Shadmi, *Supersymmetry Breaking*, arXiv: hep-th/0601076

[48] J. Wess and J. Bagger, *Supersymmetry and Supergravity*, Princeton University Press (1992).

[49] E. Witten, *Dynamical Breaking of Supersymmetry* , Nucl. Phys. B 188(1981) p. 513.

[50] P. Fayet and J. Iliopoulos, *Spontaneously Broken Supergauge Symmetries and Goldstone Spinors*, Phys. Lett. B 51(1974), p. 461.

[51] W. J. Marciano, C. Zhang, and S. Willenbrock, *Higgs decay to two photons*, Phys. Rev. D 85(2012) p. 013002.

[52] T. Hahn, *Generating Feynman Diagrams and Amplitudes with FeynArts 3*, Comput. Phys. Commun. 140(2001) p. 165.

[53] T. Hahn and M. Perez-Victoria, *Automatized One-Loop Calculations in 4 and D dimensions*, Comput. Phys. Commun. 118(1999) p. 153.

[54] M.E. Peskin, D. V. Schroeder, *An Introduction to Quantum Field Theory*, Westview Press (1995).

[55] M. Spira, A. Djouadi, D. Graudenz, and P. M. Zerwas, *Higgs Boson Production at the LHC*, Nucl. Phy. B 453(1995) p. 17.

[56] F. Wilczek, *Decays of Heavy Vector Mesons into Higgs Particles*, Phys. Rev. Lett. 39(1977) p. 1304.

[57] X. Li and M. B. Voloshin, *Remarks on double Higgs boson production by gluon fusion at threshold*, Phys. Rev. D89(2014) p. 013012.

[58] G .Ferrera, J. Guasch, D. Lopez-Val, and J. Sola, *Triple Higgs boson production at the ILC within a generic Two-Higgs-Doublet Model*, PoS, RADCOR2007 (2007), p. 043.

[59] D. Lopez-Val and J. Sola, *Neutral Higgs-pair production at Linear Colliders within the general 2HDM: Quantum effects and triple Higgs boson self-interactions*, Phys. Rev., D81(2010) p. 033003.

[60] K. J. F. Gaemers and F. Hoogeveen, *Higgs-Boson Pairproduction in e^+e^- Reactions*, Z. Phys. C 26(1984) p. 249.

[61] N. D. Christensen and C. Duhr, *FeynRules - Feynman rules made easy*, Comput. Phys. Commun. 180(2009) p. 1614.

[62] B. Grzadkowski, M. Iskrzynski, M. Misiak, and J. Rosiek, *Dimension-Six Terms in the Standard Model Lagrangian*, JHEP 10(2010) p. 85.

[63] M. Veltman, *Second threshold in weak interactions*, Acta Phys. Polon. B8(1977) p. 475.

[64] J. Donoghue, E. Golowich, and B. Holstein, *Dynamics of the Standard Model*, Cambridge University Press (1992).

[65] D. Gauthier, C. Grojean, J. Gu, and K. Wang, *The leptonic future of the Higgs*, arXiv: hep-ph/1704.02333

[66] T. Riemann, *The Z Boson Resonance Parameters*, https://cds.cern.ch/record/332962/files/9709208.pdf.

[67] A. Denner, S. Heinemeyer, I. Puljak, D. Rebuzzi, and M. Spira, *Standard Model Higgs-Boson Branching Ratios with Uncertainties*, arXiv: hep-ph/1107.5909v2.

[68] I. Aitchison, *Supersymmetry in particle physics, an elementary introduction*, Cambridge University press (2007).

[69] A. Falkowski and F. Riva, *Model-independent precision constraints on dimension-6 operators*, arXiv: hep-ph/1411.0669v3.

[70] E. Coniavitis and A. Ferrari, *Pair production of heavy MSSM charged and neutral Higgs bosons in multi-TeV e^+e^- collisions at the Compact Linear Collider*, Phys. Rev. D 75(2007) p. 015004.

[71] N. Arkani-Hamed, D. P. Finkbeiner, T. R. Slatyer, and N. Weiner, *A Theory of Dark Matter*, arXiv: hep-ph/0810.0713.

[72] Z. Zhang, *Testing the Higgs sector directly in the nonrelativistic domain*, arXiv: hep-ph/1604.07061v2.

[73] Z. Zhang, *Final state interactions at the threshold of Higgs boson pair production*, J. Phys. G: Nucl. Part. Phys. 42 (2015), p. 115003.

[74] J. L. Feng, M. Kaplinghat, and H. Yu, *Sommerfeld Enhancements for Thermal Relic Dark Matter*, arXiv: hep-ph/1005.4678 .

[75] S. Cassel, *Sommerfeld factor for arbitrary partial wave processes*, arXiv: hep-ph/0903.5307.

[76] K. Fujii et al., *Physics Case for the 250 GeV Stage of the International Linear Collider*, arXiv: hep-ph/1710.07621v3

[77] M. J. Strassler and M. E. Peskin, *Threshold production of heavy top quarks: QCD and the Higgs boson*, Phys. Rev. D 43(1991), p. 1500.

[78] S. Flügge, *Practical Quantum Mechanics*, Springer-Verlag (1994).